UNIVERSITY OF ZULULAND

Faculty of Science and Agriculture

Department of Physics and Engineering

SYNTHESIS AND CHARACTERISATION OF DLC AND DIAMOND FILMS FOR GAS SENSING APPLICATIONS

Dissertation submitted in fulfilment of the requirements for the degree of Master of Science to the:

Faculty of Science and Agriculture

Department of Physics and Engineering

University of Zululand

Supervisor: Prof. O.M. Ndwandwe

Co-supervisor: Dr B. Mwakikunga (CSIR)

Submitted by

NELISIWE PRINCESS CHONCO

NOVEMBER 2014

DECLARATION

I, undersigned, hereby declare that the work contained in this thesis is my own original work and that I have not previously in its entirety or in part submitted it at any other university for a degree.

Signature.....…

Date….....

ACKNOWLEDGEMENTS

I would like to thanks my ancestors and to the above Almighty God for His presence and provider for extending my day of living until I finish my thesis and my family for their love and support, for encouraging me to seek for myself a meaningful education.

I would also like to extend my thanks to the following people who made this project possible:
Prof. OM Ndwandwe, my supervisor, who was involved in my admission to the Manus/Matsci programme for his encouragement and advice, who designed this project, for being a good supervisor who listens and tries to solve our problems. For his unwavering support and excellent guidance, especially for encouraging and showing me the light whenever I lost hope.

- Special thanks go to my co-supervisor Dr. B Mwakikunga, Nanoscience Research Centre, CSIR Material Sciences and Manufacturing, Pretoria for his moral support, encouragement and guidance in my studies.
- Fellow students: CT Thethwayo, AP Sefage for their assistance during the time for SEM , EDS and AFM.
- NF Thabezhe was very helpful to my understanding of sputtering system.
- Dr CL Ndlangamandla for his help with Raman and interpretation of the results and for making an eye opening suggestion, which proved to be very useful for this work.
- Mrs Mothapo for being kind supportive during my research period, and all who contributed directly and indirectly, I say thank you.
- NRF/DST, iThemba LABS, University of the Western Cape and the Research Committee of the University of Zululand for your financial support during this investigation.
- Dr Linda Prinsloo and Dr Jack Nel, University of Pretoria, for sharing me with your facility and your assistance during the time for Raman and AFM measurements.

- Special thanks go to Prof. T Hillie, Dr. GH Mhlongo and Dr. B Dhonge, Nanoscience Research Centre, CSIR for their assistance and discussions through this investigation, I appreciate their support.
- Dr. P. Sechogela and Dr. C.B Mtshali, Material Research Group, iThemba Labs, for sharing with me your facility and your assistance during the time for RBS.
- Dr. R. Bucher and Mr. Z. Khumalo, Material Research Group, iThemba Labs, for sharing with me your facility and your assistance during the time for XRD.
- An exceptional warmest thank goes to Dlomo's family especially to Qin'sile for taking care of my lovely kids, S'nqobile and Mhlengi, and for their great love and passion, nothing was possible without their encouragement and support.
- I would like to sincerely my warmest thanks to my mom (umaMbatha) Khombani and the late dad Sakhowakhe Chonco with their value to my life.
- To my mother (umaNdlovu), my second father Msindisi for their love, moral support, encouragement and understanding during this journey.
- To my family for giving me endless love and support, especially my eldest brother S'phiwe and my sister Themb'sile for their financial support.
- Finally I would like to sincere my warmest thanks to my friends Ntombizile,Nelile and Thandekile for their love, support and encouragement throughout my studies

Ngibonge koGambushe,oShayimamba,oNyongande ,oMfomubi…ngithi nje nimenjalo bomabhala ngozipho abanye bebhala ngamapensela!!!!

TABLE OF CONTENTS

LIST OF FIGURES

LIST OF TABLES

LIST OF EQUATIONS

LIST OF ABBREVIATIONS

C.....*Carbon*

H.....*Hydrogen*

DLC.....*Diamond-like carbon*

nc-G.....*Non-crystalline graphite*

A-C.....*Amorphous carbon*

A-C: H.....*Amorphous hydrogenated carbon*

Ta-C.....*Tetrahedral amorphous carbon*

Ta-C: H.....*Tetrahedral hydrogenated amorphous carbon*

PLHC.....*Polymer-like hydrogenated carbon*

CNTs.....*Carbon nanotubes*

sp^2 .....*Orbital hybridization characteristic for graphite like Carbon*

sp^3.....*Orbital hybridization characteristic for diamond like Carbon*

SD.....*Sputter Deposition*

DC.....*Direct Current*

RF .....*Radio Frequency*

Sccm .....*Standard cubic centimetre*

CVD .....*Plasma Enhanced Chemical Vapour Deposition*

FE-SEM .....*Field Emission- Scanning Electron Microscope*

SE .....*Secondary electrons*

BSE .....*Backscattered electrons*

EDX/S .....*Energy Dispersive X-ray/ Spectroscopy*

AFM .....*Atomic Force Microscope*

RBS .....*Rutherford Backscattering Spectrometry*

XRD.....*X-Ray Diffraction*

LIST OF SYMBOLS

π.....*Mathematical constant, sometimes written is approximately equal to* ***3.14159****.*

μ*: .....Micron (*10^{-6}*)*

α: *.....Alpha (the first letter of the Greek alphabet means the beginning)*

v*:.....Potential difference*

Θ:*.....Theta (angle normally in degree)*

ω*:.....Raman shift expressed in wavenumber*

d: *.....Distance between the atomic planes*

λ*:.....Wavelength (nm)*

a_0***:*** *..... Lattice constant*

n*: .....An integer number / order of diffraction*

h,k,l *:.....Crystal planes*

σ:*.....Sigma*

a.u *:.....Arbitrary units*

A°*.....Angstrom=1.0 x*10^{-10}

ABSTRACT

Over the last decade diamond like carbon (DLC) and diamond films have been extensively studied. These studies were only focused on the synthesis and characterization of this material. DLC films have some unique properties as a semiconductor such as a high elastic modulus, high mechanical hardness, very low surface roughness, and chemical inertness that qualifies it to be a valuable material for several applications. Its band gap varies approximately between 1eV to 4 eV. This material has been extensively used in electronic, optical, mechanical and biomedical applications. In this research work diamond and DLC thin films are deposited on a silicon substrate (Si <100 >/<111>), alumina strips by using direct current (DC) magnetron sputtering system under varying conditions such as temperature, pressure, power, voltage, deposition rate, argon, nitrogen as well as oxygen gas flow rate. The as-deposited thin films were characterized using several characterization techniques. The roughness of the sample was studied using atomic force microscopy (AFM) and it was estimated to be 0.292- 3.2 nm. Scanning Electron Microscopy (SEM) equipped with Energy Dispersed X-ray (EDX) was used to investigate the morphology and the composition or stoichiometry of the sample. SEM confirmed that the samples are uniform and fairly smooth which is in agreement with the AFM results. X-ray diffraction (XRD) was used to study the crystallinity of the sample and the films were found to be polycrystalline with the pronounce peak of DLC. Raman analysis was used to determine the quality of the DLC films using the ratio of the areas under the sp^3 to sp^2 curves. The ratio of sp^3 to sp^2 areas under the curve was found to vary between 0.7 to 0.9 for samples prepared under different conditions. RBS was used to as a rough measure of continuity of the films or coverage of the substrates by carbon. This research was aimed at attempting to determine the gas sensing properties of DLC and diamond films at different concentrations of various gasses and at different sensor temperatures. It was found that DLC films are corrosive resistant to poisonous gasses such as H_2S. DLC films were found to respond more favourably to NO_2 and NH_3 at room temperature than to other gasses like CO, H_2 and H_2S which indicates that DLC sensors are very selective – a desirable property in a gas sensor.

CHAPTER 1: INTRODUCTION

1.1 Carbon

Carbon is one of the most remarkable elements among all other element in periodic table. It is a unique and abundant chemical element in nature, with symbol C and the ^{12}C consists of 6 protons and 6 electrons. There are three naturally occurring isotopes with ^{12}C and ^{13}C being stable while ^{14}C is radioactive decaying with half-life of about 5.7×10^3 y [1]. Carbon is unique because it is easier for the carbon atom to share its four electrons with another atom than to lose or gain four electrons. Each carbon is identical they all have four valence electrons so they can easily bond with other carbon atoms to form long chains or rings. Carbon has an outstanding ability to form different hybridization (sp^3, sp^2 and sp^1). It can form structures of various geometries with different fractions of sp^3, sp^2 bonding in crystalline and non- crystalline. Carbon can exists in more than 90% of all known chemical substances and consists of large number of allotropes which is represented in Figure 1.1.

Carbon materials appear in different crystalline forms as a result of the three different types of bonding known as hybridization, which is sp^3, sp^2 and sp^1 as shown in Figure1.2. The first hybrid is the sp^1 (linear coordination), second is sp^2 (trigonal) and the third is sp^3 (tetragonal). Diamond is known as pure sp^3 hybridization while graphite is pure sp^2 hybridization and diamond-like carbon (DLC) has a mixture of sp^3 and sp^2 hybridization. In the sp^3 configuration, in diamond, four valence electrons are assigned to be tetrahedral directed to sp^3 orbital, which makes a strong σ bond to an adjacent angle [2-3].

In the three-fold coordinated sp^2 configuration as in graphite, three of the four valence electrons enter trigonal directed sp^2 orbitals, which form σ bonds in a plane. The fourth electron of the sp^2 orbitals lies in a pπ orbital, which lies normal to the σ bonding plane [4-5]. The π orbital forms a weaker bond with a π orbital on one or more neighbouring atoms. In the sp^1 configuration, two of the four valence electrons enter σ bonds, each forming a σ bond directed along ± x-axis and the other two electrons enter π orbitals in the y and z directions [6]. The second well known form of carbon is the graphitic form called graphite. Graphite was discovered in the 15th century and its name was derived from Greek word <

graphian >, meaning *writing* and was called black lead. It is used in pencil and called pencil lead because there were feeling graphite contains lead. In the graphite structure each atom is sp^2 hybridize and is bounded trigonally with the neighbouring atoms at 120°, the bonds found in graphite are σ bonds. The unbounded electron found in a π orbital leads to an electrical conductivity of graphite [7].

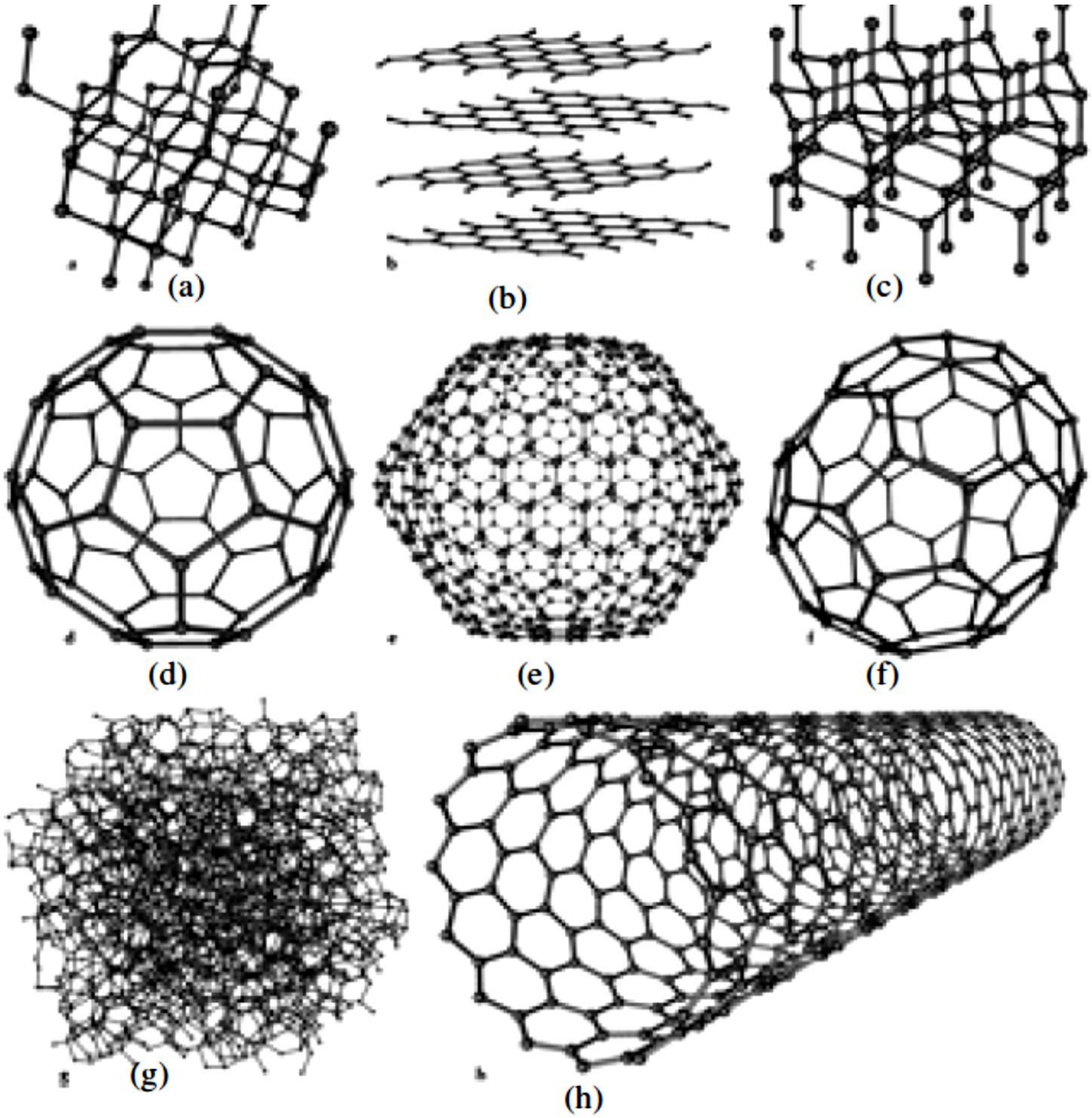

Figure 1.1: *Models of eight allotropes of carbon: (a) diamond, (b) graphite, (c) lonsdaleite, (d)C60, (e) C540, (f) C70, (g) amorphous carbon and (h) a carbon nanotube (Foursa, 2007) [2].*

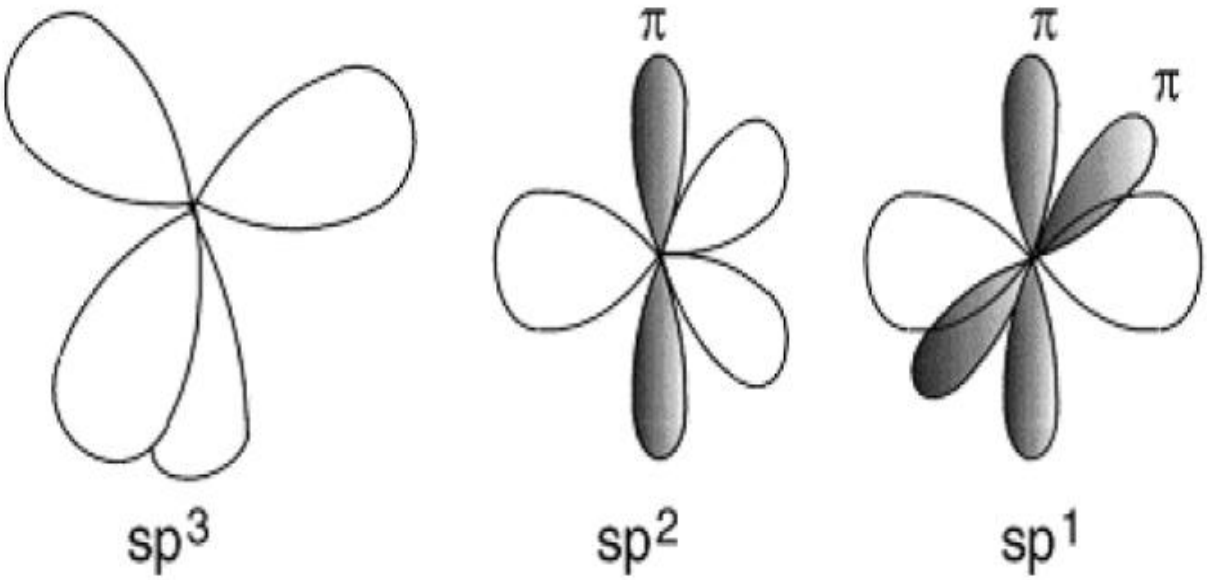

Figure 1.2 *The schematic diagram of the carbon bonds, where the shaded areas represent the π bonds and the un-shaded areas represent the σ bonds [3].*

1.2 Thin films

Thin films are defined to be layers of materials that are less than a micron in thickness. Diamond like carbon (DLC) thin films has a growing interest due to their unique properties such as high hardness, high thermal conductivity, high chemical inertness and high corrosion resistance. DLC can be used as a decorating material due to its hardness and tribological properties. DLC films exist in eight different forms all of which are amorphous [2]. The eight forms are classified in terms of sp^3/sp^2 ratio of their hybridized carbon atoms with the hardest and strongest mixture consisting of purely sp^3 bonded diamond called ta-C. This study will be focusing on diamond because of its interesting properties and potential application in various spheres of technology [9].

The first successful DLC thin film was synthesized by Aisenberg and Chabot in the early 1970 and from there a large interest has grown to look the different ways to synthesis thin films [3, 4, 6-7]. Lots of applications of thin films technology extensively depend on the thickness of the films. Among these applications the thermal barrier coating which involves coating of a metallic surface of an appliance working at a relatively high temperature such that it serves as an insulator. The most common application for thin film technology is found in mirrors. This involves a glass sheet that is coated with a thin metal to form a reflective interface [6-7].

Various deposition techniques such as physical vapour deposition (PVD), chemical vapour deposition (CVD) can be used to deposit DLC thin films. Depending on the thickness and properties of the film required a deposition method may be more favourable than the other [7]. Physical vapour deposition can be subdivided into five classes which are molecular beam epitaxy, activated reactive evaporation, thermal evaporation, ion plating and electron beam gun [6, 7-8]. Through these five deposition techniques a thin film can be deposited on the substrate by physically transforming the deposited material into vapour form in a low pressure region and use a potential difference to condense it onto the substrate to form a film [8].

Chemical vapour deposition is classified into six classes which are chemical deposition, electron deposition, solution growth, spray pyrolysis, screen printing and anodisation [8-9]. The process of cathode sputtering is based on the idea of sputtering a target with inert gas ions and collecting the sputtered materials onto the substrate. This process is subdivided into four classes which are magnetron sputtering, DC sputtering, RF sputtering and ion beam sputtering.

1.3 Outline of the project

In this study we used DC magnetron sputtering method because of its simplicity and availability at the University of Zululand. This method is powerful because it produces uniform thin films which are good for gas sensing purposes.

- Chapter one: gives an introduction about Diamond-Like Carbon and Diamond films in generally
- Chapter two: gives a survey literature review about diamond and diamond like carbon and its applications.
- Chapter three: presents the different types of characterization techniques for DLC and Diamond films.
- Chapter four: described the synthesis and characterization for DLC films
- Chapter five: discuss the sensitivity of DLC thin films on various gases
- Chapter six : represent preparation & characterization of diamond films
- Chapter seven : represent summary and conclusion

1.4 Problem identification

The question; is it possible to synthesize thick DLC coatings with low residual stress? Is it possible to increase the sp^3/sp^2 ratio of these films so that they resemble actual diamonds much more? Can we do gas sensing, and if so which gases can be sensed using DLC films?

1) Thick DLC low residual stress
2) Increase sp3/sp2 ration
3) DLC's be used for gas sensing in the following gasses: H_2.H_2S, CO, NO_2 and NH_3.

1.5 Aim of the research

The aim of this research work is to use DC magnetron sputtering method to deposit uniform DLC thin films on various substrates and characterize it using various characterization methods. As deposited DLC thin films will then be used for gas sensing applications.

1.6 Method of this research project

To use DC sputtering deposition method to deposit DLC thin films on various substrates such as Si wafer and aluminium substrates for gas sensing purposes. At the end of this research project the following are expected to be achieved.

- To use moisture to reduce the amount of unbounded carbon in DLC films.
- To use Faraday cage to see whether or not it has an effect on sp^3/sp^2.
- To grow the diamond films from the diamond seeds at high temperature by using acetylene as a source of carbon.
- To study the properties of diamond like carbon and diamond films.
- To use DLC films as a gas sensor coating after doping with nitrogen. Sometimes nitrogen has been used to dope diamond; we have not found any reference to doping DLC films with nitrogen. Nitrogen doping changes the colour of diamond. We would like to see whether nitrogen has the same effect on DLC films.
- To use an electric field to reduce the ratio sp^3/sp^2 by applying a voltage between target and substrate during sputtering.
- To determine the gas sensing properties of DLC thin films and determining such properties at different sensor temperatures.

1.7 References

[1] Furlan K .P, Klein A.N and Hortza .D, *Diamond- Like Carbon films deposited by Hydrocarbon plasma sources.* Rev.Adv.Mater.Sci, 34 (2013) 165-172.

[2] Grill .A, *Diamond-Like Carbon: State of Art, Diamond and Related Materials,* 8 (1999) 428-434.

[3] Kumari. K, Banerjee .S , Chini T.K. and Ray N. R. , *Preparation of Diamond Like Carbon Thin Film on Stainless Steel and it's SEM Characterization, Bulletin of Materials Science,* 32 (2009) 563-567

[4] Wiech G. , Auer N, Simunek A, Vackar J, Hammerschmidt A and Rittmayer G, *Diamond-Like Hydrogenated Amorphous Carbon film studied by x-ray emission spectroscopy, Diamond and Related Materials,* 6 (1997) 944-951

[5] McLaughlin J.A, Meenan B, Maguire P, Jamieson N, *Properties of Diamond – Like Carbon thin films Coatings on Stainless steel Medical Guidewire, Diamond and Related Materials,* 5 (1996) 486-491

[6] Sibiya P.S, *Nanostructured Diamond –Like Carbon by Dual Pulsed Laser Ablation-Pulsed Gas Feeding,* MSc thesis, University of Zululand (2007) 13-21

[7] Kayani. A, *Deposition and characterization Diamond –Like Carbon Films With and Without Hydrogen and Nitrogen*. PhD thesis, Ohio University, Athens,Ohio,(2003) 22- 26

[8] Jyh-Ming. T, Howard .L, *Diamond- Like Carbon Composite thin films by Sputter Deposition,* Diamond and Related Materials, 11 (2002) 1119-1123.

[9] Whang. K.W and Tae. H.S, *The properties of diamond-like carbon films prepared by R.F discharges, Thin Solid Films,* 204 (1991) 49-58.

CHAPTER 2: LITERATURE REVIEW

2.1 Introduction

There are many allotropes of carbon. Some are natural while others are synthetic. Some forms of carbon include diamond, graphite, fullerene, carbon nanotubes, amorphous carbon (a-C). DLC has some extreme properties similar to diamond such as the hardness, elastic modulus and chemical inertness [1]. The major focus of this research work is on both diamond and DLC films. DLC films are described as a metastable form of carbon containing a mixture of sp^3 and sp^2 hybridization. Diamond contains sp^3 hybridized carbon. Graphite is made of sp^2 bonded carbon [1-2].

2.2 Structure of DLC films

All DLC films are substantially amorphous, but some micro or nano-crystalline inclusions of most carbon forms can be found in the amorphous matrix. DLC 's amorphous nature make it feasible to be doped with small amounts of different elements like N, B, O, F, Si and their combinations to improve and control their mechanical ,tribological and biological properties. The structure of DLC consists of both threefold coordinated sp^2 and four fold coordinated sp^3 .While the sp^2 controls the electrical properties like band gap, sp3 controls the mechanical properties like hardness and rigidity of the film. Figure 2.1 shows a typical DLC film structure [2].

Amorphous carbon (a- C) and hydrogenated amorphous carbon (a–C: H) can be categorized into different forms based on the content of hydrogen as shown in Figure 2.1. The properties of DLC films depend strongly on the ratio of hybridization sp^3/sp^2. The amorphous carbon film rich in sp^3 content is described to be tetrahedral amorphous carbon. These films, ta-C, are highly stressed and are easily flaked off from the substrate.

2.3 An overview of Diamond- like carbon (DLC) films

The Diamond-Like Carbon (DLC) was first synthesized in the Laboratory using carbon ions in 1971 and proved to have several interesting properties of diamond. DLC is metastable and amorphous in nature. DLC can be deposited at temperatures less than 325°C [3]. The properties of DLC films depend strongly on the ratio of the hybridization ratio of sp^3 and sp^2 coordination. During the synthesis of ta-C the amount of sp^3 may be increased by decreasing the relaxation time, when the temperature is high, in which the hybrids change into sp^2 thereby inducing more graphite than diamond properties. The presence of hydrogen in DLC films has been said to promote the formation of sp^3 hybrids thus increasing the sp^3/sp^2 ratio. Amorphous carbon containing hydrogen (a-C: H) is known by its specific physical states such as it softness combined with its higher degree of optical transparency compared to other hydrogen free forms. The different types of DLC coatings can be presented in a ternary diagram shown in Figure 2.2 [4].

DLC films is divided into the following types, first is amorphous carbon (a-C), second is hydrogenated tetrahedral amorphous carbon (ta-C: H) and third is hydrogenated amorphous carbon (a-C: H) or polymer like hydrogenated carbon (PLCH). The first type of DLC contains relatively high degree of sp^2 bonding. The second type of DLC contains high degree of sp^3 bonding with hydrogen content. The third type contains high sp^3 bonding. The amount of hydrogen on the films has been used to increase the sp^3/sp^2 ratio [5].

In all three cases, the sp^3/sp^2 ratio is considered as a signature of diamond or graphite nature. As one moves from ordered graphite to non -crystalline graphite (nc-G) to amorphous carbon (a-C) and at the end to sp^3 bonded ta-C, the sp^2 groups become first smaller, then disordered and finally change from ring structure to chain configurations. a- C (PLCH) is known as polymer-like hydrogenated amorphous carbon, highest hydrogen content (40-60 %) and this film has a large amount of sp^3 hybridization up to 70 % of overall bonding. The film is soft and has low density with the band gap ranging between 1- 4 eV [6].

(a-C:H) hydrogenated amorphous carbon second class, are films with an intermediate hydrogen content which is between 20-40% and have less sp^3 hybridization compared to the polymer like a-C as described in first class. DLC films have lower sp^3 content; they have

more C-C sp^3 bonds than the polymer like hydrogenated carbon. They exhibit better mechanical properties with an optical gap ranging between 1 to 2 eV. These films are called diamond-like a-C:H (DLCH) [4, 5] (ta-C:H) hydrogenated tetrahedral amorphous carbon films third class, are the class of diamond like carbon hydrogenated (DLCH) in which the C-C sp^3 content can be increased while keeping a fixed hydrogen content, because of the higher sp^3 content of about 70% and 25-30% atomic. This film has a higher density of the order of 2.4 $g.cm^3$ and associated to Young's modulus of 300 GPa and has an optical band gap of 2.4 eV [6, 7].

GLCH family is called graphite-like which is the last class of hydrogenated amorphous carbon with 20% hydrogen content and large content of sp^2 hybridization. They exhibit a low band gap of about 1 eV. They can be produced via plasma enhanced chemical vapour deposition and magnetron sputtering at high bias voltage [3-5]. Therefore the amount of hydrogen in deposited films increases the optical gap, electrical resistivity and stabilizes the diamond structure by maintaining the sp^3 hybridization configuration [7].

According to Robertson, 2002 [7], bombardment of a target with ions promotes the formation of sp^3 bonds. The DLC coatings with the highest amount of sp^3 hybrids was produced from the bombardment of the substrate as well as growing film of with C^+ ions having an energy of 100 eV [8]. When highly energetic carbon ions bombard the growing film, the hybridization adjusts itself accordingly in order to accommodate the change in density. The hybridization may change to sp^2 at low density and more sp^3 at higher density. The increase in the ion energy leads to an increase in both the ion range and the penetration depth of the ions into the films [9].

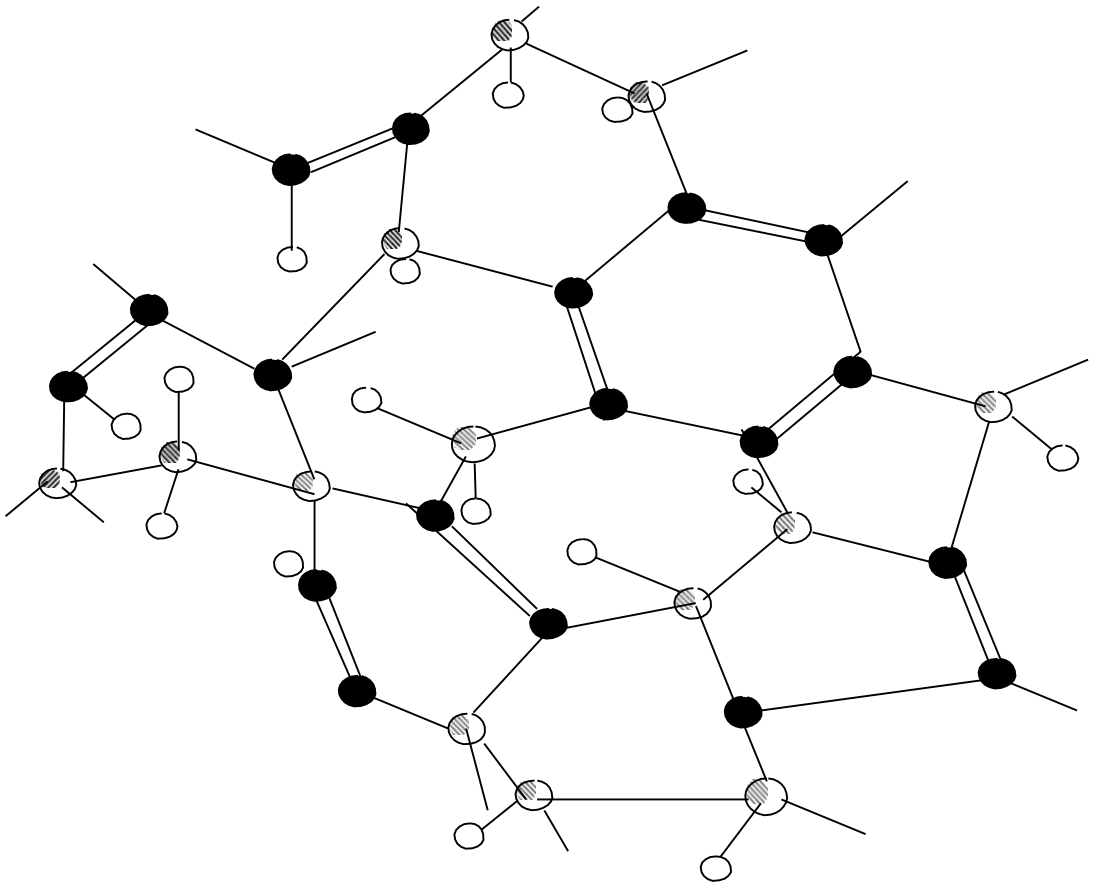

***Figure 2. 1*:** *The 2-D representation of diamond-like carbon film structure* ● sp^2 carbon atom; ▨ sp^3 carbon atom; hydrogen atom. *This diagram was adopted from ref [3]*

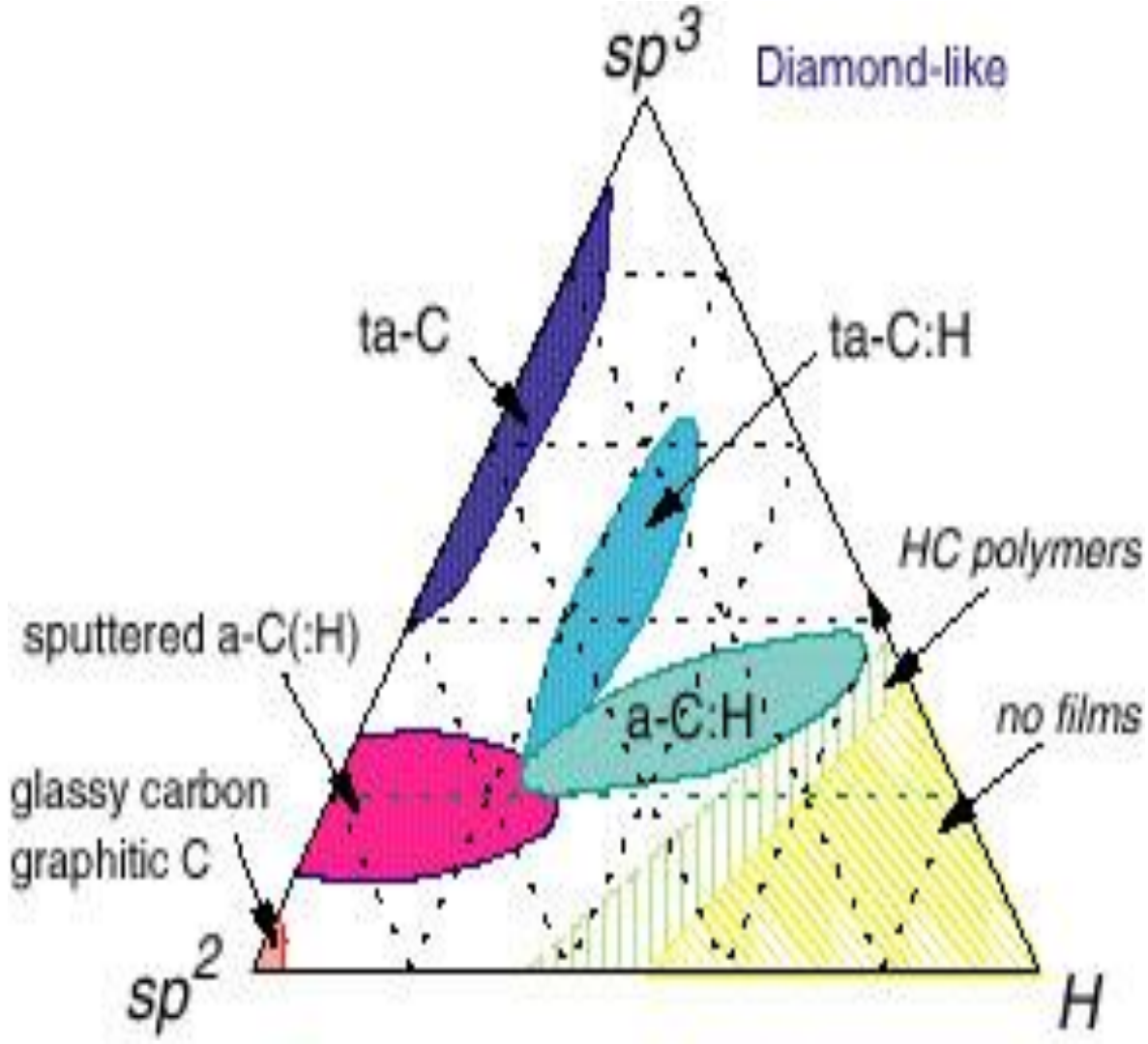

***Figure 2.2**: Phase diagram of DLC coatings depending on the sp^2 and sp^3 hybridization. This diagram was adopted from ref [9]*

2.3.1 Biomedical applications of DLC

DLC films have many applications: DLC is used as protective coatings from razor blades to magnetic tapes. It is also used as anti-reflecting coating for silicon solar cell, High hardness combined with a low coefficient of friction makes DLC the best material for MEMS applications, anti –scratch coatings for optical applications, infrared optics, sunglasses, optical lenses and biocompatible material for orthopedic implants [10]. DLC films have been adopted for biomedical applications due to its biocompatibility with the human body. DLC can also be used in biomedical applications.

The coronary stents are surgical devices implanted on a patient's restricted artery to support the walls of the artery and keep them open for greater blood flow [10]. Previous stents showed two problems; one being the formation of blood clots along the inside of the stent and the other being an unfavorable reaction of body cells with the metal ions released from the stent [10]. DLC coated stents, because of the inertness of the DLC no metal ions are released and the hemocompatible nature of DLC films reduces clotting of blood along the stent. Diamond-like carbon (DLC), known as amorphous carbon, is a class of materials with excellent mechanical, tribological and biological properties, which makes them particularly attractive for biomedical applications as shown in Figure 2.3.

2.3.2 Artificial joints

Seriously damaged joints and joints with chronic joint pains are surgically replaced with a new man made joints. Depending on the material used in the production of these artificial joints wear and debris formation are the two major problems regarding joint replacement. Previous joints were coated with Polyethylene which produced wear and debris leading to joint failure. Coating artificial joints with DLC thin films reduces wear and debris formation making joint replacement long lasting [11].

2.4 Properties of carbon

Carbon is a unique and abundant chemical element in nature and is found in group 14 of the periodic table. Carbon can form structures of various geometries with different fractions of sp^2 and sp^3 bonding in both crystalline and non-crystalline forms. Diamond and graphite are well known crystalline forms which have very important applications in science and technology. There are approaches that are being developed to find new forms of materials based on carbon and these have led to new forms of materials, e.g. C_{60} and Carbon Nanotubes (CNTs) [10,12].

2.4.1 Physical properties of DLC films

The physical properties of DLC films can be determined from the concentration of hydrogen along the relative ratio of hybridized carbon bonds (sp^2 and sp^3). Hydrogenated amorphous carbon with low hydrogen concentration is termed as "hard "a-C: H due to its high hardness. This hard a-C: H contains a considerable amount of sp^2 carbon in addition to sp^3 carbon. Hydrogenated amorphous carbon with high hydrogen concentration is termed as "soft" a-C: H. Most of the excess hydrogen is bonded to the film in the sp^3 configuration which results in soft a-C: H having a high percentage of sp^3 bonding [10-11].

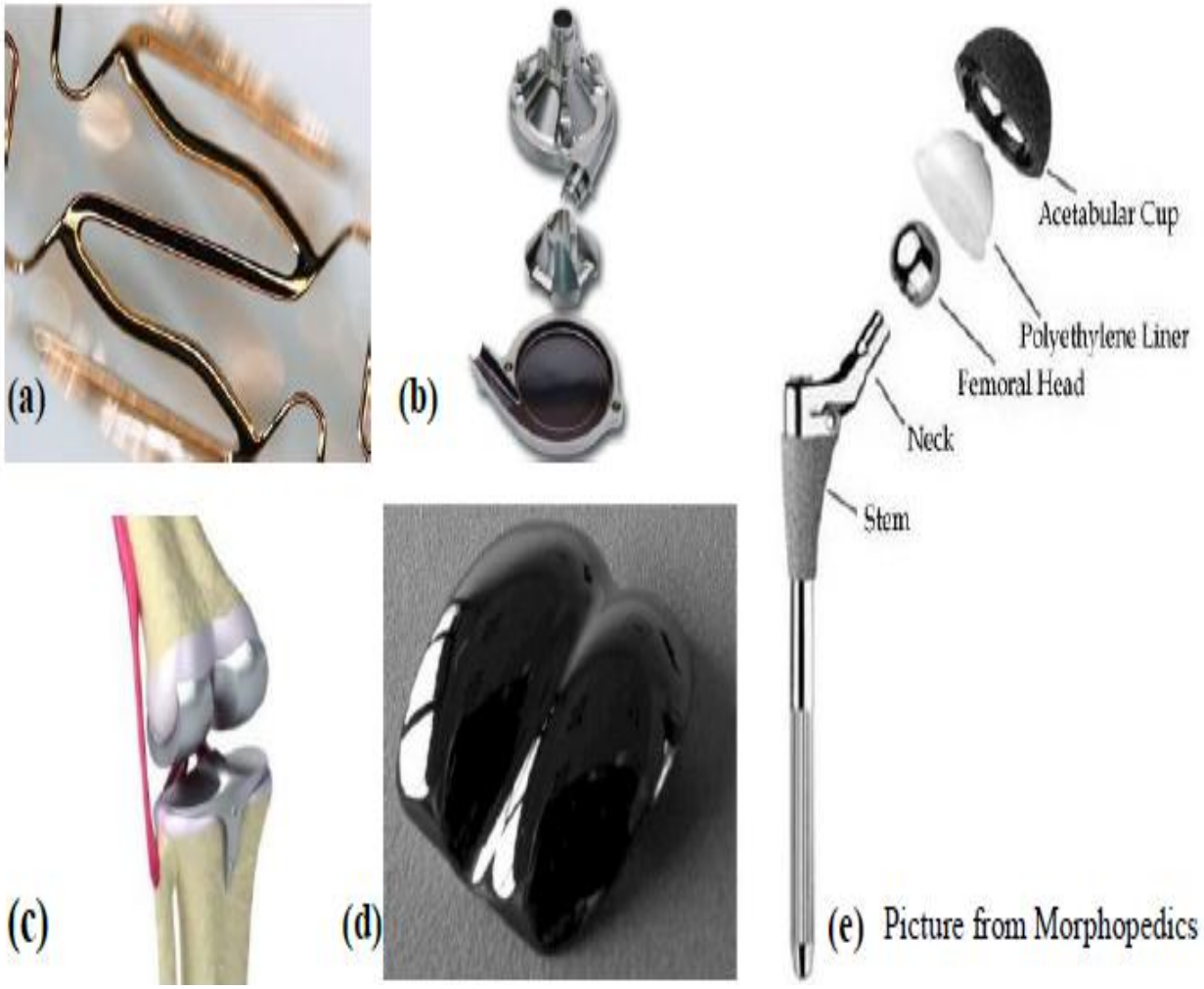

Figure 2. 3: *DLC coated products (a) Stent [12] (b) Left ventricular assist device heart pump [13] (c) artificial joint [13] (d) Ankle joint [14] (e) Hip Joint [15]. This diagram was adopted from ref [15]*

2.5 References

[1] McLaughlin J.A, Meenan B, Maguire P, Jamieson N, *Properties of Diamond –Like Carbon thin films Coatings on Stainless steel Medical Guidewire, Diamond and related materials,* 5 (1996) 486-491

[2] Sigmund. P, *Recollections of fifty years with sputtering*. *Thin Solid Films* 520 (2012) 6031-6049.

[3] Hassan M.K, "*Plasma Enhanced Chemical Vapor Deposition and Electrical Characterization of Diamond-Like Carbon Thin Films*"PhD thesis (2007), Kochi University of Technology

[4] Aisenberg .S and Chabot. R "*Ion beam deposition of thin films of diamond –like carbon"* Journal of applied physics 42 (1971) 2953-1971.

[5] Watson T.J, "*Diamond-Like Carbon: state of art*" Diamond and Related Materials 8 (1999) 428-434

[6] Sibiya P.S, *Nanostructured Diamond –Like Carbon by Dual Pulsed Laser Ablation-Pulsed Gas Feeding*, MSc thesis, University of Zululand (2007) 13-21

[7] Robertson, J.,*Diamond-like amorphous carbon. Materials Sciences and Engineering R Reports: A Review Journal* 37 (2002) 129-381.

[8] Postek M.T ,Howard K.S ,Johnson A.T ,McMichel K.L ,*Scanning Electron Microscopy, Ladd Research Industries*, Holly Cort, Williston, Vermont, 83 (2001) 533-537

[9] Wiech G. , Auer N, Simunek A, Vackar J, Hammerschmidt A and Rittmayer G, *Diamond-Like Hydrogenated Amorphous Carbon film studied by x-ray emission spectroscopy*, Diamond and related materials, 6 (1997) 944-951

[10] Mroz W, Burdynska S, Prokopiuk A, Jedynski M, Budner B and Koorwin-Pawlowski M.L, *Characterization of Carbon films Deposited by Magnetron Sputtering*, ActaPhysicaPolonica, 116 (2009) 120-122

[11] http://www.jstentech.de/eng/momo_dlc.html(2013.10.15)

[12] http://www.modernapplicationsnews.com/web/archives.php (26/07/2012).

[13] Hauert. R., *A review of modified DLC coatings for biological applications*, Diamond and Related Materials12 (2003) 583-589.

[14] http://morphopedics.wikidot.com/total-hip-arthroplasty(2013.10.15)

[15] Thompson L.A., Law F.C,.Rushton N., Franks. J., *Biocompatibility of diamond-like carbon coating,* Biomaterials 12(1) (1991) 37-40.

[16] Das T, Ghosh D, Bhattacharyya T.K, Maiti T.K, "*Biocompatibility of diamond like nanocomposite thin films"* Materials in Medicine 18 (2007) 493-500

CHAPTER 3: DEPOSITION AND CHARACTERIZATION TECHNIQUES

3.1 Introduction

3.3.1 Characterization techniques

This chapter gives a brief description of important characterization techniques used to characterize the synthesized diamond like carbon thin films. Sample preparation and deposition methods are discussed. The samples were characterised using different techniques such as Field Emission Scanning Electron Microscope (FE-SEM) to study the composition of the film, Energy Dispersive X-ray spectroscopy (EDS/EDX) was done to confirm the local elemental composition found within the sample. Rutherford Backscattering Spectroscope (RBS) was used to study the thickness of the sample surface. X-Ray Diffraction (XRD) was used to study the crystal structure of the sample**.** Raman spectroscopy was used to study the purity, bond hybridization of DLC films. Atomic Force Microscope (AFM) was used to study the roughness surface, topographical structure 2D and 3D surface morphology, grain size of the samples.

3.2 Deposition techniques

3.2.1 Sputtering deposition technique

Sputtering is the process in which atoms are physical deposited on the surface of a substrate. The most common industrial process for the deposition of DLC is sputtering. The most common form uses the DC or RF sputtering of a graphite electrode by Ar plasma because of low sputter yield of graphite [1]. The sputter process does not require any thermal evaporation of a substrate during the deposition process. In this case the target i.e. carbon graphite is bombarded with inert gas ions such as argon, the sputtered atom, ions and atom cluster originating from the target are directed to the surface of the substrate via an applied

voltage. There are three basic techniques of sputtering: DC sputtering, RF sputtering and magnetron sputtering. DC sputtering approach allows high yield of DLC and uniform coatings with good adhesion. The sputtering is the most widespread industrial process for the deposition of DLC films [1, 2]. Figure 3.1 represent the sputtering process using ionized sputtering gas argon gas (Ar^{+}) which enters the vacuum as gas molecules, and then get ionized to form plasma as it is shown in the schematic diagram presented in Figure 3.1.

3.2.2 Direct Current (DC) sputtering

DC sputtering deposition technique is also known as a planar diode sputtering deposition technique. DC bias can be applied to the substrate to vary the ion energy and to avoid the localized charge effects. The a-C: H is produced by reactive sputtering by using plasma of argon and hydrogen or methane. The main disadvantage of DC sputtering is that it only uses metal to sputter the target. If the target is a semiconductor a high voltage is needed which tends to affect the plasma with a lot of arcing experienced during deposition [2].

3.2.3 Magnetron sputtering deposition technique

Magnetron sputtering is the most universal configuration, because of low sputtering yield of graphite. External magnets are placed surrounding the target to induce a spiral motion of electrons in the plasma due to the Lorentz force so increase their path length and the ionization rate in the plasma. As ion bombardment helps the formation of sp^3 bonding, the magnetic field can be configured to pass across to the substrate, so this cause the Ar ions to also bombard the substrate to give an unbalanced magnetron. Magnetron sputtering is often used to increase the deposition rate [3]. Figure 3.1 shows a schematic diagram of a magnetron sputtering technique.

3.2.4 RF sputtering deposition technique

RF stands for radio frequency sputtering and is shown in Figure 3.2. The RF power produces plasma between the electrodes. RF also gives the ability to bombard insulating surfaces since the oscillating electrons do not reach the electrodes. The normal operating frequency for RF glow discharge deposition is 13.56 MHz The advantages of radio frequency are that one can apply at high voltage to the target for long time [3-4].

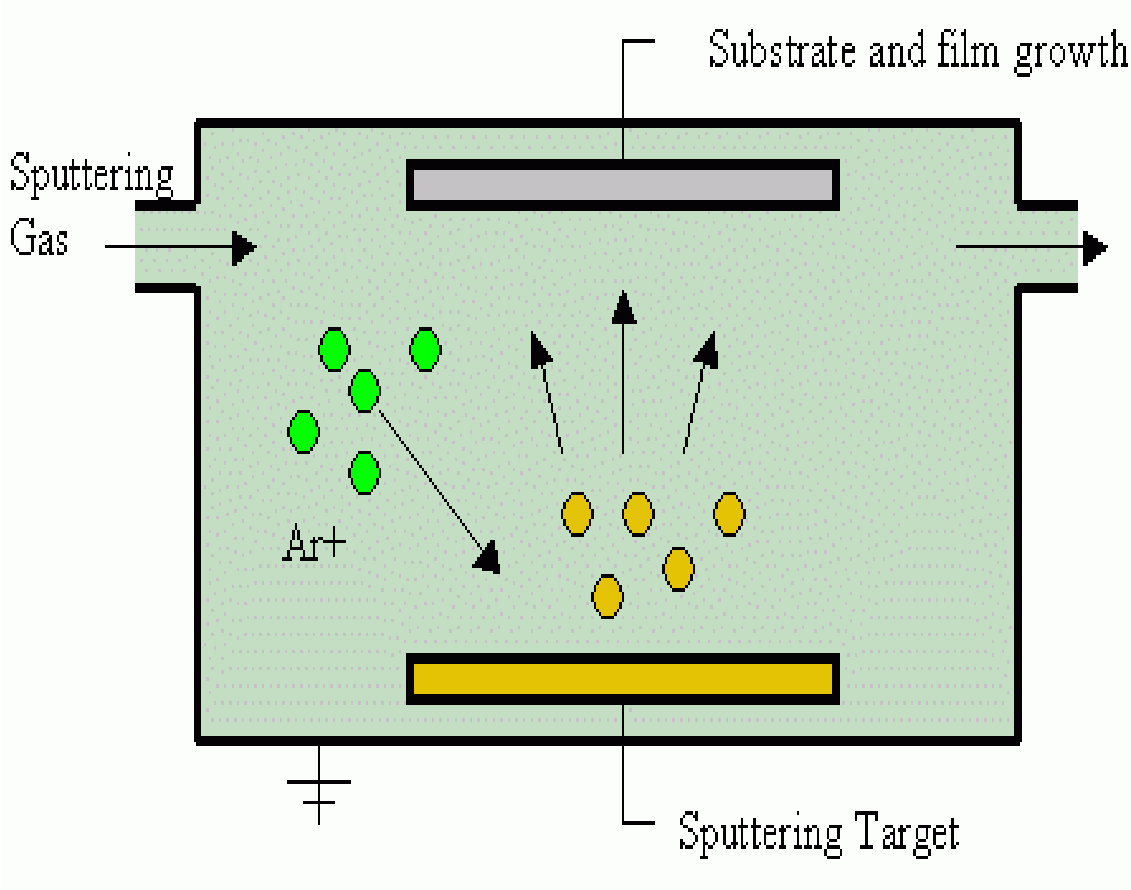

Figure 3. 1: *The schematic diagram of a Sputtering process from a solid target within an ionized argon gas. This diagram was adapted from ref [1]*

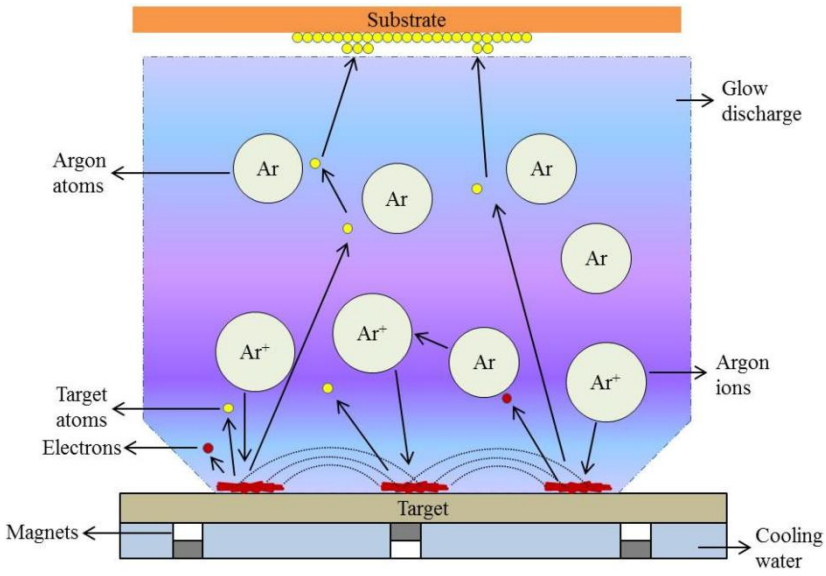

Figure 3. 2: *Schematic diagram showing the setup of magnetron sputtering deposition. This diagram was adopted from ref [1]*

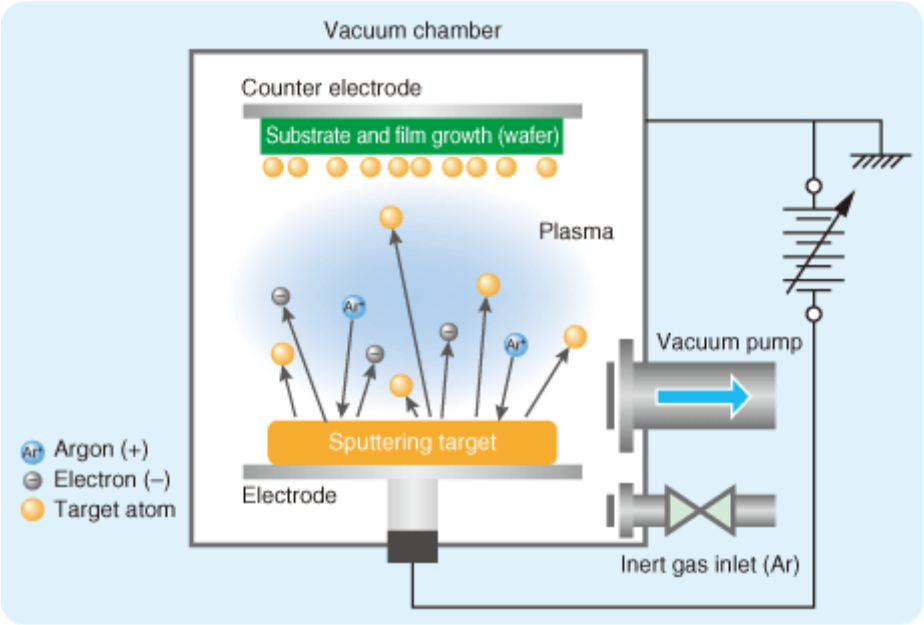

Figure 3. 3: *Schematic diagram showing the RF sputtering deposition. This diagram was adopted from ref [3]*

3.3 Characterization techniques

3.3.1 Scanning Electron Microscope (SEM) Technique

Scanning electron microscopy is the most widely used techniques to study surface morphology, microstructure analysis, elemental mapping and chemical composition. The scanning electron microscope images the sample surface by scanning it with a highly focused beam of electrons. The interaction of electrons with the sample ranging from a few nanometres to a micrometre depending on the properties and sample types, results in backscattered and emitted secondary electrons.

- Uses beam of electrons instead of light to form an image.
- Image displayed on TV screen.
- Provides two dimensional image of sample surface with a large magnification.
- Large depth of field allowing more of a specimen to be in focus.
- Sample is placed in the chamber than at lower level.

The SEM uses magnetic lenses to direct a high energetic beam of electrons towards the direction of specimen. Radiations are collected by the detectors in the chamber and are displayed on the screen. The final image gives details about the sample's morphology, topography, crystallographic arrangement and element composition. The advantage of SEM is that it provides a clear image which is similar to a normal photo [3, 4]. The image of an SEM is shown in Figure 3.4 while its detailed schematic diagram is shown in Figure 3.5.

The Figure 3.6 represents the interaction that produces a variety of radiation signals from the surface of the specimen. Several signals generated during the primary electron beam specimen interaction, the two signals: (a) secondary electrons and (b) characteristic x-rays were collected by detectors to form the image of the sample on a screen. These signals come from the beam of electrons striking the surface of the specimen and interacting with the sample. Interactions between the electron beam and the sample's electrons causes shell transitions which results in the emission of secondary electrons by inelastic scattering and the emission of electromagnetic radiation (characteristic x-rays). During inelastic interactions between incident electrons and sample's electrons, the electrons lose much of their energy and the result of this process is the emission of low energy electrons termed secondary electrons [3, 4].

Figure 3. 4: *Scanning electron microscopy at University of Zululand*

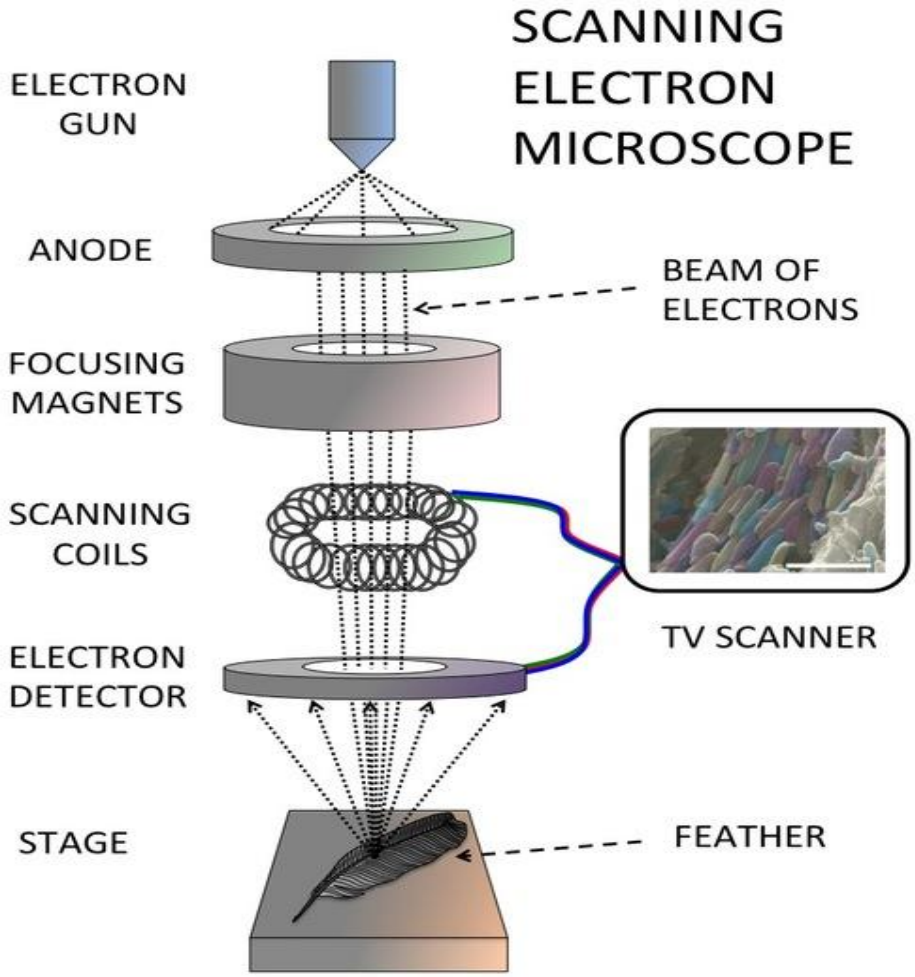

Figure 3. 5: *Schematic diagram representation the basic components of SEM. The diagram was adopted from ref [3]*

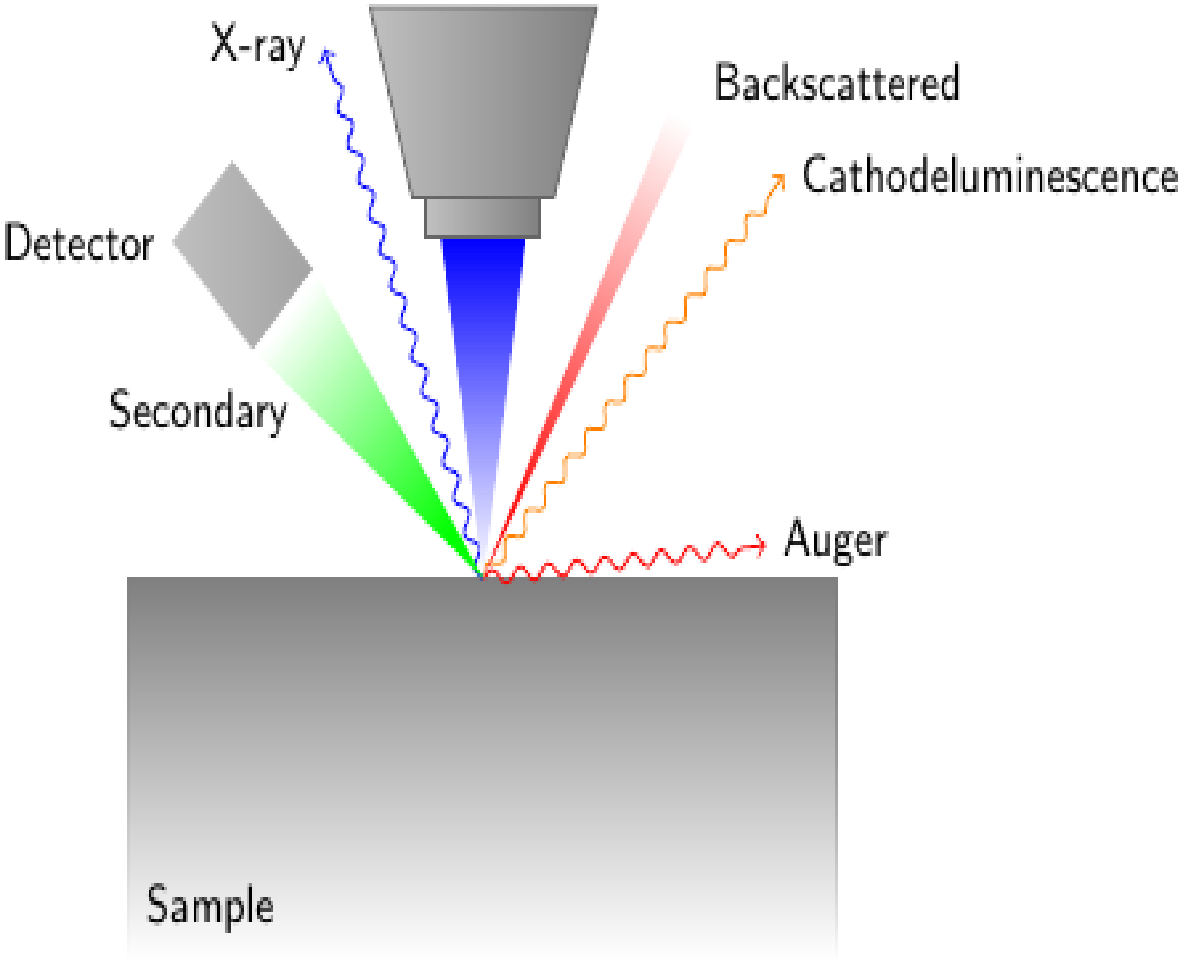

Figure 3. 6: *Schematic demonstration of the interaction of incident beam and radiation signals generated during interaction. This diagram was adopted from ref [4]*

3.3.2 Atomic Force Microscopy (AFM) technique

Atomic force microscopy is a very powerful tool which is widely used for studying the surface roughness of thin and thick films coatings. This technique can be useful for characterizing materials such as thin film coatings, ceramics, composites, glasses, synthetic and biological membranes, metals, polymers and semiconductors. In recent years AFM provides advanced tools for studying the surface topography of thin films such as 3-D image profiling and it can even be used to measure samples at the nano scale [2, 3]. Figure 3.7 shows the operation of AFM.

During the measurement the sample is placed on the electromechenical stage. In order to obtain the image of topology of the the sample, a tip is tapped across a sample surface and the change in vertical position which reflects the topography of the surface is fed back to a photo-detector. During the scanning process, the probe tip does not touch the sample because the atomic forces reflect the probe tip before a collision occurs [3, 4].

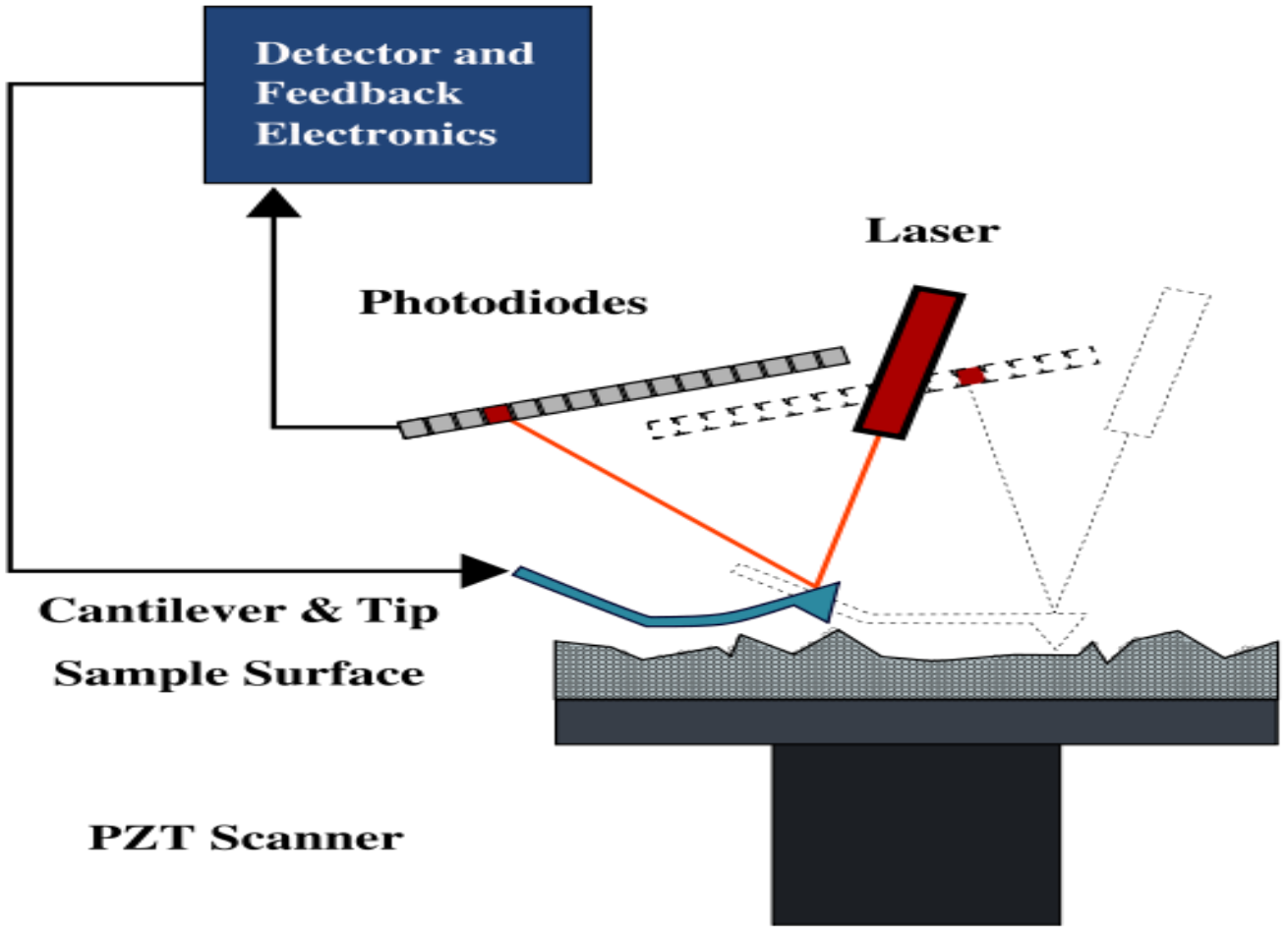

Figure 3.7: *Schematic representation of an atomic force microscopy (AFM). This diagram was adapted from ref [5]*

3.3.3 Rutherford Backscattering Spectrometry (RBS)

The Rutherford Backscattering Spectrometry (RBS) is a well-known thin film analysis technique where light ions having low energies. This technique is ideal for conducting quantitative analysis of element composition of the film thickness and depth profiling of samples. It measurements of energetic particles scattered from an ion beam incident upon the film to be analysed.

In RBS a sample is bombarded by light ions with energies ranging from 1-3 MeV which get scattered by the target samples [5]. At these low energies only elastic collision occur ,and this way nuclear reactions are avoided . A mono energetic ion beam (H^+ ,He^+ ,or He^{++}) is directed to the samples and then a solid state detector is used to analyzer the backscattered particles. We will use the resonance Energy Dispersive X-Rays (EDX) to check how much oxygen and nitrogen in the diamond films.

The Figure 3.9 represents the Rutherford backscattering can be described as an elastic collision between high kinetic energy particle from the incident beam and a stationary particle of the target material. Since it is an elastic collision, we can assume the conservation laws of momentum and kinetic energy, such that the energy E_1 of the scattered projectile can be given the formula as follows:

$$\frac{E_1}{E_0} = K = \left[\frac{m\cos\theta + (M^2 - m^2\sin^2\theta)^{1/2}}{m+M} \right]^2 \qquad \textbf{Equation 3.1}$$

The ratio K is also called kinematic factor. Particle 1 is the incident ion of energy E_0, particle 2 is the target nucleus while θ_1 and θ_2 represent the backscattered angles of the particles relative to the incident trajectory.

The analysis of RBS depends on the energy, angle and particle mass region in which the scattering is expected to take place. There are two major important aspects of RBS:

Kinematics of the elastic collision and Elastic scattering cross section.

The energy of the scattered particle can be deduced easily if the kinematic factor K is known hence the inelastic scattered ions can be separated. Indeed, the above equation does give us information about the energies of the scattered particles; however it does not tell us anything about the angular distribution of the backscattering probability. To determine this probability, we need to know the differential cross-section of the backscattering:

$$\frac{d\omega}{d\Omega} = \left(\frac{z_1 z_2 e^2}{4E_0} \right)^2 \frac{1}{(\sin\theta_1 / 2)^4} \qquad \textbf{Equation 3. 2}$$

where Z_1 and Z_2 represent the atomic numbers of the incident particle and target nuclei respectively. The amount of energy lost when the particles penetrate the surface of a sample depends on the following: the type of atom which the alpha particle scatter on, the scattering angle and the distance that the particles have to travel before scattering.

The large- angle scattering occurs as a result of ions scattering from the target nuclei while scattering from the sample electrons results in inelastic small angle scattering hence resulting to a decreased number of deep penetrating ions such that backscattering from interior nuclei occurs with a lower “effective “ incident energy . The amount of energy lost by the ion as it traverses a certain distance within the sample material refers to the stopping power of the material and is dependent on electron distribution and is given by:

$$S(E) = -\frac{dE}{dx} \qquad \textbf{Equation 3. 3}$$

For high energy ions the stopping power is proportional to $\frac{Z^2}{E}$

In Figure 3.8 x-rays are produced as a result of ionization of an atom when an inner shell electron has been removed by the incident electrons. When an ionized atom returns from its excited state to its ground state, an electron from a higher energy outer shell fills the vacant inner shell and then releases an amount of energy equal to the potential energy difference between the two shells [8]. When particles are implanted onto a surface of a material they lose energy due to collisions (see Figure 3.9) [9].

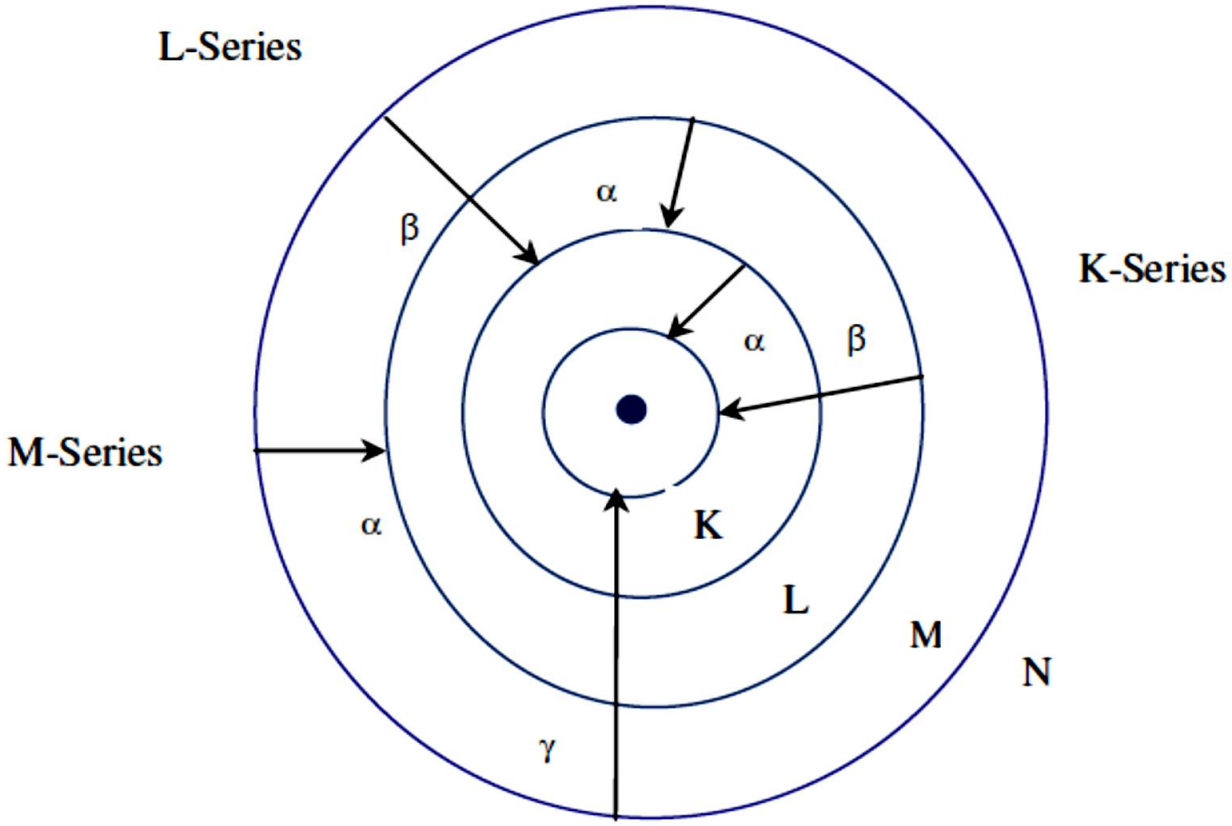

Figure 3. 8: *A schematic diagram of Atomic Energy Levels with K, L and M-shells. This diagram was adapted from ref [8]*

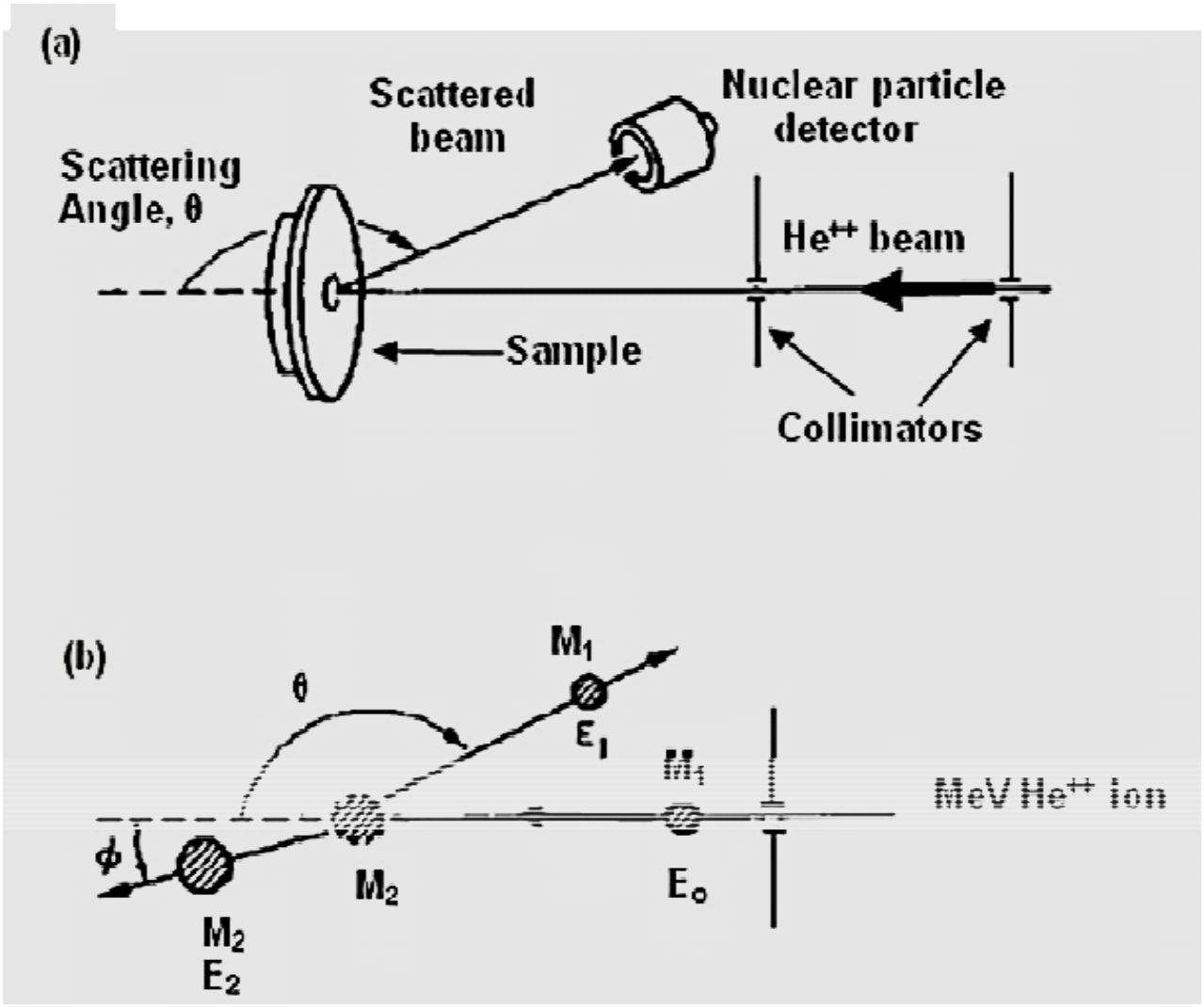

Figure 3. 9: *Experimental setup for RBS technique in (a). A beam of 2 MeV ions is directed to a sample. Particles scattered by target atoms are detected by a nuclear particle detector, (b) Schematic showing elastic collision between nucleus of incident atoms and nucleus of target atoms [9].*

3.3.4 Raman spectroscopy

Raman spectroscopy offers very detailed sample characterisation by probing individual chemical bond vibration, as a result a Raman spectrum is rich and contains data relating to the specific chemical structure of the samples being analysed. Raman spectroscopy is a very fast technique typically requiring just a few seconds to obtain a good quality spectrum. The Raman spectrum of DLC films excited by visible light is usually composed of two bands, the D and G bands [10].

The shape of the spectra varies with substrate material composition. The position of D and G peak can be shifted due to film structure, light source of Raman spectroscopy, Gaussian fitting method. The D band (which is around 1332 cm^{-1}) correspond to breathing mode of sp^2 atoms in hexagonal ring formed by graphite structure, which means the disorder of bond angle resulting due to disappearance of the long range translation symmetry of polycrystalline graphite and amorphous carbon films, while G peak is around 1588 cm^{-1} is related to c-c bond stretching vibration of all pairs of sp^2 atoms in both ring and chains of graphite layer for single crystalline graphite structure [10-11]

Experiments on deposition of DLC have been conducted and a number of samples were made. These samples were then characterized with Raman spectroscopy at University of Pretoria to investigate their bonding whether predominantly sp^3 or sp^2. Results from the Raman spectroscopy showed that some of these samples were DLC in nature whiles others were not. From these results new samples have been synthesized with slight adjustment of parameters to optimize the chances of obtaining DLC thin film. [15, 18] as can be seen in Figure 3.10.

Raman spectroscopy is a complementary technique to infrared absorption. It gives information about vibration and rotational transition in molecules. When light is scattered from a molecule most photons are elastically scattered. The scattered photons have the same energy and wavelength as the incident photons. The inelastic collision between a photon and a molecule is known as the Raman effect. The energy difference between two energy the inelastic scattered photons and the incident photons is exactly the difference between two energy levels of a molecule vibration [12].

Most of scattering proceeds elastically called Rayleigh scattering; if it is not elastic the process is Raman Effect. In 1928, Chandrasekhara Venkata Raman discovered the phenomenon now known as the Raman Effect. It is simple phenomenon where the monochromatic light is focused on the sample and scattered light is analysed for the required information. Most of vibrational states are not excited at room temperature the inelastic scattering is mostly observed with lowering the photon energy, vs - nv_i of laser energy it is called Stokes scattering. The anti –Stokes scattering with vs + nv_i, is a lower intensity which can be increased by raising the temperature because this transition originate from vibrational excited states.

A Raman spectrometer was deployed on the Viking moon landers in 1972. Raman spectroscopy has important scientific applications in studying molecular structure. The energy difference between the incident and scattered photons is represented by the arrows of different length in Figure 3.11 [10-13].

Numerically the Raman shift in wavenumber (cm^{-1}) is calculated by using equation below:

$$\Delta\omega = {}^{1}\!/\!_{\lambda_{incident}} - {}^{1}\!/\!_{\lambda_{scattered}} \qquad \textbf{Equation 3. 4}$$

Where $\Delta\omega$ is the raman shift, λ's are the wavelength in (cm) of the incident and Raman scattered photon respectively.

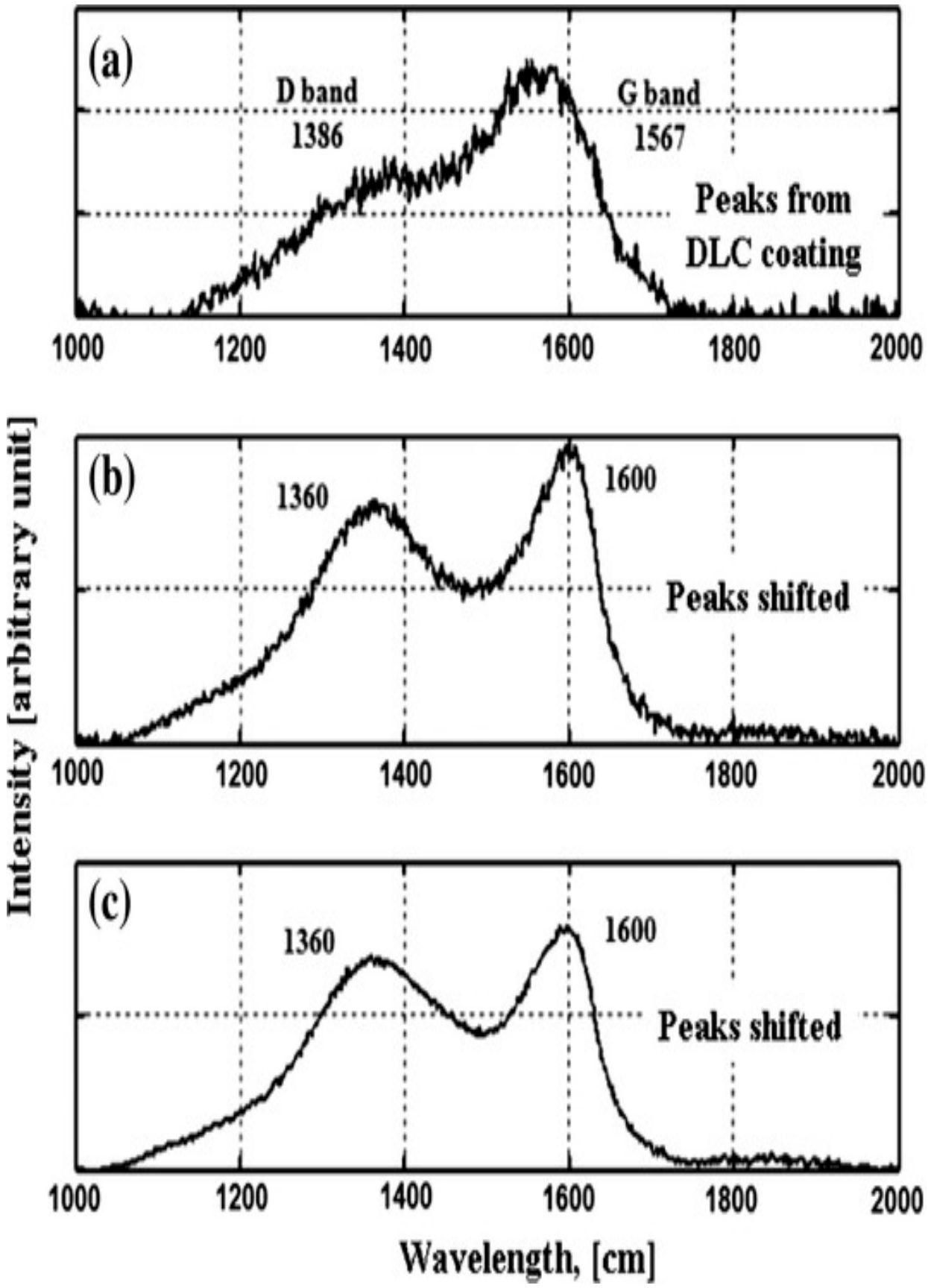

Figure 3. 10: *Spectrum of DLC Coating. This diagram was adapted from ref [18]*

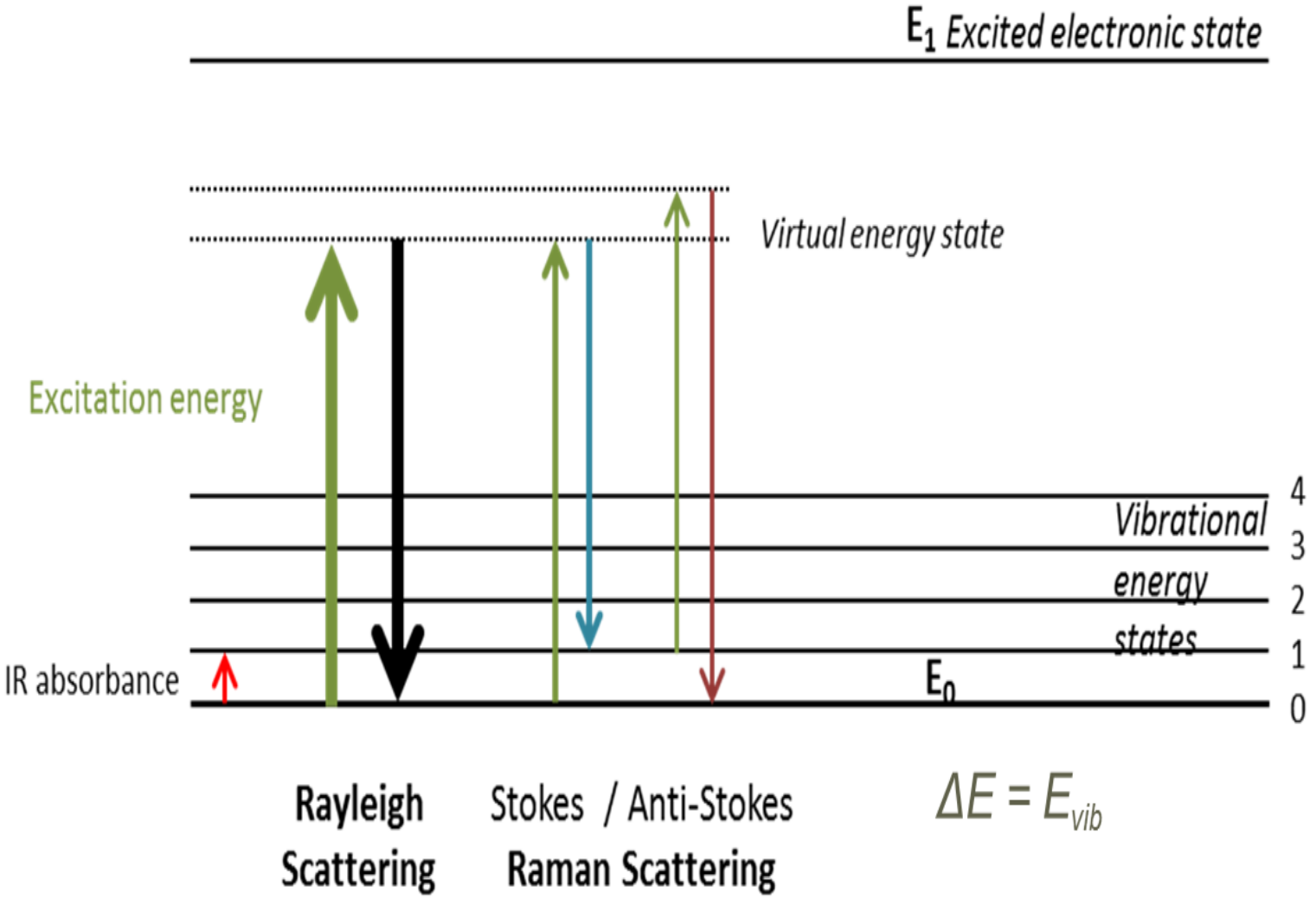

Figure 3. 11: *Energy level diagram for Raman scattering. This diagram was adapted from ref [10]*

3.3.5 X-ray diffraction technique

Figure 3.12 and Figure 3.13 represent a schematic diagram of x-ray diffractometer. The X-ray diffraction is a non-destructive analytical technique used for microstructural determination of materials by probing a sample with a beam of X-rays. The measurements are based on the diffraction of the electromagnetic waves. X-rays are electromagnetic wave of high frequency and hence small wavelength. Electrons emitted from the heated cathode by thermionic emission in vacuum are accelerated towards the target by a large potential difference V [12-13]. X-rays are produced in the X-ray tube and directed to the sample. A position sensitive detector was used to detect diffracted X-rays. In this configuration the detector and the X-ray tube move in a locked coupled mode. This mode is usually called a θ-2θ scan mode [13], the detector move angle θ for each θ the X-ray tube move while the sample is kept in a fixed position. The X-ray tube was operated at voltage of 40 kV and a current of 40 mA.

During this process, x-ray are diffracted into a direction of angle 2 θ resulting in destructive and constructive interference of the diffraction beam as shown in Figure 3.13: When a monochromatic x-ray beam with wavelength λ, on the order of lattice spacing d, is projected onto a crystalline materials at an angle θ, X-ray diffraction patterns are produced by constructive interference of monochromatic beam scattered from each set of lattice planes at a specific angles. Constructive interference gives the diffraction peaks according to Bragg's law [13- 14].

$$\mathbf{n\lambda = 2d \sin \vartheta} \qquad \textbf{Equation 3.5}$$

where n = is an integer number n = 1,2,3,…is called order of diffraction

d= is the distance between atomic planes

λ= is the wavelength of the incident x-rays

A lattice constant for cubic systems can be calculated by using equation 3.6:

$$\frac{1}{d^2} = \frac{h^2 + k^2 + l^2}{a^2} \qquad \textbf{Equation 3. 6}$$

where a is the lattice constant h,k,l - are crystal planes

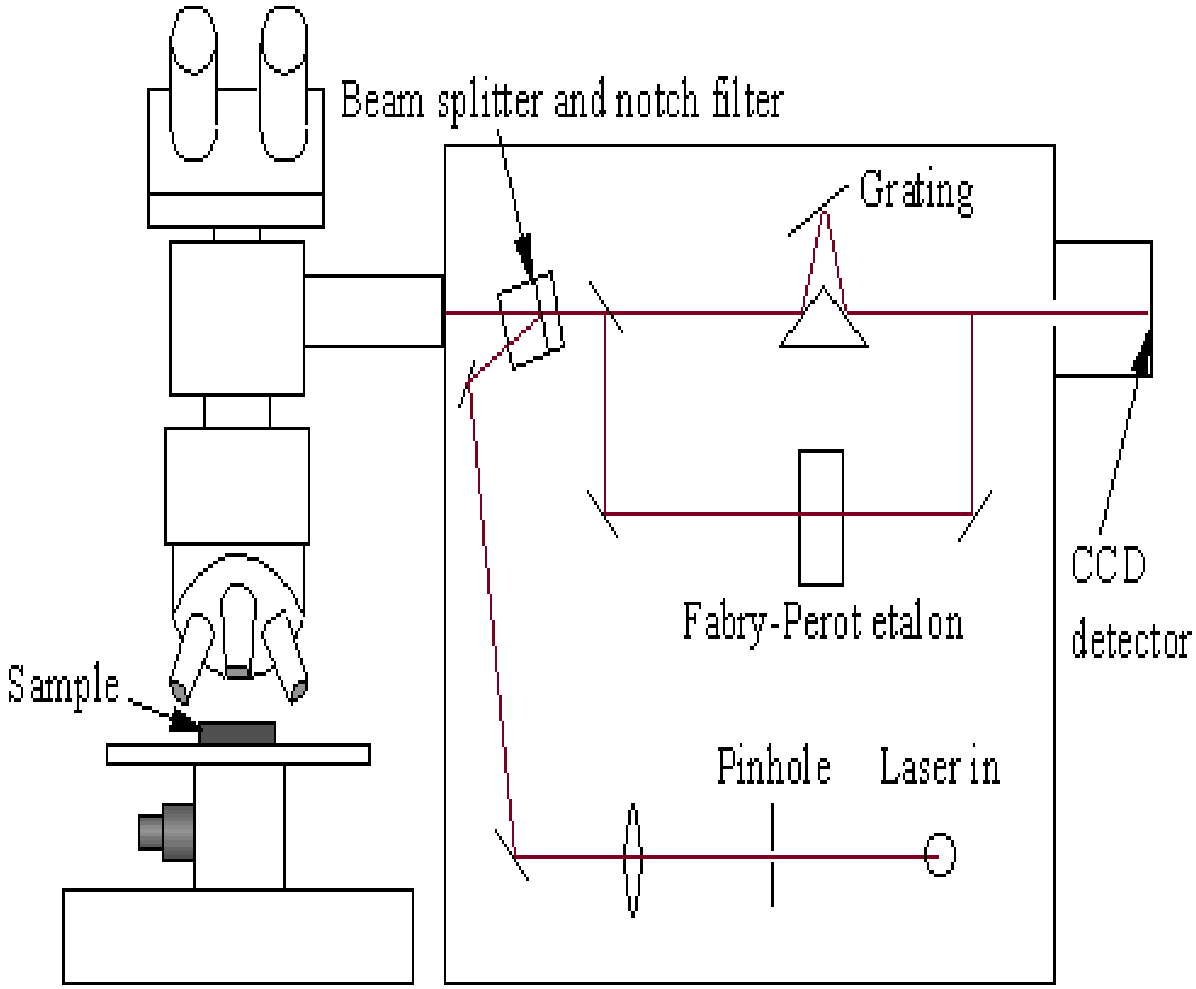

Figure 3. 12: *Schematic diagram of a Raman spectrometer adapted from ref [15]*

1

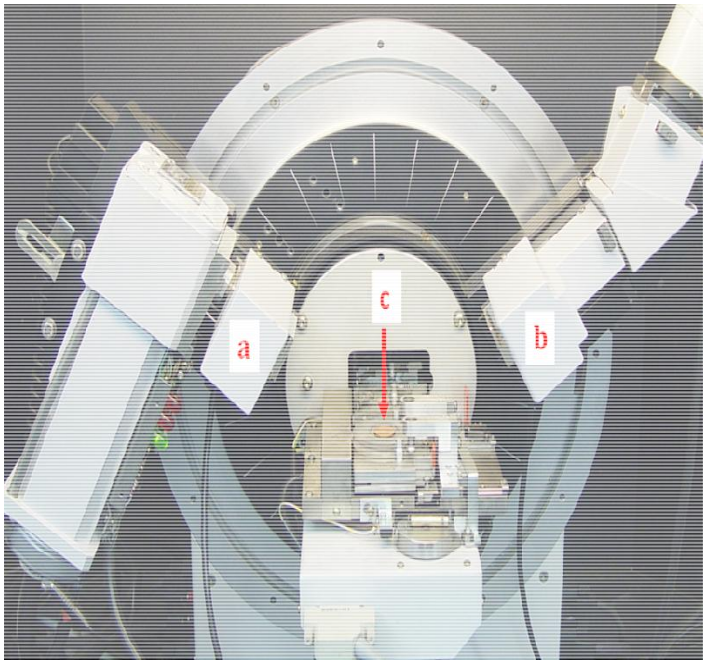

2

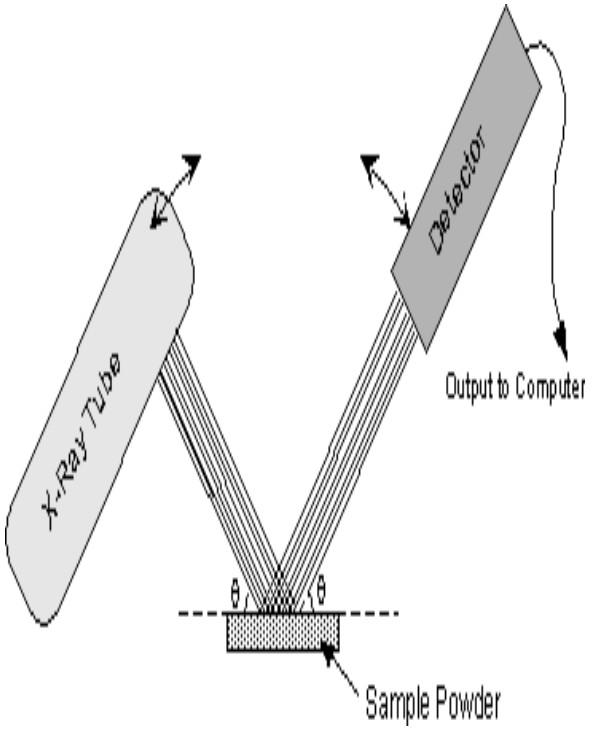

Figure 3. 13: *(1) Bruker Advance 8 X-ray diffractometer at iThemba LABS. (a) X-ray tube, (b) Detector, (c) Sample stage. (2) Schematic diagram showing the setup of XRD technique as adopted from ref [16]*

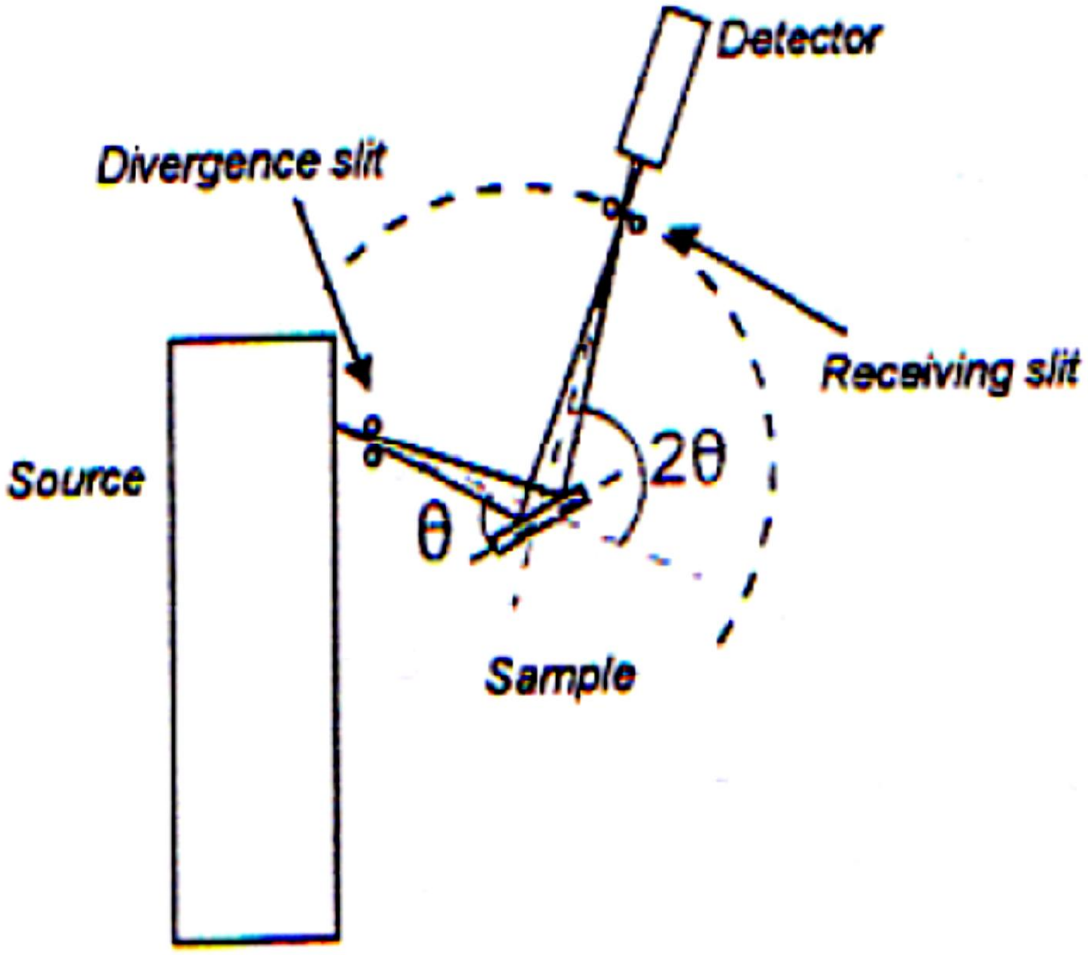

Figure 3. 14: *A schematic showing specular reflection of two parallel X-rays after interaction with atoms in a sample as adapted from ref [17]*

3.4 References

[1] Liu. D, Zhang .S, Ong S.E, Bensetter .G, Du .H, *Surface and electron emission properties of hydrogen- free diamond-like carbon films investigated by atomic force microscopy*.Mat.Sci.Eng.A-Struct.,426 (2006) 114-120

[2] Voutou B.,. Stefanaki. E.C, Giannakopoulos K.. *Electron microscopy: the basics*. Surface and Coating Technology; 133-134 (2008) 183 – 179.

[3] [www 1] http://en.wikipedia.org sighted (25/06/2010).

[4] [www2] http://www.ijs.si/ctp/ktrdeprevlekeA.html-12 sighted (30/06/2010).

[5] http://en.wikipedia.org/wiki/Atomic_force_microscopy sighted (26/07/2010)

[6] http://www.sv.vt.edu/classes/MSE2094_NoteBook/96ClassProj/experimental/optica.html(27/07/2010)

[7] Hussain .S, Investigation of Structural and Optical Properties of Nanocrystalline Zn, MSc. Thesis. (04 November 2009)

[8] Goodhew .P.J,Humpreys.T, Branland.R, Electron Microscopy and analysis Third Edition. 122-166 (Taylor & Francis Group, Jan 2001)

[9] Chu W.K, Mayer.J.W,Nicolet.M.A, Backscattering Spectroscopy, (ACADEMICS PRESSS,New York,1978) 1-48

[10] http://en.wikipedia.org/wiki/Raman-spectroscopy (2010)

[11] Dresselhaus.M.S, Dresselhaus.G, Saito.R, Jorio. A. *Raman spectroscopy of carbon nanotubes.* Physics Reports 409 (2005) 47 – 99.

[12] Kumamoto.A, Ono.R, Oda. T. *Raman spectroscopy of molecule density in hydrogen-Air mixture premixed gas ignited by spark discharge.* Proc. 2012 Joint Electrostatics Conference

[13] Ferrari A.C and Robertson .J, *Interpretation of Raman spectra disordered and amorphous carbon. Physical.Review B* (2000), 61(20)91-107.

[14] Müller, U.; Falub, C.V.; Thorwarth, G.; Voisard, C.; Hauert, R. *Diamond-like carbon Coatings on a CoCrMo implant alloy: A detailed XPS analysis of the chemical states at the interface*. Acta Mater. *59 (*2011) 1150–1161.

[15] www.chm.bris.ac.uk/pt/diamond/stuthesis/chapter2.htm (2010)

[16] Haberkorn R and Bruker *Analytical X-ray Systems, Introduction to Powder X-ray Diffraction*, Bruker AXS 21 (1999) 1-56

[17] http://epswww.unm.edu/xrd/xrdclass/01-XRD-Intro.pdf (2010)

[18] Robertson J, *Deposition and properties of diamond-like carbon. Material Research Society Symposium Proceedings*. 555, (1999) 12-14.

CHAPTER 4: SYNTHESIS AND CHARACTERISATION OF DLC THIN FILMS

4.1 Sample preparation for DLC thin films

Sputtering is a useful method for depositing a wide range of thin films. It provides good control over film properties, such as thickness, uniformity over a wider area compared to e-beam evaporation (for example). It is also possible to form ceramics and even to sputter coat in an oxygen environment to form a metal oxide. Results from sputtering are fairly reproducible if one does not change sputtering parameters. Deposition of all samples was done on Si <100> substrates. Substrates in which DLC coatings were to be deposited were subjected to chemical cleaning using high grade chemical solutions. Chemical solutions were used in the following order:

- Methanol
- Acetone
- Trichloroethylene
- Acetone
- Methanol
- De-ionized water

All beakers were rinsed clean using the above chemicals in an ultrasonic bath followed by cleaning of the substrates which were then dried using dry nitrogen gas and then loaded into the main chamber of a sputtering system. The chamber was first evacuated to about $2x10^{-7}$ Torr, pre-heated to 800 ^{o}C each time and then cooled to room temperature in order to drive out any moisture and contaminants before loading any samples.

Figure 4.1 is the image of the sputtering machine used during the deposition, AJA's ORION-5 magnetron sputtering that has three magnetrons, each of which has a holder for a sputtering target. DC magnetron sputtering was used to deposit DLC thin films onto the surface of < 100 > silicon wafers. This machine is available at the University of Zululand Solid State Laboratory.

A cylindrical piece of carbon (99.99% pure) with a thickness of 6.35 mm and diameter of 50.8 mm was used as a target material. The target to the substrate distance was maintained at 36 cm while varying the gas flow rate. When desired the samples were annealed either in nitrogen (N_2) or oxygen (O_2) in order to dope them, Magnetron power was changed from 50 W to 200 W, bias voltage between 100 V to 300 V), substrate temperature between 100 ^{o}C to 500 ^{0}C, and the deposition time from 2 hrs to 3 hrs.

Figure 4.1 presents the image of the AJA's ORION-S magnetron sputtering machine used in the deposition that has three shutters labelled 1, 2 and 3 are on top of chimneys that house magnetrons. It is possible with this machine to do balanced magnetron depositions from a DC power supply suitable for depositing metals, unbalanced magnetron deposition from a DC power supply for depositing magnetic materials, and RF magnetron for depositing ceramics.

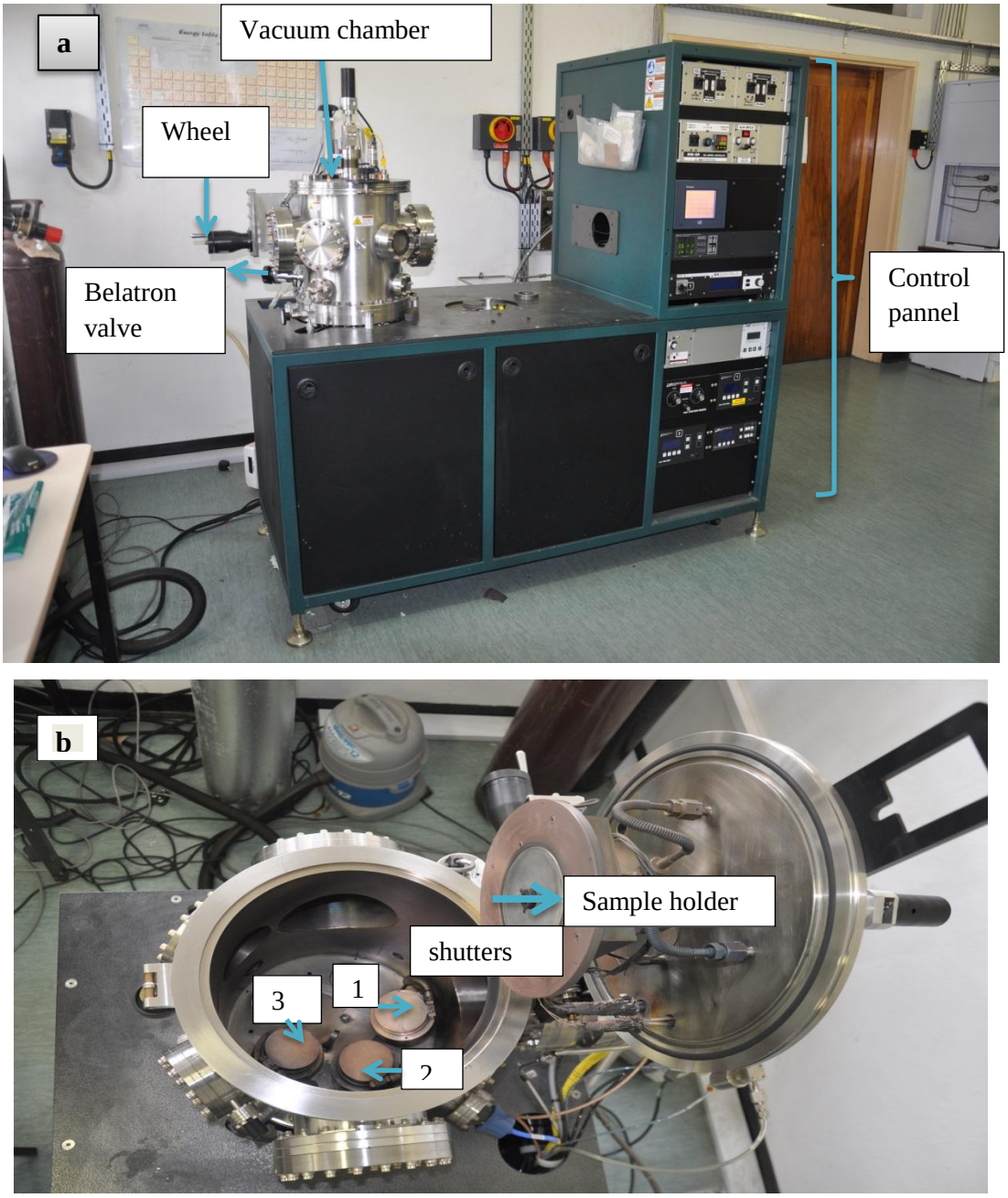

Figure 4. 1: *An AJA Orion 5 Sputtering System at University of Zululand showing various parts referred to in the text.*

4.3 Deposition of DLC thin films

DLC thin films were successfully deposited on silicon substrates and then characterised using various methods. DLC thin films can be synthesized in different ways but in this study we chose to use DC magnetron sputtering deposition method. It was used because of its simplicity and its sample reproducibility.

The following parameters were used during the deposition of DLC thin films under different conditions using the sputtering machine. In all cases a graphite target was used.

- Substrates : Si wafer < 100 > , aluminium strip and glass substrate
- Varied temperature between 100°C to 300°C.
- Pressure was kept at $3x10^{-3}$ Torr for all depositions.
- Varied power between 100 W to 300 W.
- Argon flow rate between 2 sccm to 8 sccm.
- Rate of deposition 2 hrs to 3 hrs.

The solid target material (graphite in our case) is a source of atoms that are sputtered off the cathode and then deposited on top of the substrate (silicon wafer). The electric field was used in order to increase the sp^3/sp^2 ratio by applying a voltage between the target and the substrate. The target and the substrate are placed in a vacuum chamber during deposition process [1].

4.4 Characterization of DLC Thin Films

4.4.1 SEM analysis of DLC thin Films

All SEM micrographs show that DLC films deposited under different experimental conditions have smooth featureless surfaces (see Figure 4.2). The following parameters were used: Temperature 200°C, power 150W, pressure $3x10^{-3}$ Torr, voltage 120 V , duration 2 hrs and argon flow rate 8 sccm. Image **(a)** in Figure 4.2 represents a DLC film deposited from a carbon target, **(b)** deposited from a carbon target but where the substrate had been placed inside a faraday cage and an electric field applied between target and substrate **(c)** where the deposition was from a carbon target and an electric field (voltage) applied between target and substrate. The reason for applying a voltage between target and substrate is to increase the speed of the carbon atoms impinging on the substrate. The speculation is that higher energy impacts will increase sp^3 bonding in the DLC film (as compared to sp^2 bonding). Figure 4.2(a) (b) and (c) present the SEM results for DLC thin films which were deposited on Si substrate using same parameters listed and deposition was done on different conditions as listed. It then concluded that the DLC films are fairly smooth and uniform in all conditions.

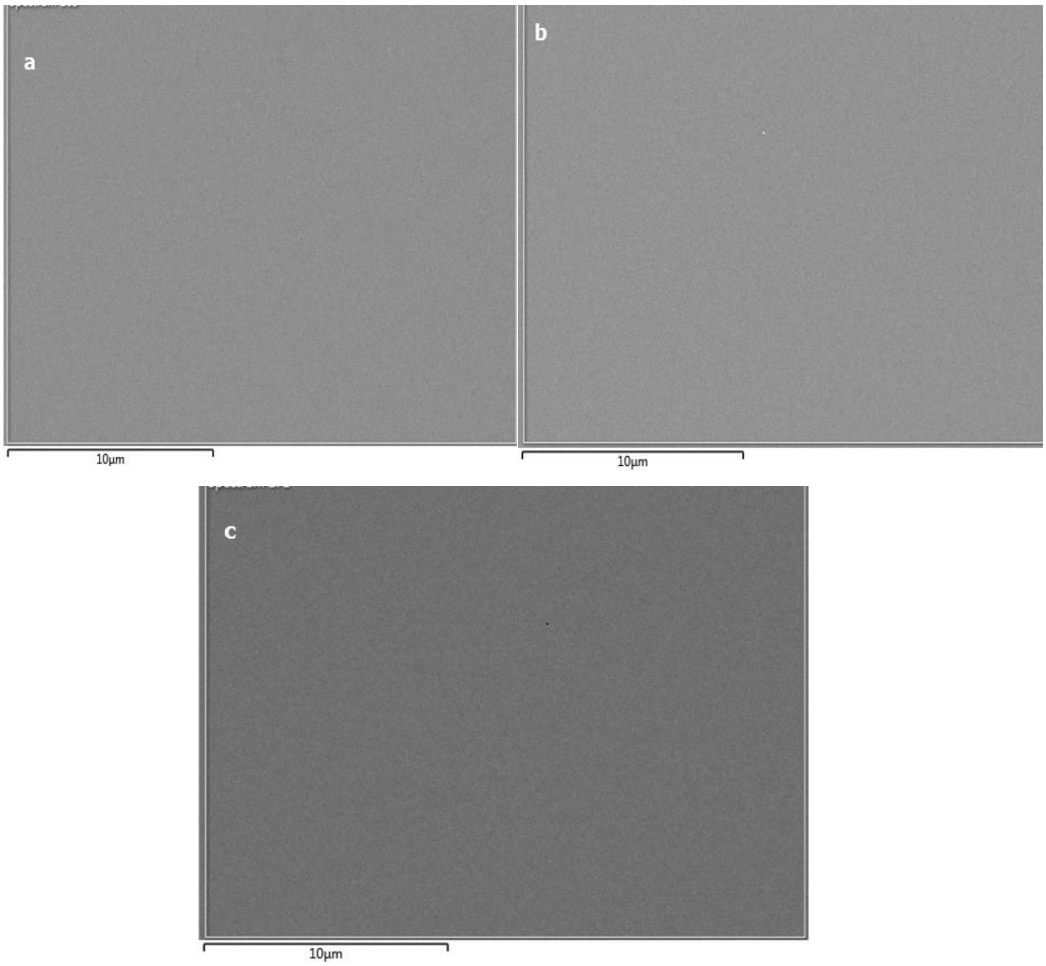

Figure 4. 2: *The SEM results of DLC films obtained from the sample deposited on Si substrate*

4.4.2 XRD analysis of DLC Thin Films

The X-ray diffraction patterns of the samples were obtained from a Bruker D8 Advance X-ray diffractometer using a Cu Kα (λ = 1.54 Å) radiation source. The measurements were extracted at the voltage of 40.0 kV and the current of 40.0 mA. The data was obtained in the Bragg-Brentano geometry as from 2Θ = 20° to 60° with a step size of 0.0134° for all samples. Figure 4.3 represents the XRD results of a DLC film grown on Si substrate and that is why we also see some signal from Si. There is a pronounced peak pattern appearing at 2Θ = 47.9° which does not belong to silicon. This peak is a signature of DLC. Therefore DLC was successfully deposited on an Si substrate.

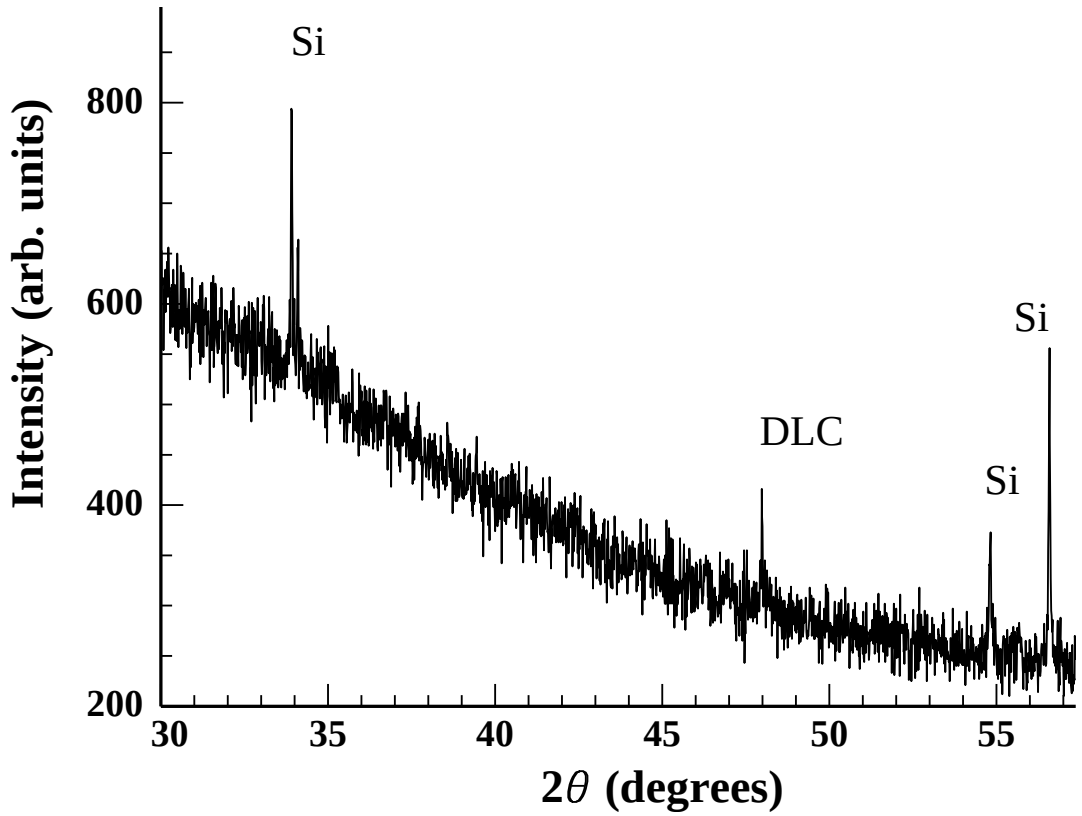

Figure 4. 3: *The XRD patterns of a sample obtained under a voltage bias of 120 V, magnetron power of 150W for a period of 2hrs. A peak belonging to DLC is seen at 47.9^o and 28.4^o belonging to Si values of 2θ.*

4.4.3 AFM analysis of DLC Thin Films

The surface roughness of DLC films were analysed using an Atomic Force Microscope (AFM). Figure 4.4 shows an AFM image of DLC films in two dimensional (2D) and three dimensional (3D) views.

The AFM analysis is presented in Figure 4.5. It has been estimated that the mean surface roughness (R_a) and maximum peak-to-valley height (R_{max}) of the DLC films is 0.292- 3.2 nm. It can then be concluded that DLC films produced using sputtering are fairly smooth and uniform. The results are shown in Figure 4.4 - 4.5.

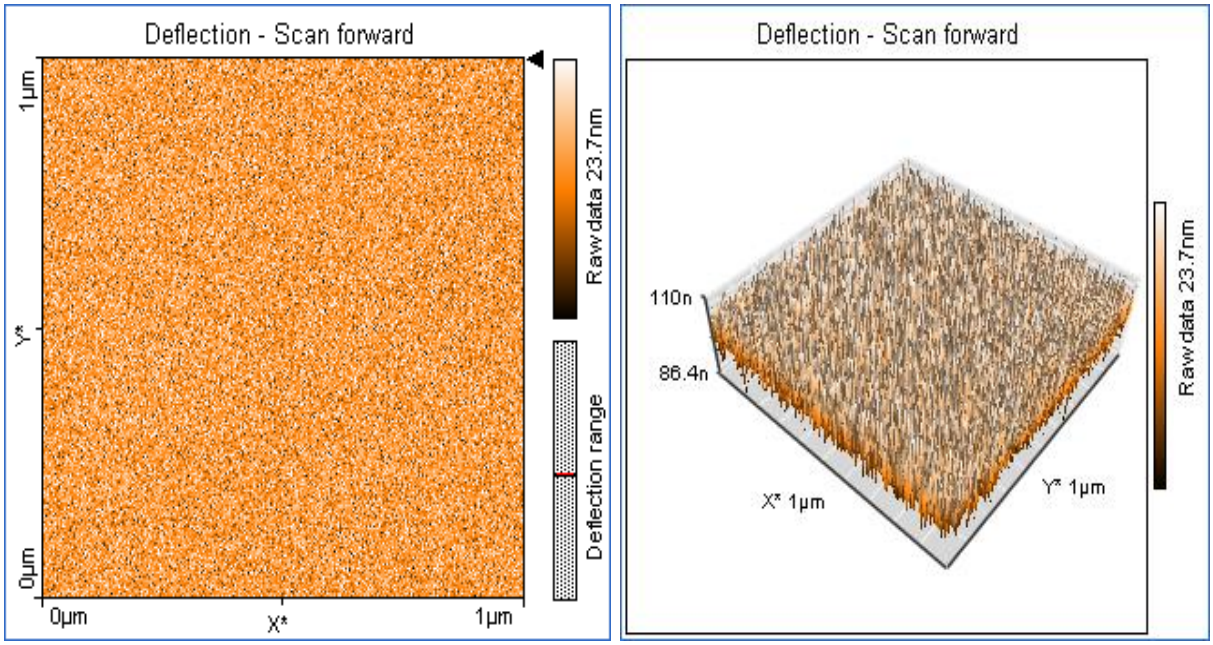

Figure 4. 4: *AFM images of DLC films deposited on Si substrates by using carbon graphite 2D view is on the left and 3D is on the right @ temperature of 200°C, power*

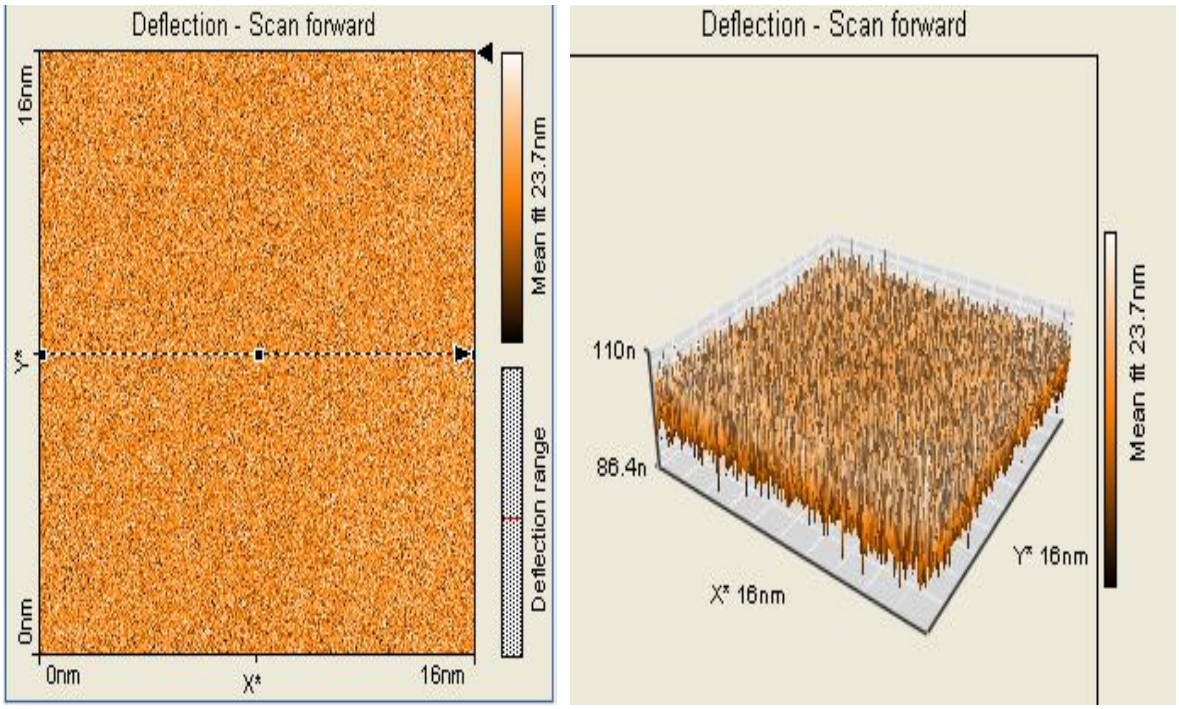

Figure 4.5 ***:*** *AFM results of DLC film 2D and 3D image @ 16nm deposited on faraday cage at temperature of 200°C, Power 150 W, The chamber pressure was kept at* $3x10^{-3}$ *Torr, Argon flow rate 8sccm deposition time 2hrs.*

4.4.4 Raman analysis of DLC Thin Films

The Raman spectra of Diamond –Like Carbon films are shown in Figure 4.6. It represents multi-peak Raman spectra from different DLC films deposited on silicon substrates under various conditions. There are two Raman peaks named D and G which are characteristic of the DLC films. Figure 4.7 to Figure 4.10 show the Raman spectra fitted with a Gaussian D and G peaks. The position of D and G peak are shifted to larger wavenumbers due to the degradation of the film because of laser heat [3-4]. The D peak belong to sp^3 hybridized carbon and a larger more prominent D peak shows that a film is of higher quality (i.e. more diamond like and less graphite like). The fitted data is shown in Figures 4.7-4.10 as well as in Table 4.1- 4.5 respectively. The target used during the sputtering to make DLC films was graphite. Argon was used as a sputtering gas with a flow rate of 8 sccm, deposition time was 2 hrs, magnetron power 150 W, temperature 200°C and the voltage of 120 V.

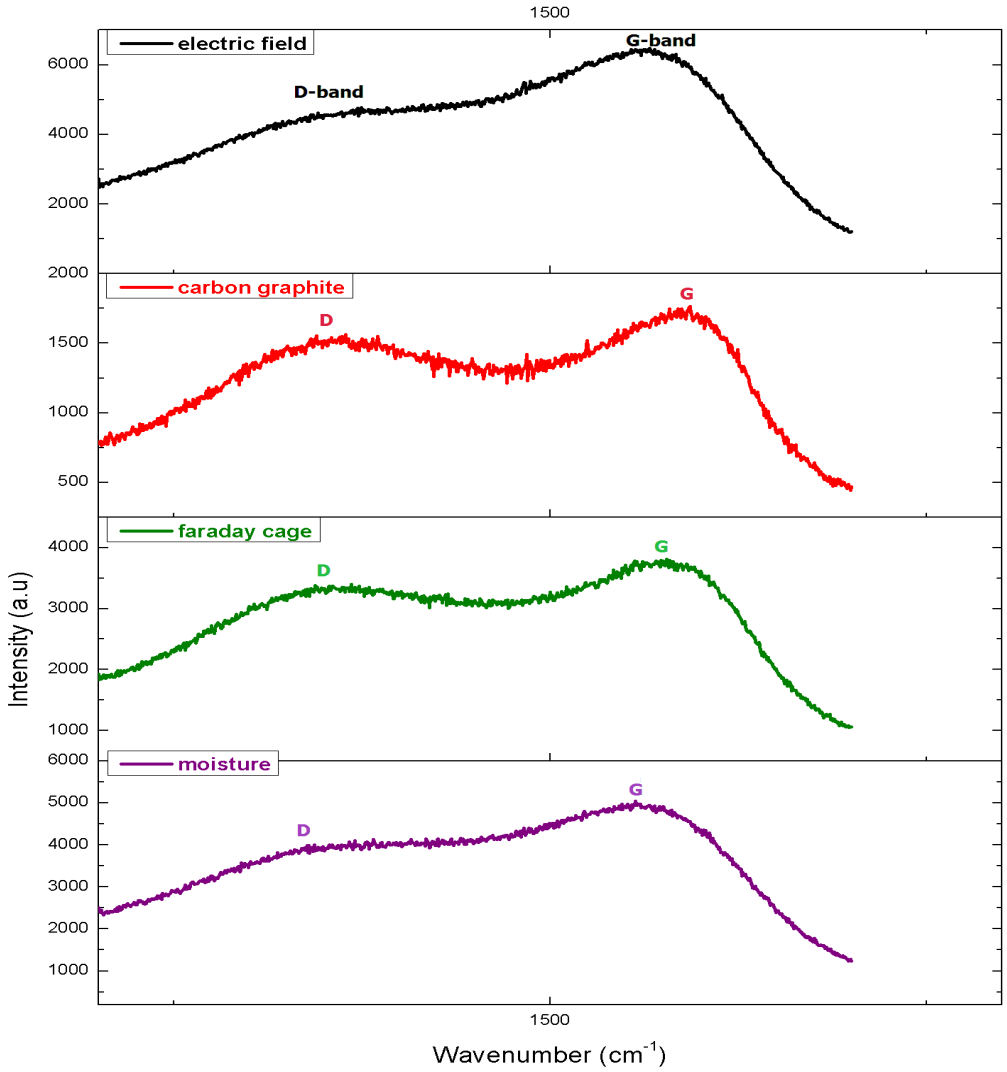

Figure 4. 6: *Shows Raman multipeak results for samples prepared using various approaches. The D peak which is sp^3 (diamond) is found at a Raman shift of 1332cm^{-1}while the G peak which is sp^2 (graphite) is at 1588 cm^{-1}*

The spectra in Figure 4.7 to Figure 4.10 show different peaks when fitting Raman results for different samples. The sample names are as follows: **A, B**, **C** and **D**.

Moisture **(A) -** the spectrum in figure 4.6, labelled 'moisture' was prepared within a chamber that had moisture. It shows that peaks belonging to both sp^2 and sp^3 bonded carbon are negligible. The spectrum is for a sample prepared by using moisture in order to reduce the unbounded carbon atoms in diamond like carbon. This method has been used successfully in the past during Carbon Nanotube preparation to reduce unbound carbon. It was used here expecting a similar result. Visual inspection of the film showed that very little material had been deposited. We therefore cannot conclude whether the use of moisture during the growth of DLC films is helpful. The sp^3/sp^2 ratio found is 0.2.

Faraday cage **(B)** - the purpose of using faraday cage is to check whether it has an effect on the sp^3/sp^2 ratio. Our experience on growing CNTs shows that an electric field encourages sp^2 hybridization of carbon. Our thinking is that sp^3 hybridization is encouraged in an electric field free environment. We however want higher impacts of carbon atoms onto the substrate to bring carbon atoms closer to form diamond-like bonds. The trick therefore is to apply a voltage between target and substrate that accelerates the carbon atoms. We however place the substrate within a metal grill (Faraday cage) to prevent the existence of a field on the substrate. Orbital re-configuration happens within femtoseconds. A carbon atom travel from target to substrate might be in an sp^2 configuration while within a field but should relax in the short distance as it enters an electric field free region. The sp^3/sp^2 ratio for this sample was found to be 3.2 which means it is of better quality when compared to samples prepared using other methods(except for the one where a voltage is used). Our Group is the first to devise this method.

Plain samples **(C)** - these samples were prepared using a graphite target. No voltage was applied between target and substrate. The sp^3/sp^2 ratio was found to be 0.04.

Electric field **(D)** - the spectrum in figure 4.6 is for a sample prepared by using a bias voltage of 120V. The sp^3/sp^2 ratio for this sample was found to be 0.7. This is the highest ratio obtained. We however think that film thicknesses between this case and the one where both a voltage bias and a Faraday cage are used differ, with the one where a cage is used being lower due to film thicknesses. This will happen because some of the sputtered carbon will land on the cage itself.

For all samples which is shown in Figure 4.6 magnetron power used was 150 W, argon flow rate 8 sccm and the pressure within the chamber was kept at $3x10^{-3}$ Torr, temperature 200° C and deposition time was 2 hrs. It was observed that the ratio of areas under the curve for sample A and C are both small. In sample D where we deposited the DLC films by applying a voltage between target and substrate during sputtering in order to increase the sp^3/sp^2 ratio, the ratio was found to be 5.4. It is therefore higher than for a sample where there was no voltage bias. Voltage bias therefore helps to increase the sp3/sp2 ratio. Sample B where the deposition of film was done by using faraday cage, the sp^3/sp^2 ratio increased to 0.9.

***Table 4.1**: Representative Raman results for DLC samples deposited on Si wafer from a carbon target. No voltage was applied between target and substrate, the substrate was not within a cage and no moisture was let into the system during deposition. The ration under the D and G curves was found to be 3.2.*

Sample name	*Position (Xc)*	*Width (w)*	*Area (A)*	*FWHM*	*Height (H)*	*Band (D or G)*
C	1589. 6	109.27	16119.4	256.19	1177.7	D
	1372.7	261.73	430220.56	276.65	1311.5	G

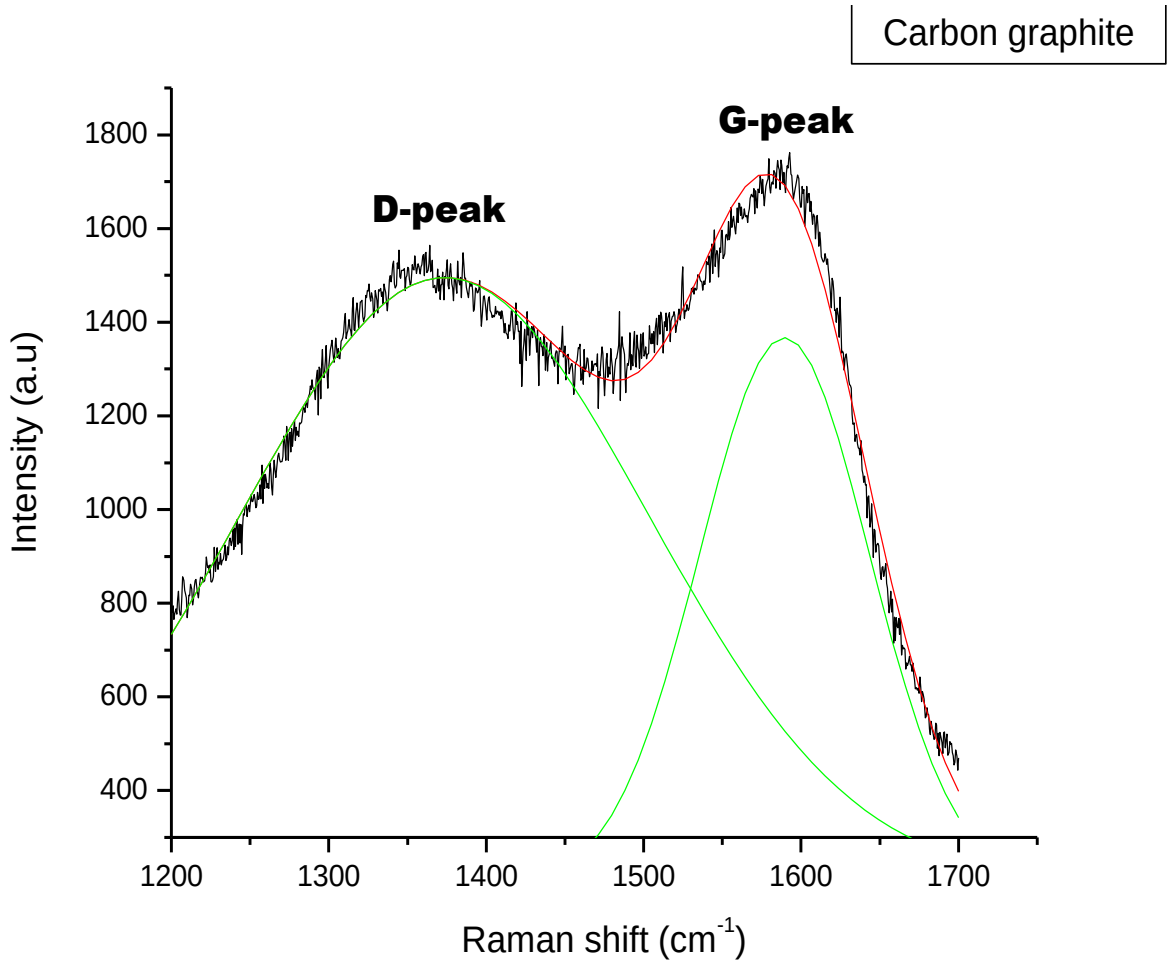

Figure 4. 7: *The Raman spectra shows the dependencies of the peak position (Xc), the full width at half maximum (FWHM) and the area (A). All peak positions move toward higher wavelengths. We used the areas under the curves to calculate the ration D/G or sp^3/sp^2.*

***Table 4. 2*:** *Representative Raman results for DLC samples deposited on Si wafers under a voltage bias.*

Sample name	*Position (Xc)*	*Width (w)*	*Area (A)*	*FWHM*	*Height (H)*	*Band (D or G)*
D	1575.4	116.8	$3.489x10^5$	363.09	2383.6	G
	1394.4	366.4	$1.89x10^6$	392.26	4126.6	D

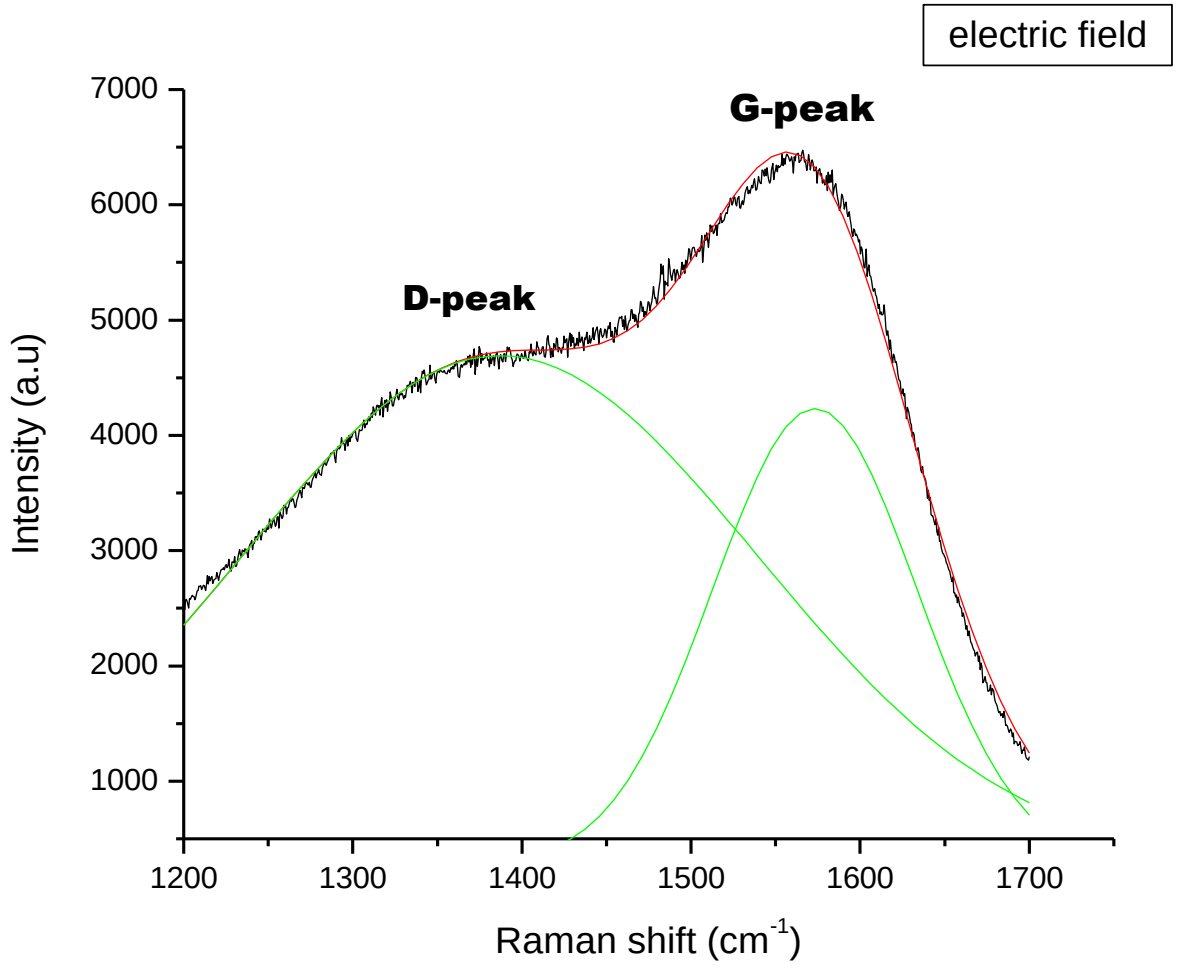

Figure 4. 8: *The Raman spectra shows the dependencies of the peak position (X_c), the full width at half maximum (FWHM) and the area (A) under the curve. All peak positions move towards higher wavelengths. The G-peak position shows a small increase in intensity while D-peak shifted to higher wavelengths. This Raman spectrum is that of a DLC films deposited under a voltage bias of 120V.*

***Table 4. 3*:** *Representative Raman results for DLC samples deposited on Si wafer using a faraday cage.*

Sample name	*Position (Xc)*	*Width (w)*	*Area (A)*	*FWHM*	*Height (H)*	*Band (D or G)*
B	1585.8	112.64	323894.06	264.73	5197.42	G
	1376.8	282.48	1022096.13	264.19	2264.33	D

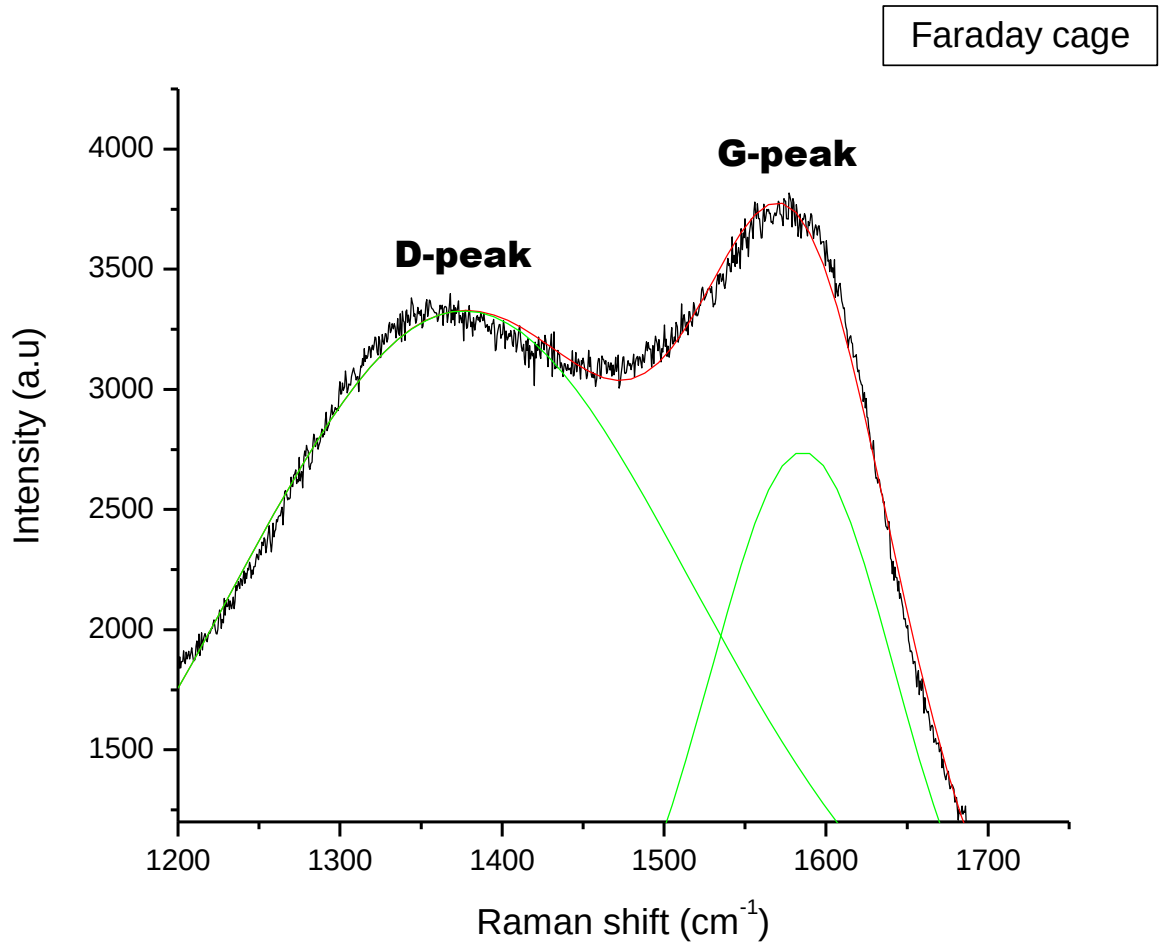

Figure 4. 9: *The Raman spectra show dependencies of the peak positions (Xc), the full width half maximum (FWHM) and the area (A). All peak positions move toward higher wavelengths. The G-peak position shows small increase intensity while D-peak shifted to high wavelength. Raman represent of the DLC films deposited using a faraday cage.*

Table 4. 4*: Representative Raman results for DLC samples deposited on Si wafer under moisture*

Sample name	*Position (Xc)*	*Width (w)*	*Area (A)*	*FWHM*	*Height (H)*	*Band (D or G)*
A	1585	112.64	323894	1319.9	83807.25	G
	1377	282.48	1022096	340.8	2981.87	D

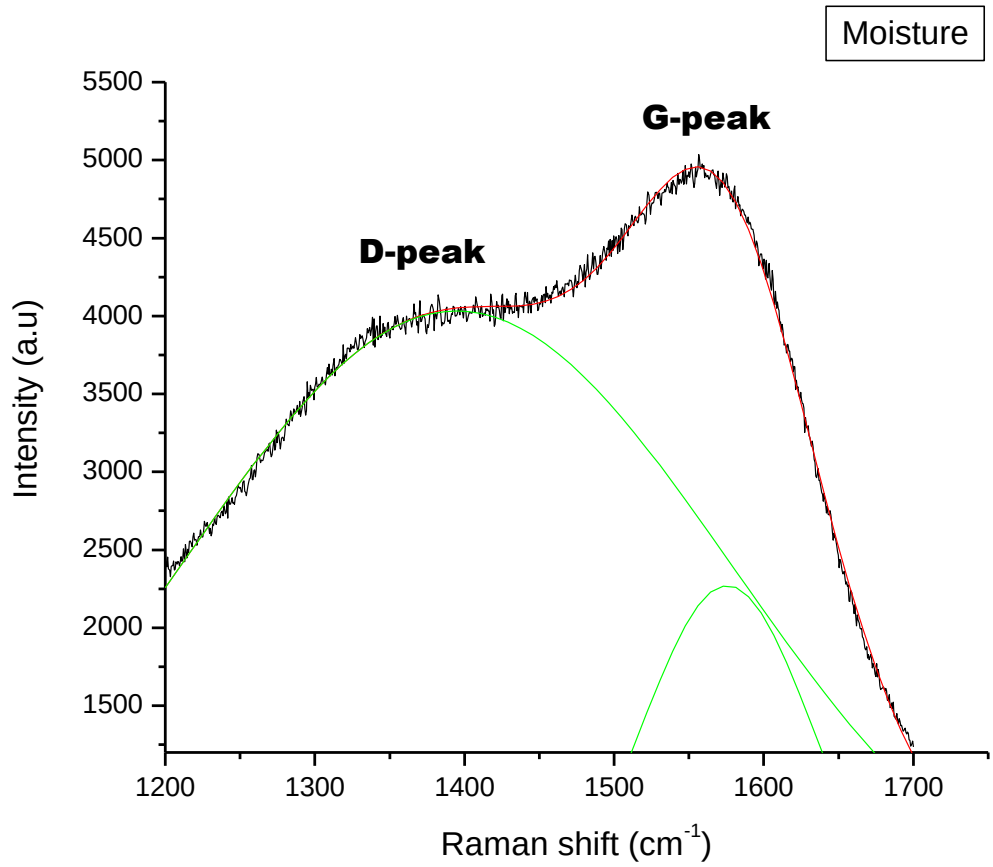

Figure 4. 10: *The Raman spectra shows the dependencies of the peak position (Xc), the full width half maximum (FWHM) and the area (A). All peak positions move toward higher wavelength. The G-peak position shows slight increase intensity while D-peak shifted to high wavelength. Raman represent of the DLC films deposited under moisture.*

Table 4. 5*: Summary of* sp^3/sp^2 *ratios for different samples.*

Sample name	$I_{diamond}$	$I_{graphite}$	I_D / I_G
D	4500	6500	0.7
C	1500	1700	0.8
B	3250	3750	0.9
A	4000	5000	0.8

4.5 Conclusion

DLC films sputter deposited from a graphite target were obtained. Various conditions were used in order to increase the sp^3/sp^2 ratio so as to obtain good films. These various conditions are: sputter deposition while maintaining a voltage bias between sample and target in order to increase the impact energy of carbon atoms on surface of sample; deposition in the presence of moisture in order to remove unbound carbon; deposition onto a substrate that has been placed within a Faraday cage in order to eliminate an electric field on the substrate and finally just normal sputtering from the target. It was found by means of Raman characterisation that the best films are those where a voltage bias had been maintained between sample and target. The next best film was the one where both a voltage bias between a target and substrate had been maintained during deposition and a Faraday cage used. XRD was done and the results agree with Raman results that those are DLC films. AFM results agreed with SEM results in that the surfaces of the films are smooth and featureless. The films should therefore be good for gas sensing applications(see next Chapter).

4.6 References

[1] Angus J.C and Hayman C.C., *"Low-pressure,metastable growth of diamond and diamond-like phase,* " Science, 241 (1988) 913-921.

[2] Morris.V.J, Kirbv. A.R, Gunning. A.P, *Atomic Force Microscopy for Biologists,*Imperial College Press, London,1999.

[3] Chi-Ruey L, Chun-His S,Chien-Kuo C,Da-Hua W, Deposition of Diamond –Like Carbon Films and Metal-DLC thin films on PCBN substrates by RF Magnetron sputtering method,Symposium (2009) 4-5

[4] Khalid Alamgir .M, Zaka Ansar .M, Arif S, Arif. M, *Deposition of Diamond- Like Carbon thin film by Pulse Laser Deposition for Surgical Instruments*, World Applied Sciences Journal 32 (6) 2014 1110-1114

CHAPTER 5: SENSITIVITY OF DLC FILMS TO VARIOUS GASES.

5.1 Introduction

Diamond-Like Carbon (DLC) thin films have been studied extensively in the past. Some of these desirable properties of DLC films are its high hardness and a high degree of smoothness of their surfaces as well as a low coefficient of friction [1]. Carbon is well-known to crystallize in the forms of diamond (sp^3) or graphite (sp^2) and mixtures thereof. Most of the carbon surfaces are chemically stable and hence they are inert species under static environments. These can interact with liquids or gases under the influence of sliding or abrasive contacts such as terminating bonds on the surface.

DLC as a noncrystalline carbon (an amorphous) carbon with a high fraction of diamond-like (sp^3) bonds, and it is also named to be an amorphous hydrogenated carbon (a-C:H), if it contains hydrogen. Typically, thin films of hydrogen-free DLCs with very high sp^3 configuration have been prepared by filtered cathodic vacuum arc, pulsed laser deposition (PLD), or mass selected ion beam deposition in the past. In addition, hydrogenated amorphous carbon with sp^2 configuration has been produced by reactive sputtering or plasma enhanced chemical vapour deposition (PECVD). The sp^3 bonding is generated by ensuring that the deposition flux contains a sizeable fraction of medium energy ions with energy ~100 eV [2-3].

Diamond-like-carbon films constitute a new research area in electrochemistry. They have been used as electrodes in electrochemical microgravimetry on quartz crystal electrodes [4] as nitrogenated DLC films (N: DLC) for metal tracing analysis and as coatings for polycarbonate membranes used as selective barriers in glucose oxidase biosensors.
In gas sensing applications, materials that will withstand gas poisoning from dangerous gases such as H_2S are sought. DLC has some unique properties, such as high elastic modulus, high mechanical hardness, very low surface roughness, and chemical inertness that qualify it to be a valuable material for these applications. It is also a semiconductor with a band gap, which can be varied from approximately 1 to 4 eV [5-6].

Amorphous DLC electrodes has been reported as a glucose amperometric biosensor [6-7] and DLC microelectrodes for medical diagnosis of human immunodeficiency virus (HIV), human hepatitis B virus (HBV), and human hepatitis C virus (HCV) [8]. Depending on the deposition process and conditions, the Carbon-sp^3/Carbon-sp^2 hybridization ratio may be adjusted and controlled and can be doped to form conductive material thus allowing tailoring the film properties depending on the application. Due to these properties, it has found applications in a variety of areas such as electronic, optical, mechanical and biomedical applications [9].

Reports on DLC as being an active chemical sensor for gases such as NO_2, CO, H_2S, H_2 and NH_3 and a wide variety of gases are not available in contemporary literature. In this work, the sensing properties such, as response and recovery rates from the listed gases will be presented, the adsorption and desorption rates as well as lowest detection limits and saturation limits will be presented.

5.2 Sample preparation method

The Diamond-Like Carbon (DLC) films were deposited using DC sputtering within an Orion Stilleto Sputtering System from AJA Inc. All depositions were done on aluminium strips substrates and then placed in the chamber and the chamber evacuated to $2x10^{-7}$ Torr. The chamber was heated to 800 ^oC for one hour while pumping to remove moisture and impurities. It was then cooled to room temperature. A cylindrical piece of carbon (graphite) having purity of 99.99% , thickness 6.35 mm and diameter of 50.8 mm was used as a sputtering target. In order to find the best conditions for depositing DLC films. We do several depositions by using different parameters then after that it then concluded that at temperature of 200°C,power of 150 W,voltage of 120 V are good parameters for depositing DLC films.i.e films with highest sp^3/sp^2 ratio magnetron power was at temperature of 200°C,power of 150 W and voltage bias of 120 V

5.3 Gas sensing with DLC films

A sensor is a technological device that senses a signal, physical condition and chemical compounds. Sensors are most electronic and based on semiconducting oxides and have been used to detect poisonous and combustible gas in air [8-9]. Gas sensing materials can be classified into two types, namely organic and inorganic. More recent work has shown that DLC films on gas sensors are also able to respond to gas at room temperature and slightly above

The following equation for response was adopted

$$S = \frac{|R - R_0|}{R_0} \qquad \textbf{Equation 5. 1}$$

where R and R_0 are the resistances of the DLC film when in presence and absence of the gas under test. Langmuir isotherms were fitted to each response-time line shapes in order to obtain adsorption and desorption constants:

$$S = S_{\max}\left(1 - e^{-Qt}\right) \qquad \textbf{Equation 5. 2}$$

where are maximum response, S_{max}, and the growth coefficient, Q, depend on the both the adsorption coefficient,α and the desorption coefficient, δ. Lastly, the response-concentration curves were fitted with the Dose-Response equation in order to obtain the critical concentrations for each gas for the purposes of comparing among the gases:

$$S = S_1 + \frac{S_2 - S_1}{1 + 10^{(\log C_0 - C)p}} \qquad \textbf{Equation 5. 3}$$

where S_1 and S_2 are minimum and maximum responses at low and high doses respectively and C_0 is the critical dose of gas for the sensor and *p* is an exponent.

5. 4 Gas sensing results and discussion

The sensing tests were performed in a Kinosistec system capable of measuring resistance of the DLC film while automatically changing the temperature of the sensor, the concentrations of the gas as well as the gas type. The schematic view of the gas sensor structure with interdigitated Ni electrodes, measuring 5x5mm is shown in Figure 5.1 [10].

Gas sensing response curves for DLC sensing H_2, H_2S, CO, NH_3 and NO_2 at different temperatures are shown in Figure 5.2. It shows some response curves in time for the gases considered at varying temperatures: H_2, H_2S, CO, NH_3 and NO_2. The effect of humidity on these films and how they might affect gas sensing has also been studied. The gases studied are, H_2; H_2S; CO; NH_3 and NO_2. It is noticed that the DLC sensor responses to H_2, CO and H_2S are quite similar for the concentrations chosen in this study. The responses to NH_3 and NO_2 are much higher than those from H_2, CO, H_2S showing that the DLC has preferential response to nitrogen-containing molecules. It is then possible to envision that the N sites in both NH_3 and NO_2 are the most preferred centres of interaction with the sp^3 bonding in the DLC layers.

The response-concentration curves in Figure 5.4 shows the similar trends as in Figure 5.3. Figure 5.3 represents the resistance-time profiles of the DLC based sensor when exposed to varying concentrations of CO, H_2, H_2S, NH_3 and NO_2 at temperatures of 25, 100 and 200°C.

It is observed in Figure 5.4 that our sensor has a better response to NO_2 and NH_3 at all concentrations than on other gasses. The curves in Figure 5.4 are fitted with the traditional dose-response equation given in Equation 3. The parameters of EC_{50}, C_0, S_{max} and S_{min} after fitting summarized in Table 5.1.

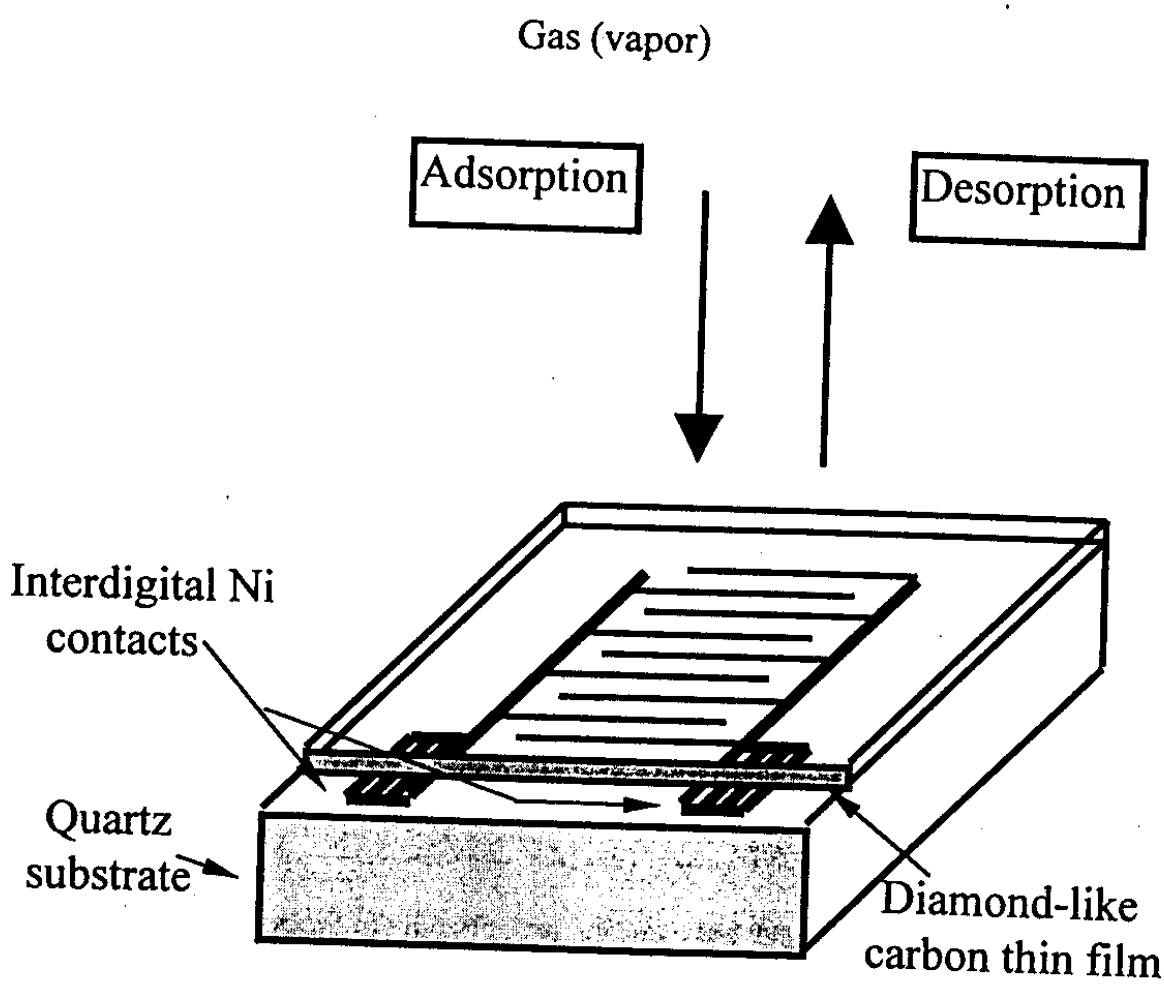

Figure 5. 1: *Schematic view of the new gas sensor. This diagram was adapted from ref [10]*

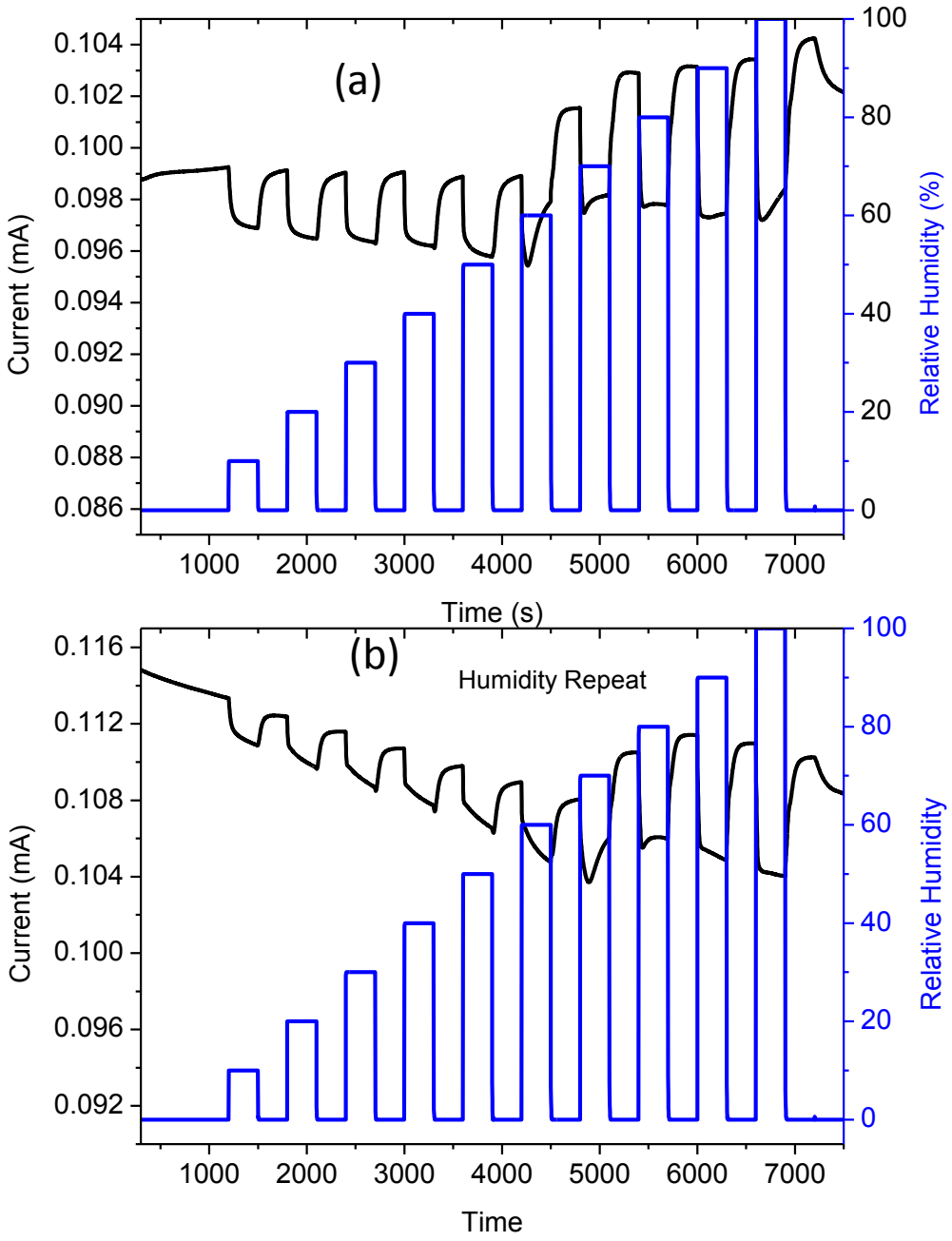

Figure 5. 2: *Response of the DLC sensor to relative humidity shows an intriguing change in the response profile between the relative humidity level 50% and 60%.*

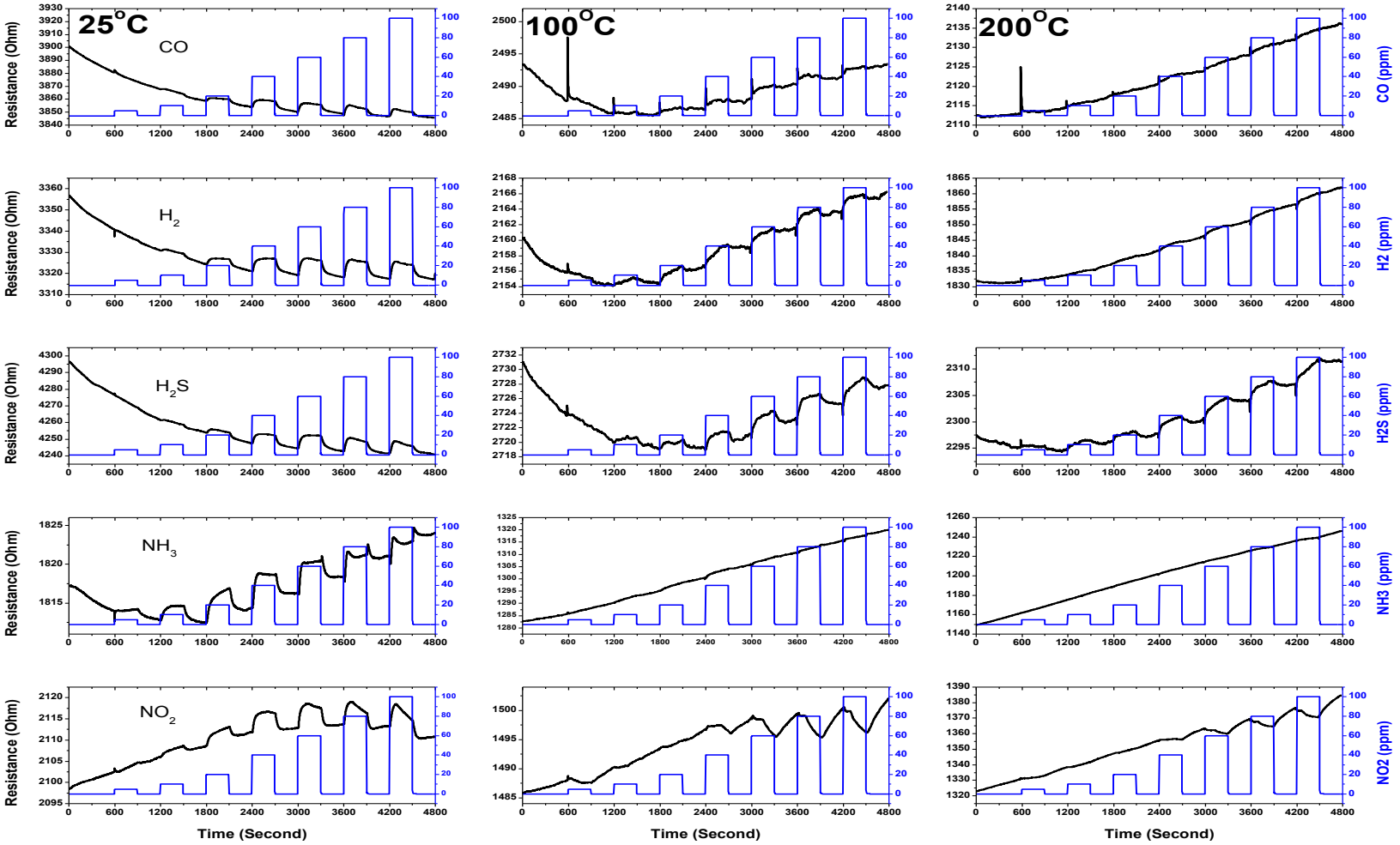

Figure 5. 3: *Resistance-time profiles of the DLC based sensor when exposed to varying concentrations of CO, H_2, H_2S, NH_3 and NO_2 at temperatures of 25, 100 and 200 ℃.*

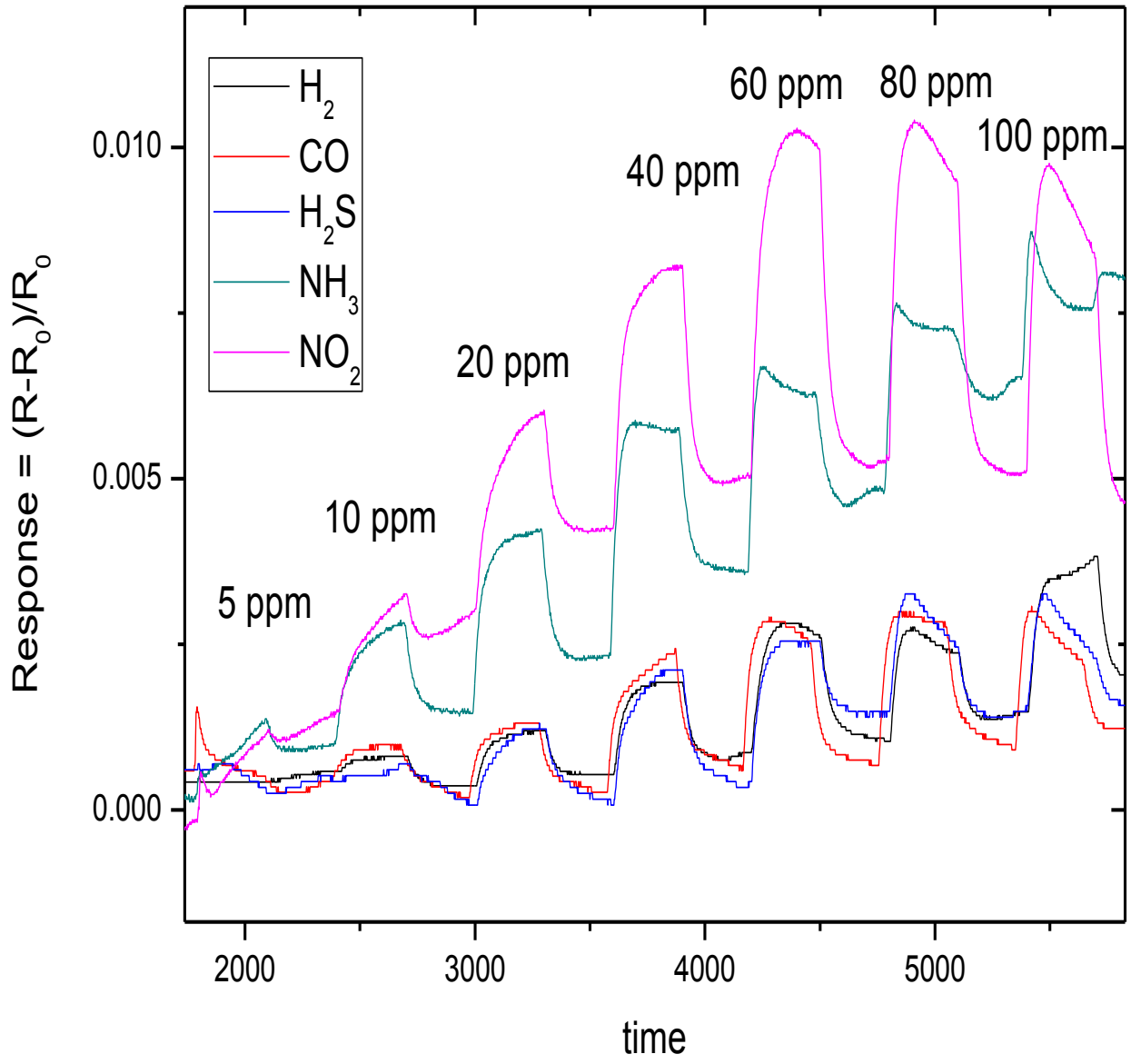

Figure 5. 4: *Response versus time curves for ON and OFF on each gas type and each gas concentration considered this was done at room temperature.*

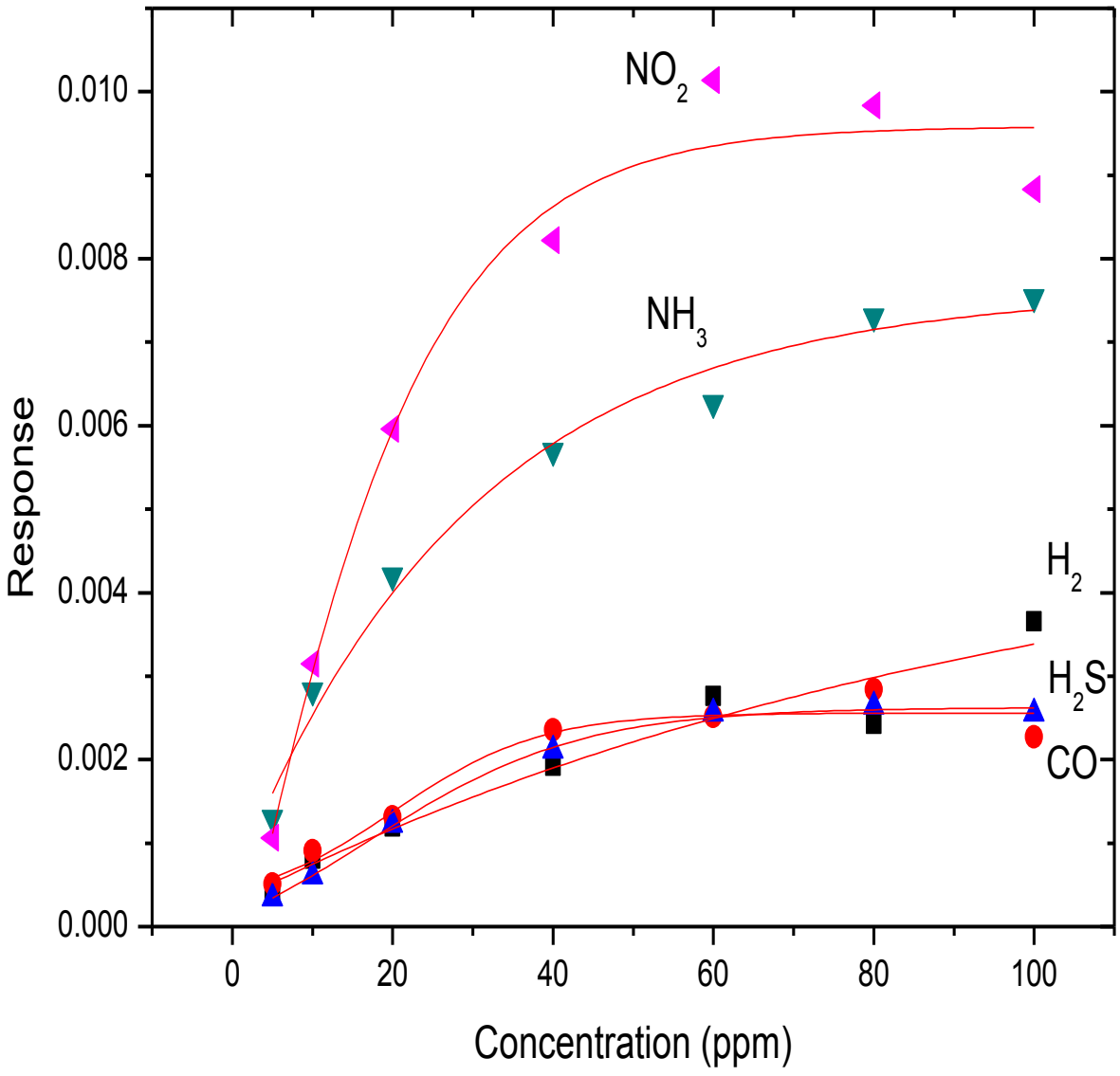

Figure 5. 5: *Response –concentration curves fitted with the Dose-Response*

Table 5. 1: A *summary of the parameters in the dose-response and the Langmuir isotherm equations after fitting to the response-concentration data of the DLC sensor*

Gas	**Smin**	**Smax**	**Log Co**	**p**	**EC50**	**S0**	**Smax1-S0**	**Q1**	**Smax2-S02**	**Q2**
H_2	-0.86192	0.00518	-512.932	0.00438	0	2.11E-04	7.93E-04	17.62166	3.27E+12	1.39E+17
	1812.193	0.02192	215676.7	0.06531		9.32E-04	0.00135	73.86405	4.52E+12	2.47E+17
CO	2.16E-04	0.00256	20.20714	0.04786	1.61E+20	-1.08E-04	0.00137	21.96479	0.00137	21.96455
	9.32E-04	1.58E-04	9.21258	0.03467		9.11E-04	12811.04	3.12E+06	12811.04	3.12E+06
H_2S	-5.89E-04	0.00262	16.85478	0.03281	7.16E+16	-2.54E-04	0.0015	27.02589	0.0015	27.02649
	4.94E-04	4.56E-05	4.52089	0.00537		3.70E-04	--	970110.2	--	970127.9
NH_3	-10.2096	0.00762	-214.031	0.01474	9.31E-215	-0.00161	0.00617	65.89196	0.0044	6.06873
	21942.54	8.01E-04	63518	0.01489		0.00203	8.52E-04	52.65115	0.00143	4.89801
NO_2	-0.01724	0.00958	-5.73105	0.03129	1.86E-06	-0.00189	0.00578	17.28971	0.00578	17.28936
	0.07019	5.14E-04	59.4999	0.02294		0.00261	31563.8	645986	31563.8	645980.8

5.5 Conclusion

Diamond-Like Carbon thin films have unique and desirable properties useful for many applications. They however have not been studied extensively for their gas sensing properties. A sensor made up of DLC films will be chemically stable, a property desirable for sensing corrosive gases. Further, there is a possibility of tailoring the sp^3/sp^2 ratio of the films such that it is either more conducting or less conducting.

We have studied the gas sensing properties of DLC films including the recovery rate of these films after they had been exposed to various gasses. Detection limits were also studied as well as saturation limits. Sensing tests consisted of measuring changes in resistance of the DLC film when exposed to various concentrations of gas at varying temperatures. The effect of humidity on these films and how they might affect gas sensing has also been studied. The gases studied are, H_2; H_2S; CO; NH_3 and NO_2. Comparing the sensitivity of the DLC sensor to various gases it was found that it responds better to NH_3 and NO_2 gases compared to H_2; CO and H_2S. The conclusion made is that the DLC film senses nitrogeneous gasses preferentially as compared to hydrogeneous gasses. The interaction sites for gas molecules are most likely sp^3 bonding sites.

Further we notice also that the sensors are effective even at room temperature. This is an advantage because heating a sensor is costly, thus a sensor that functions well at room temperature is much more desirable. The sensors saturate at about 40 ppm and are effective to as low as 10 ppm.

5.6 References

[1] Wang.C, Yu .X, Hua. M, *Microstructure and mechanical properties of Ag-containing diamond-Like Carbon films in mid-frequency dual-magnetron sputtering, Applied Surface Science*, 256 (2009)1431-1435.

[2] Paik .N, *Raman and XPS studies of DLC films prepared by magnetron sputter-type negative ion source, Surface & Coatings Technology*, 200 (2005) 2170-2174

[3] Nebel, M., Neugebauer, S., Kiesele, H., Schuhmann, W., *Local reactivity of diamond-like carbon modified PTFE membranes used in SO_2 sensors Electrochimica Acta*,55 (27) (2010) 7923-7928

[4] Möller, S., Lin, J., Obermeier, E. *Material and design considerations for low-power microheater modules for gas-sensor applications, 1995 Sensors and Actuators: B.Chemical* 25 (1-3), 343-346

[5] Polyakov V.I., Rukovishnikov, A.I., Khomich, A.V., Ghosh, T.K., Loyalka, S.K. *Surface phenomena of the thin diamond-like carbon films Authors of Document Year the Document was Publish 1999 Source of the Document Materials Research Society Symposium - Proceedings* 555, 345-350

[6] Kulisch, W., Popov, C., Zambov, L. *Deposition, Characterization and Applications of Nitrogen-Rich Amorphous Carbon Nitride Films 2001 New Diamond and Frontier Carbon Technology* 11 (1), 53-76

[7] Ohlckers, P., Skotheim, T., Dmitriev, V.K., Kirpilenko, G.G. *Advantages and limitations of diamond-like carbon as a MEMS thin film material 2008 TechnicalProceedings of the 2008 NSTI Nanotechnology Conference and Trade Show, NSTI-Nanotech, Nanotechnology* 2008 1, 63-66

[8] Tanaka, Y., Furuta, M., Matsura, H., Fujisima, A., Honda, K. *Development of high-Sensitive gas -sensor for B_2H_6 using gas-permeable conductive DLC membrane (2008) ECS Transactions* 16 (11), 387-391

[9] Xiao, Q., Yang, B.-H., Zhu, S.-S. *Characterization of DLC films prepared by magnetoactive-RF-PECVD method in low temperature 2010 Guangdianzi Jiguang/Journal of Optoelectronics Laser* 21 (9), 1332-1336

[10] Nebel, M., Neugebauer, S., Kiesele, H., Schuhmann, W., *Local reactivity of Diamond- like carbon modified PTFE membranes used in SO_2 sensors 2010 Electrochimica Acta* 55

CHAPTER 6: PREPARATION AND CHARACTERIZATION OF DIAMOND FILMS

6.1 Introduction

Diamond is a metastable allotrope of carbon where each carbon atom is bonded covalently with other surrounding four carbon atoms. The physical properties of diamond are greatly affected by the presence of defects like point defects, dislocation etc. Diamond lattice has boron, nitrogen, hydrogen and oxygen as a substitution defects. Presence of nitrogen leads to less thermal conductivity [1, 2 - 3]. Diamonds usually have eight sides forming double pyramids, some have six sides and they form cubes.

The followings are the interesting properties of diamond:

- Diamond is insoluble in all liquids.
- It has a high refractive index extraordinary brilliance.
- It is a hardest substance and also it is bad conductor of electricity because it lacks of free electrons.
- Naturally diamond is transparent to X-rays while artificial diamond is opaque to X-rays.
- Diamond dies are used to make thin tungsten wires.
- Small pieces of diamond are used for cutting glass and drilling rocks.

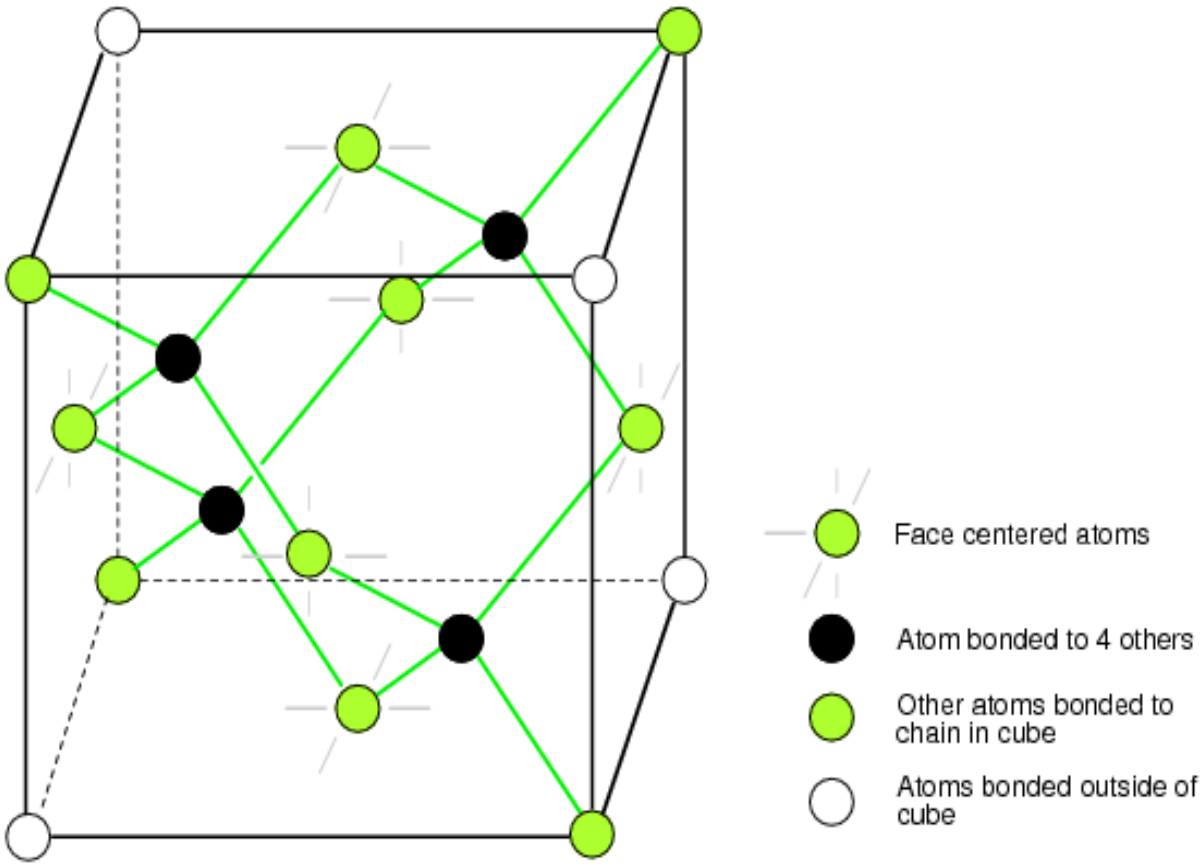

Figure 6. 1: *Schematic diagram of diamond structure. This diagram was adopted from ref [3]*

Table 6. 1*:* *Provides a brief summary of the ideal properties of diamond [2]*

No.	**Properties**	**Diamond**
1.	Density ($g.cm^{-3}$)	3.52
2.	Young's modulus (GPa)	910- 250
3.	Compression strength (GPa)	8.68- 6.53
4.	Thermal conductivity at 25°C ($W.m^{-1}.C^{-1}$)	600- 1000 (type Ia)
		2000- 2100 (type IIa)
5.	Specific heat at 25C ($kJ.kg^{-1}.K^{-1}$)	0.502- 0.519

6.2 Preparation of diamond films by spin coating

High purity diamond powder (99.9%), whose particle sizes were about 1μm average diameter was obtained from Alfa Aesar. The powder was then mixed with methanol to form a consistent paste. Methanol was chosen because it evaporates easily. The paste was used for spin coating on Model Cee 200X spin coater from Brewer Science Inc. The substrates on which the diamond films were made were silicon wafers that had been chemically cleaned using the same method described in Chapter 4. The spin speed used was 300 rpm for duration of 5min.

The films were allowed to dry in air before putting them in a chamber for further processing. The vacuum chamber was evacuated to a base pressure of $2x10^{-7}$ Torr. It was then annealed at temperatures from 650 ^{o}C, 750 ^{o}C and 850 ^{o}C. Acetylene (C_2H_2) was then bled into the chamber at a flow rate of 4 sccm at a chamber pressure of $3x10^{-3}$ Torr. This was done to either grow the diamond seeds or at least to form conduction bridges between diamond grains. Some of the samples were doped with nitrogen while others were doped with oxygen at these various temperatures. All doping was done at a pressure of $3x10^{-3}$ Torr.

6. 3 Characterization of diamond films

Diamond films were characterised using various techniques. We were interested to find out whether the films were of good quality or not. We checked for uniformity and continuity of the films, grain size and whether we had managed to obtain adequate doping levels with nitrogen and oxygen. We also wanted to find out whether the CVD process had produced any graphitization or only growth of diamond particles [4].

6.3.1 SEM and EDX analysis of the deposited Diamond Thin Films

SEM images were obtained for all synthesized thin films. Scans over vast areas of a film could tell whether a film was uniform or not. This enabled us to choose good uniform films for further processing. It was noticed also that the films did not peel after subjecting them to high temperature and to various gases (C_2H_2, N_2 and O_2). Figure 6.2 shows that (a) and (b) are good films whereas (c) is discontinuous. It is noticed also that the films contain grain

sizes of about 1 µm in diameter. The surface looks rough. This is desirable since a rougher film contains a bigger surface area per given volume. The films should be good as gas sensors. It is however not clear whether the films are continuous electrically for them to act as gas sensors, hence a need to process them in C_2H_2 at high temperature.

EDX is the technique that was used to check doping levels in the samples. Table 6.2 summarises results of our EDX analysis. The aim was to obtain doping levels of between 1 and 4 atomic percent in the dopants. The data presented in Table 6.2 are all acceptable. We also doped some of the samples with oxygen. Doping levels are summarised in Table 6.3. The doping with oxygen was done at 650 ^oC and 850 ^oC. It was observed that the oxygen doping level at 750 ^oC proved to contain 13% of oxygen which is regarded as excessive.

6.3.2 RBS Analysis of Diamond samples

Rutherford Backscattering Spectrometry (RBS) was carried out using 2 MeV alpha particles on a 6 MeV Van de Graaf Generator belonging to iThemba LABS, Cape Town, South Africa. Rutherford backscattering energy spectra were analysed using the RUMP simulation package [3]. All samples were deposited using DC sputtering from a graphite target.

The structure of the sample is Si<100>/diamond, i.e. a diamond film deposited on a silicon wafer. In Figure 6.3 there is a Si signal that pronounced evidence of surface position. It means that some of the alpha particles from the beam reach the Si wafer without being scattered by diamond particles. This happens because the diamond film is grainy and some alpha particles can pass through these to reach the Si wafer. Simulation using RUMP and normalization on the carbon signal reveals that the Si signal does not reach its expected height confirming that there are holes in the diamond film. The Carbon/diamond signal appears at its surface position (see Figure 6.3). It was not possible to determine the thickness of the diamond film from the RBS results due to the reason mention above. During the CVD process C_2H_2 was allowed to flow in to the chamber over diamond films. It is known that C_2H_2 breaks down to hydrogen and carbon at temperatures above 300 ^oC [5]. The hydrogen may either combine with oxygen to form steam at these elevated temperatures and may simply be pumped out. The carbon attaches itself to diamond particles. This helps to fill the

gaps between the diamond particles,therefore a better coverage is achieved. This is why the height of the Si signal is reduced in Figure 6.4.

Figure 6.5 is the result of CVD deposition method with C_2H_2 at an even higher temperature which shows a further reduction of the height of the Si signal (compare to Figures 6.4 and 6.3). It means that the conversion of C_2H_2 to hydrogen and carbon at higher temperatures is even better thus allowing more carbon to attach itself to diamond particles

Figure 6.6 is the RBS spectra obtained from the undoped diamond films synthesized using CVD synthesis method at different temperatures. These spectra were obtained on thin films with substantial covering of diamond on a substrate. The deposition was done at temperatures between 750 ^{o}C and 800 ^{o}C using acetylene gas. It is evident that the Si signal is reduced as the deposition temperature is increased. This is because C_2H_2 bonds are getting broken at around 300 ^{o}C and therefore the carbon atoms get attached on to the diamond grains thereby increasing the diamond grain size to close the gaps between each other to stop the alpha particles from reaching the Si substrate [5, 6].

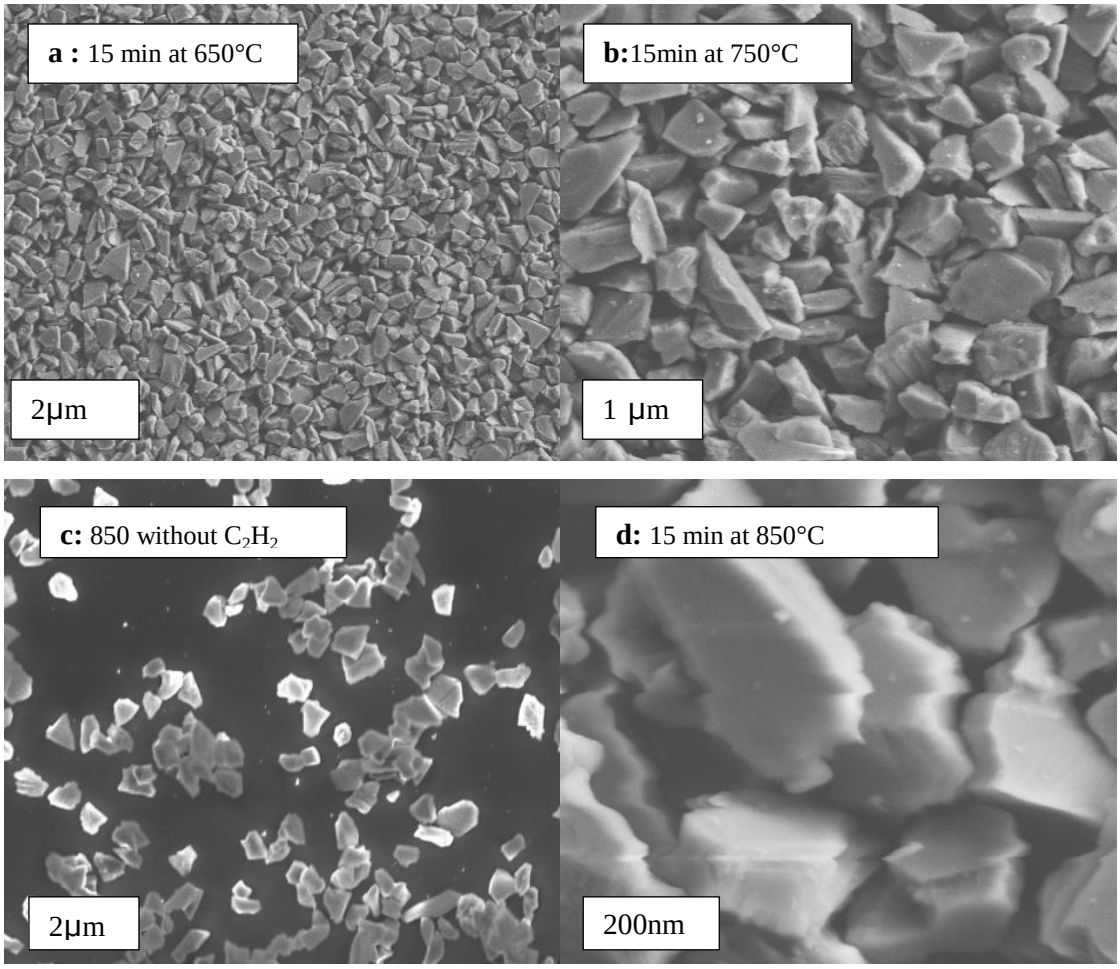

Figure 6. 2: *Illustrate the SEM image of diamond films synthesized at different annealing temperatures varied from 650°C-850°C, (a) show a CVD at 650°C,(b) CVD at 750°C (c)and (d)CVD at 850°C but c before treating with acetylene.*

Table 6. 2: *EDX results showing different chemical compositions at different temperatures after annealing of deposited diamond particles in a nitrogen atmosphere at 650°C , 750°C and 850°C. The nitrogen flow rate was 4 sccm at a chamber pressure of $3x10^{-3}$ Torr for 20 minutes.*

Elements	650°C (At %)	750°C (At %)	850°C (At %)
Carbon	98.46	98.7	98.04
Nitrogen	1.54	1.3	1.96
Total	100	100	100

Table 6.3: *EDX results showing different chemical compositions at different temperatures after annealing deposited diamond particles in an oxygen atmosphere at 650°C , 750°C and 850°C. The nitrogen flow rate was 4 sccm at a chamber pressure of $3x10^{-3}$ Torr for 20 minutes. It is noticed that doping in the sample annealed at 750 ^{o}C is too high.*

Elements	650°C (At %)	750°C (At %)	850°C (At %)
Carbon	97.96	86.3	98.69
Oxygen	2.04	1.37	1.31
Total	100	100	100

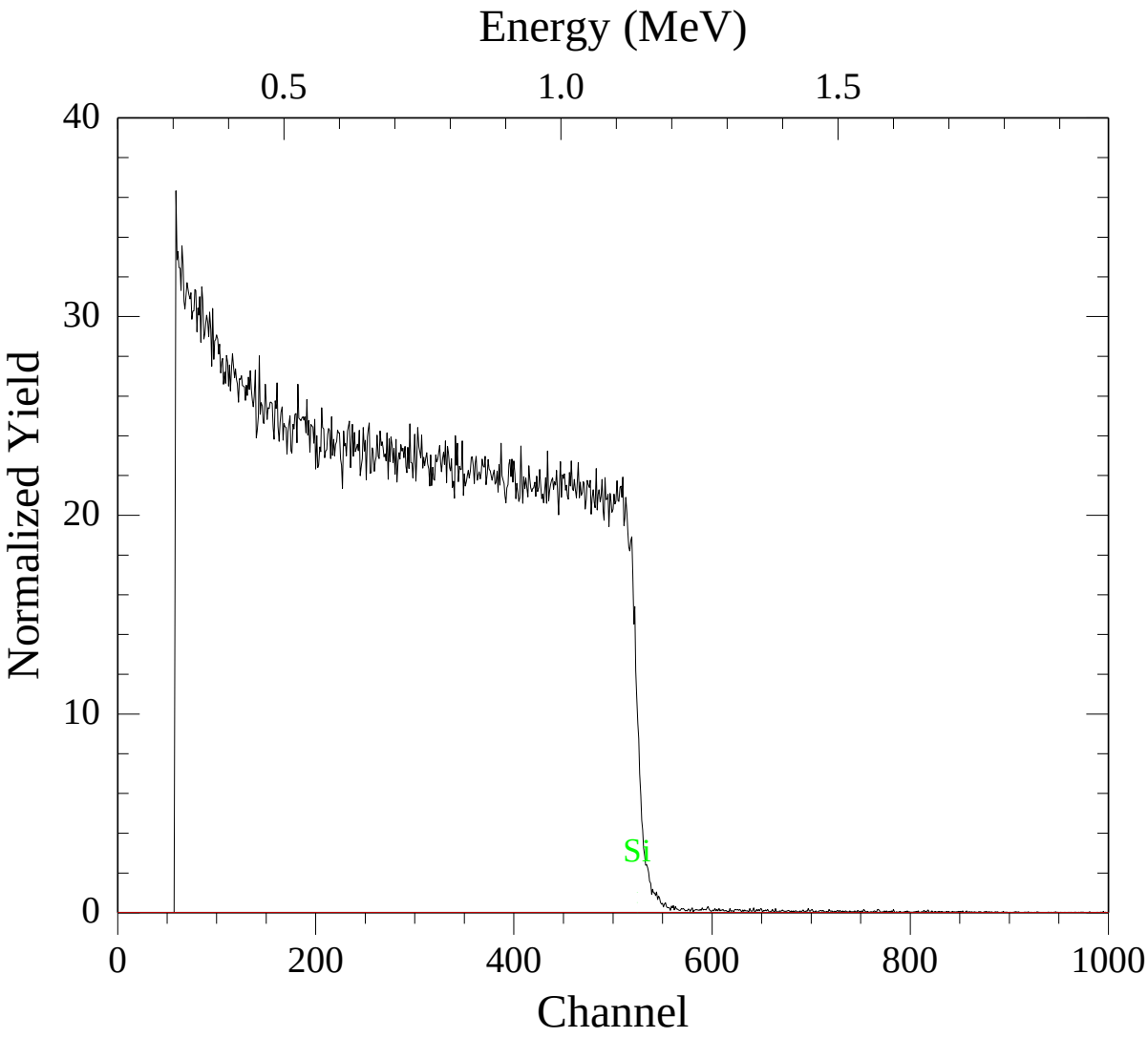

Figure 6. 3: *Representation for a calibration curve for diamond films deposited on silicon substrate for 2 hrs*

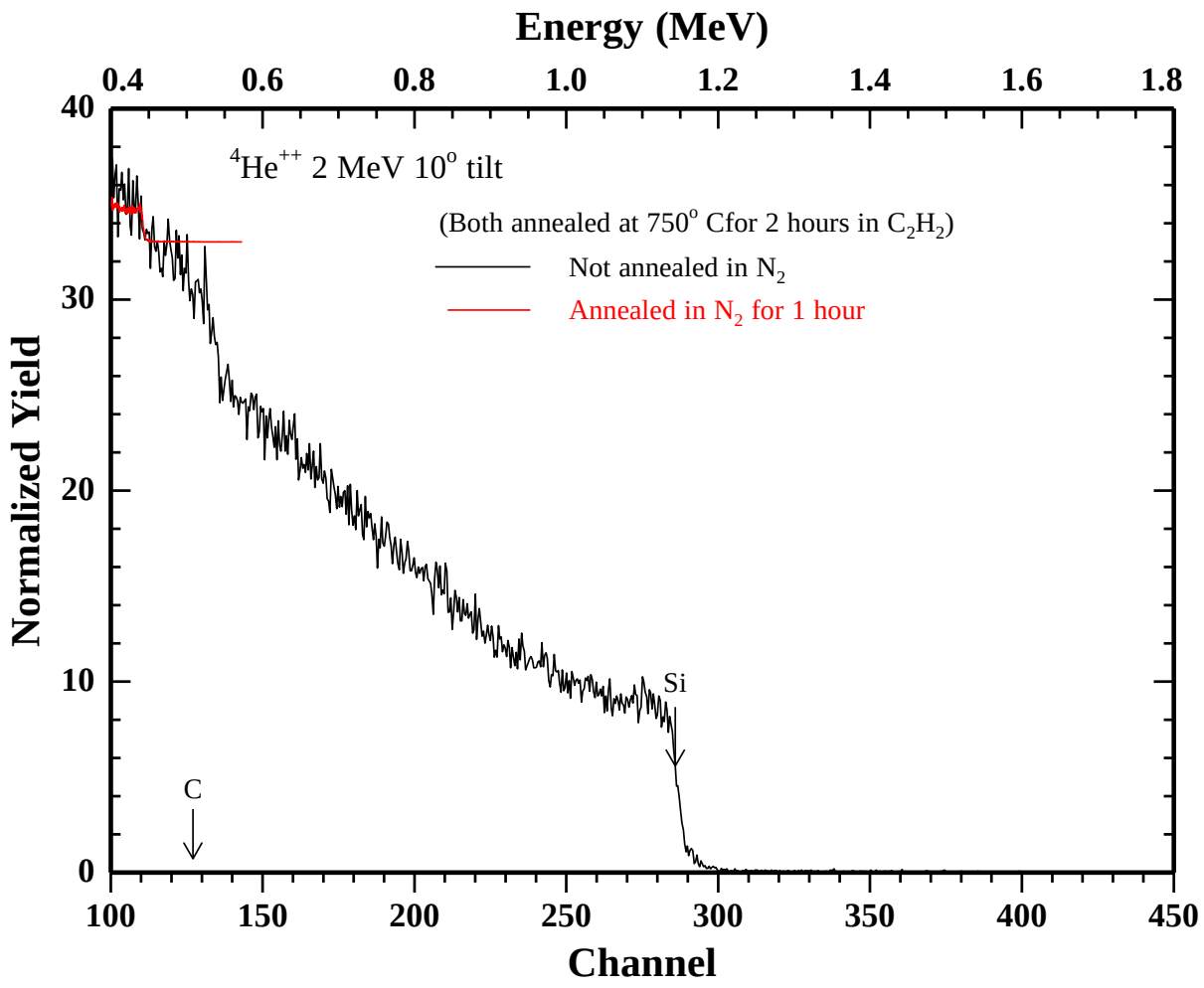

Figure 6. 4: *RBS spectra for diamond films deposited on silicon substrate and annealed with C_2H_2 for 2 hrs. See* ***Appendix*** *for a calibration curve.*

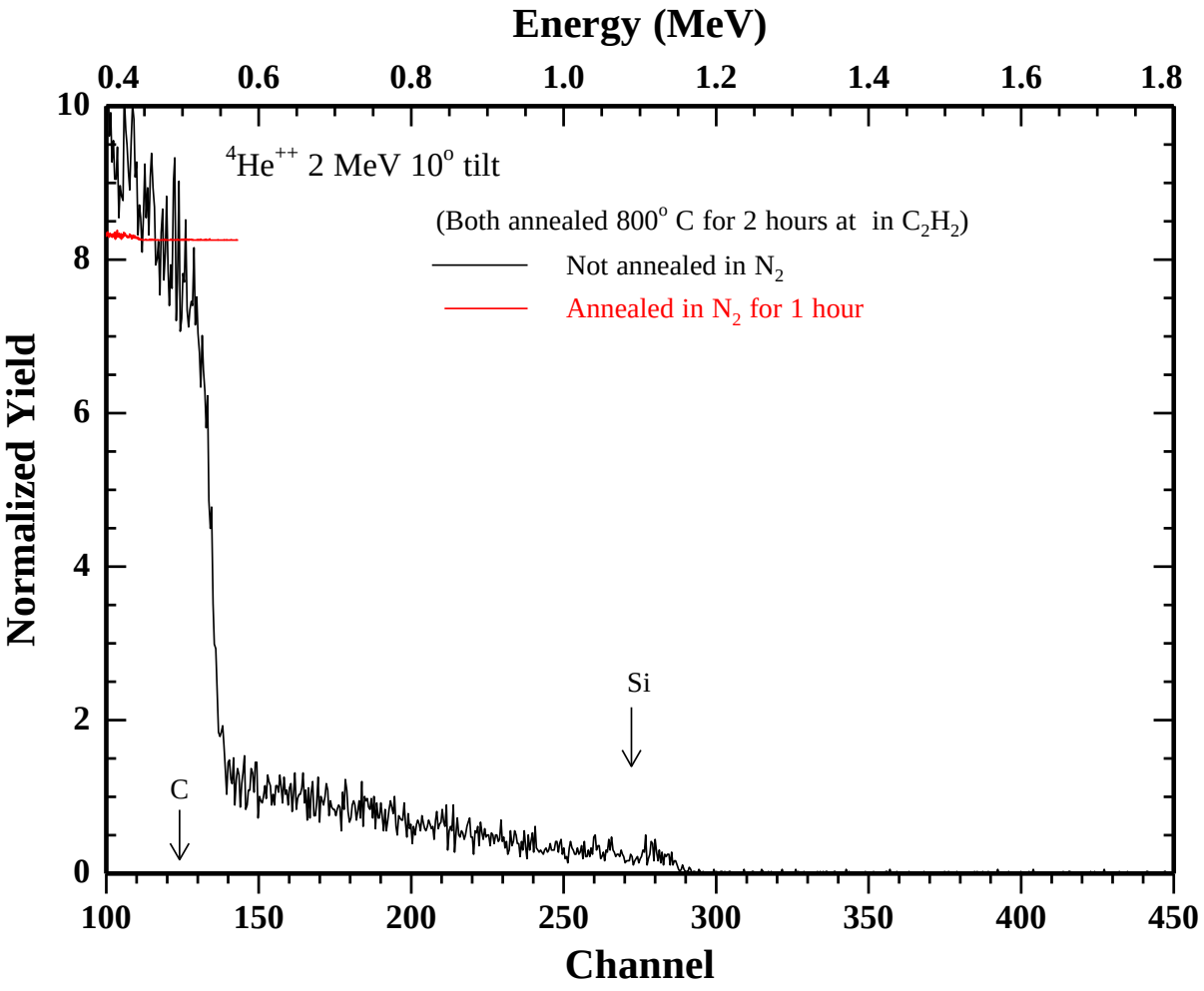

Figure 6. 5: *RBS spectra for diamond films deposited on silicon substrate and annealed with C_2H_2 for 2hrs at 750°C.*

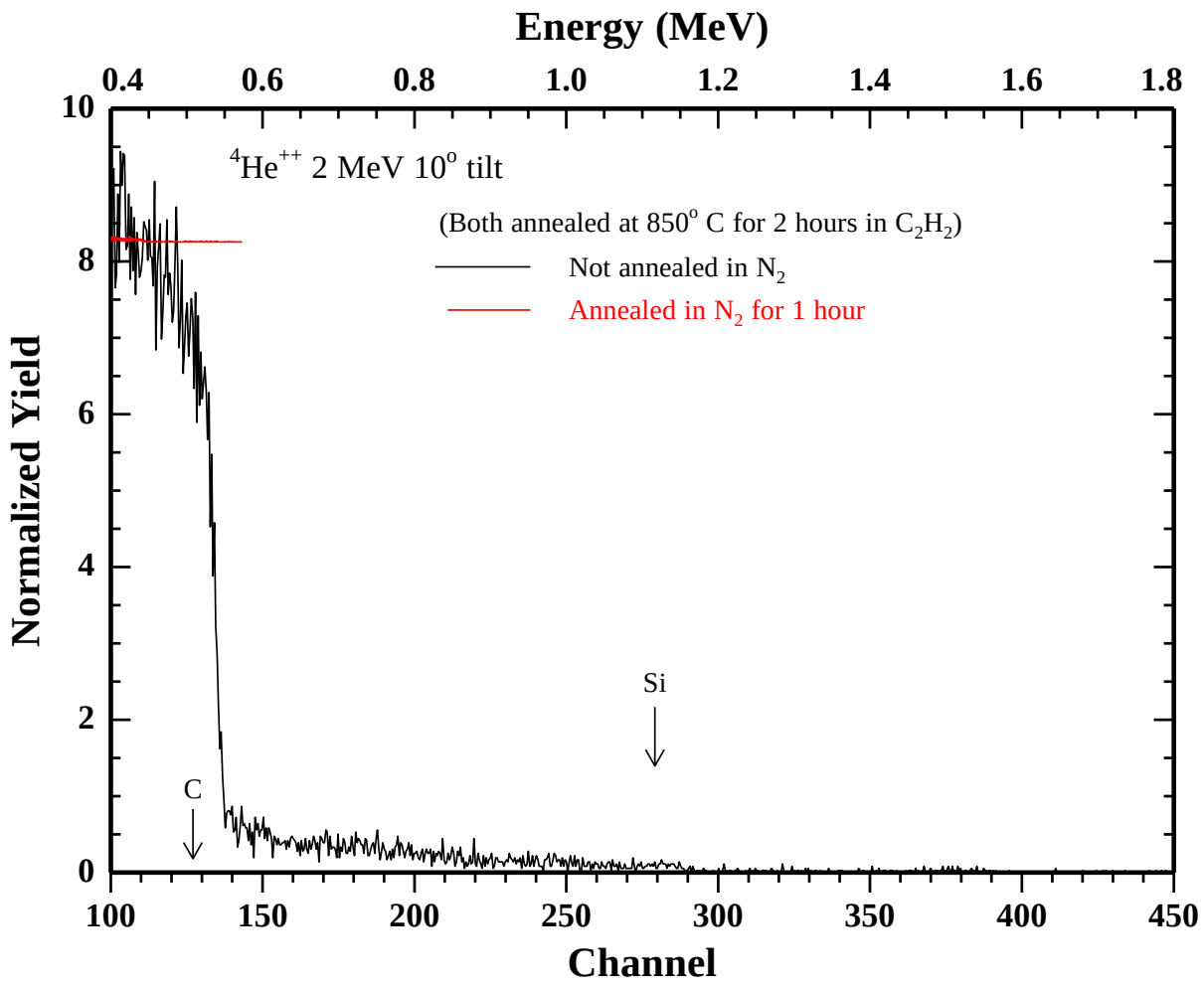

Figure 6. 6: *RBS Spectra of both doped and undoped Diamond films with nitrogen prepared using CVD synthesis method at the C_2H_2 environment and annealed at 850 ^oC for 2hrs.*

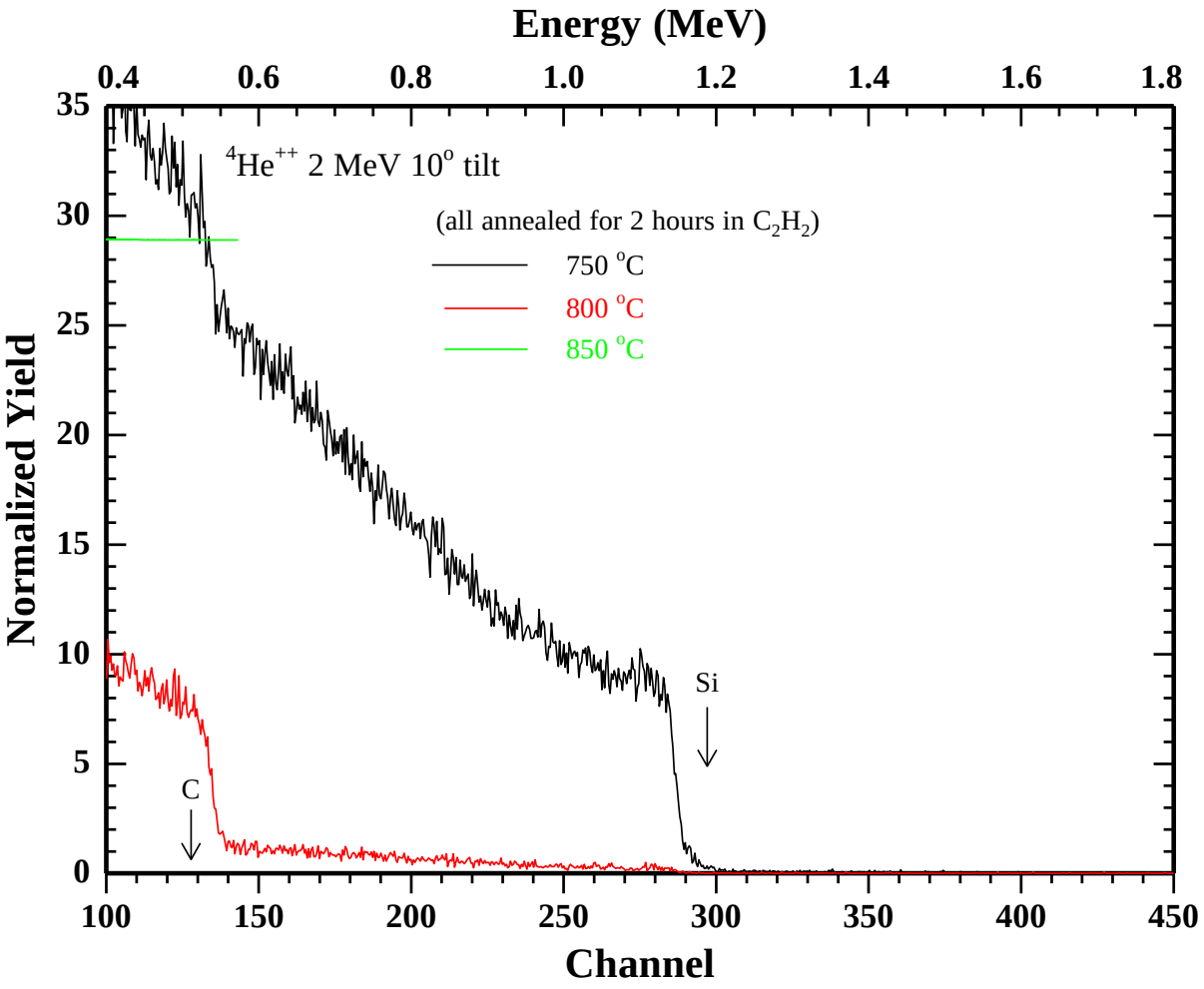

Figure 6. 7: *RBS spectra obtained from the undoped diamond films synthesized using CVD method at different temperatures. These spectra were obtained on films with substantial covering of diamond on a substrate. The deposition was done at temperatures between 750 ^{o}C and 800 ^{o}C using acetylene gas.*

6.3.3 XRD analysis of diamond sample

XRD was used to investigate the structure of diamond samples after annealing at high temperature. Figure 6.7 shows an XRD pattern for diamond films that had been annealed in C_2H_2, then flowing nitrogen for doping purposes at various temperatures. The samples are on Si <100> substrates. The samples were annealed at 650 ^oC, 750 ^oC and 850 ^oC in the environment where nitrogen was flowing at a rate of 4 sccm into the chamber with pressure of $3x10^{-3}$ Torr. It was observed from XRD spectra that the diamond is still crystalline even after the heat treatment. It cannot be ascertained however whether the CVD process introduced a graphitic material in between the diamond grains, especially if the graphite remains amorphous [7].

Figure 6.8 shows XRD spectra of diamond films deposited at different temperatures, the undoped diamond films with less peak of diamond and silicon peak. Unfortunately, XRD has a limitation when comes to graphitic carbon identification on the samples therefore a non-destructive instrument called Raman Spectroscopy was used.

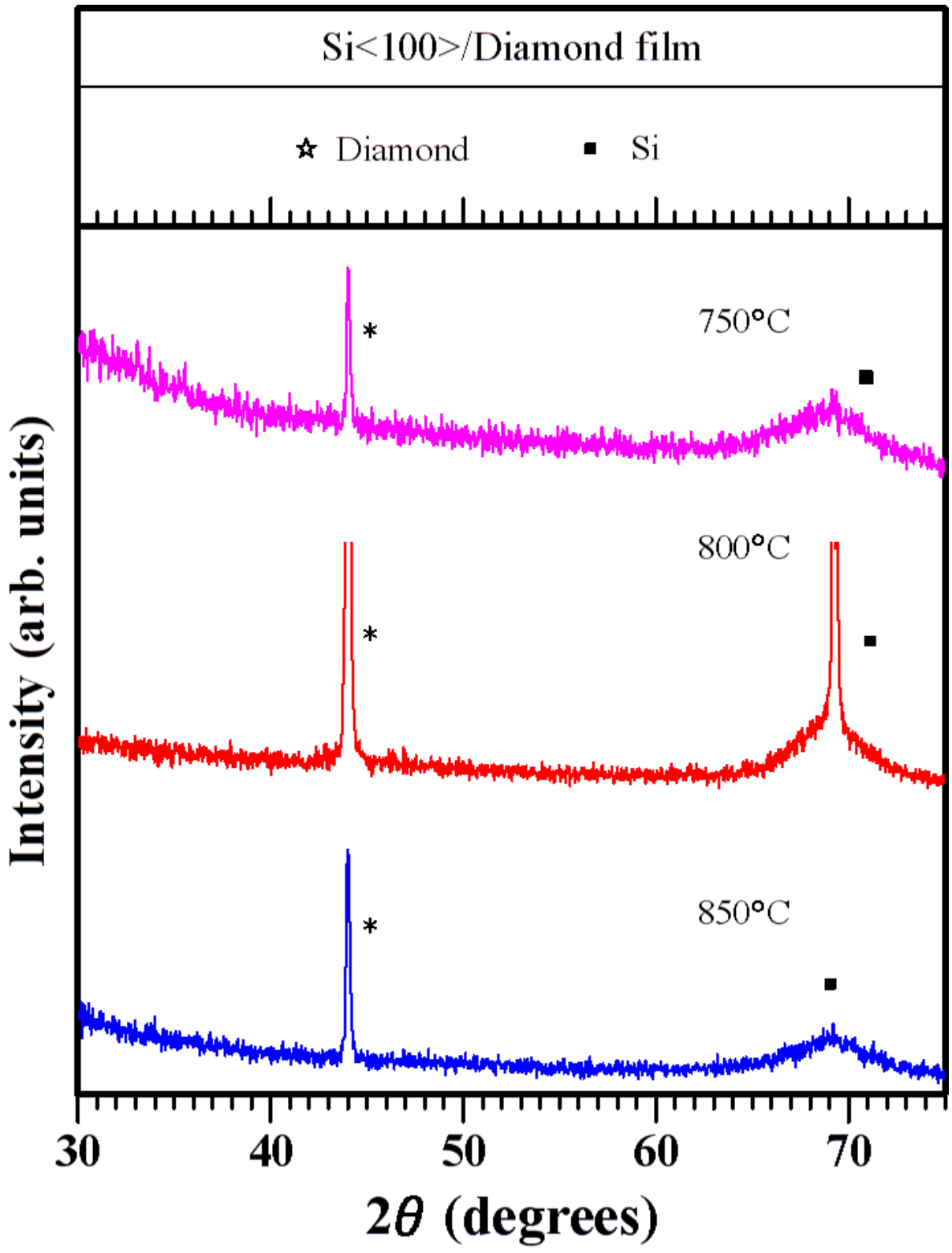

Figure 6. 8: *XRD peak patterns of doped diamond films with nitrogen and annealed at 750 ^{o}C, 800 ^{o}C and 850 ^{o}C.*

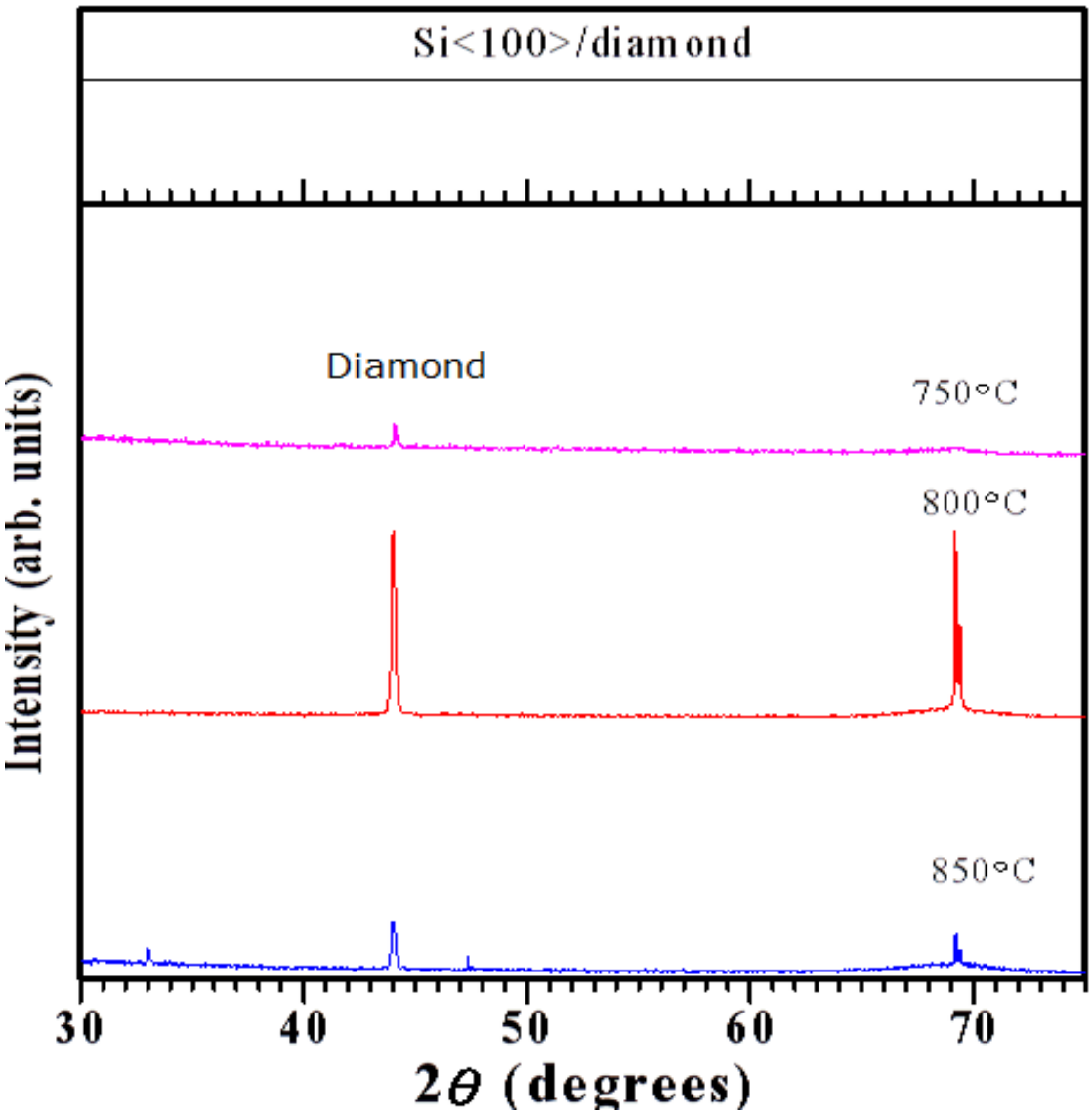

Figure 6. 9: *Represent the XRD peak pattern of undoped diamond films annealed at750 °C, 800 °C and 850 °C.*

Table 6. 4*: show the powder diffraction pattern of XRD of diamond* [3]

hkl	2θ	Relative intensity
111	41.9	100
220	75.3	2.5
311	91.3	16
400	119.5	8
X-ray source: CuKα1 (λ =1.5405 A°)		

6.3.4 Raman analysis of the diamond films

Some of the diamond films that were obtained during spin coating were annealed at temperatures 850 ^{o}C, 750 ^{o}C and 650 ^{o}C in order to find out whether these high temperatures would lead to graphitization of the films. Figure 6.9 shows Raman spectra from these samples. It can be seen that no G band representing graphite develops. These temperatures therefore do not lead to any graphitization of our films.

We then performed Raman measurements on samples on which CVD had been done using C_2H_2. Some of the samples had also been doped with ether nitrogen or oxygen. Figure 6.10 shows Raman spectra from samples on which CVD had been done (and also doping with nitrogen and oxygen on some). The diamond peak appears at 1332 cm^{-1} while the graphitic peak is at 1588 cm^{-1} [8]. Figure 6.10 show Raman spectrum of Diamond films deposited on silicon substrate at different temperature 650°C,750°C and 850°C and all samples were deposited using gas composed gas acetylene (C_2H_2) and all samples were annealed with Oxygen(O_2)and Nitrogen (N_2).

The samples deposited at varying conditions are labelled A2, F2, and H2 these samples were annealed with oxygen at different temperatures 650°C, 750°C and 850°C at a flow rate of 4sccm with duration of 20 minutes while G2, K2 and M were annealed with nitrogen at different temperatures with a flow rate of 4sccm in 20 min. It may be concluded that some of the carbon settles on the film to form graphite.

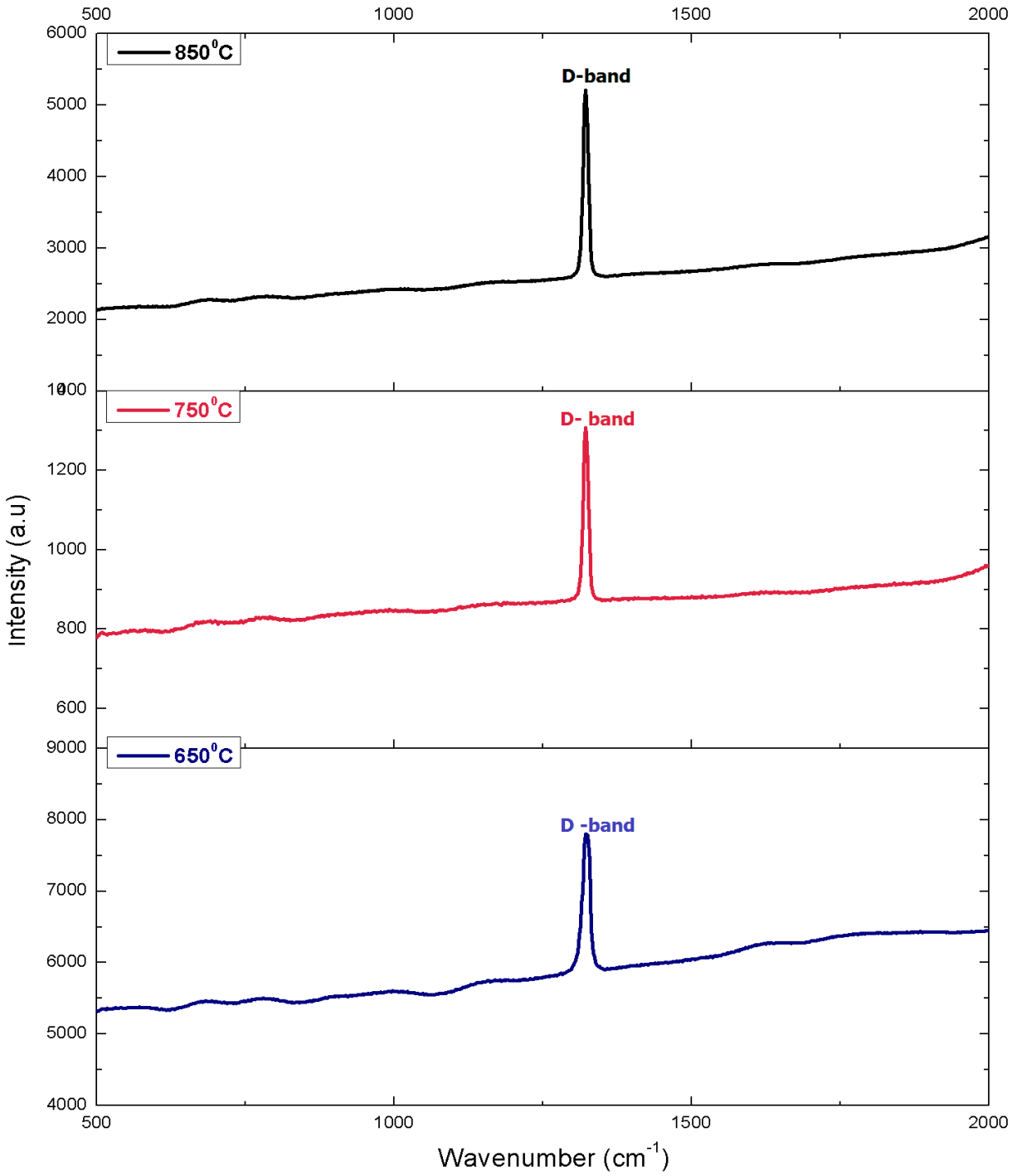

Figure 6. 10: *Raman shifts of as deposited diamond Film and annealed in vacuum at 650°C,750°C and 850°C and the pressure was recorded to be $3x10^{-3}$ Torr.*

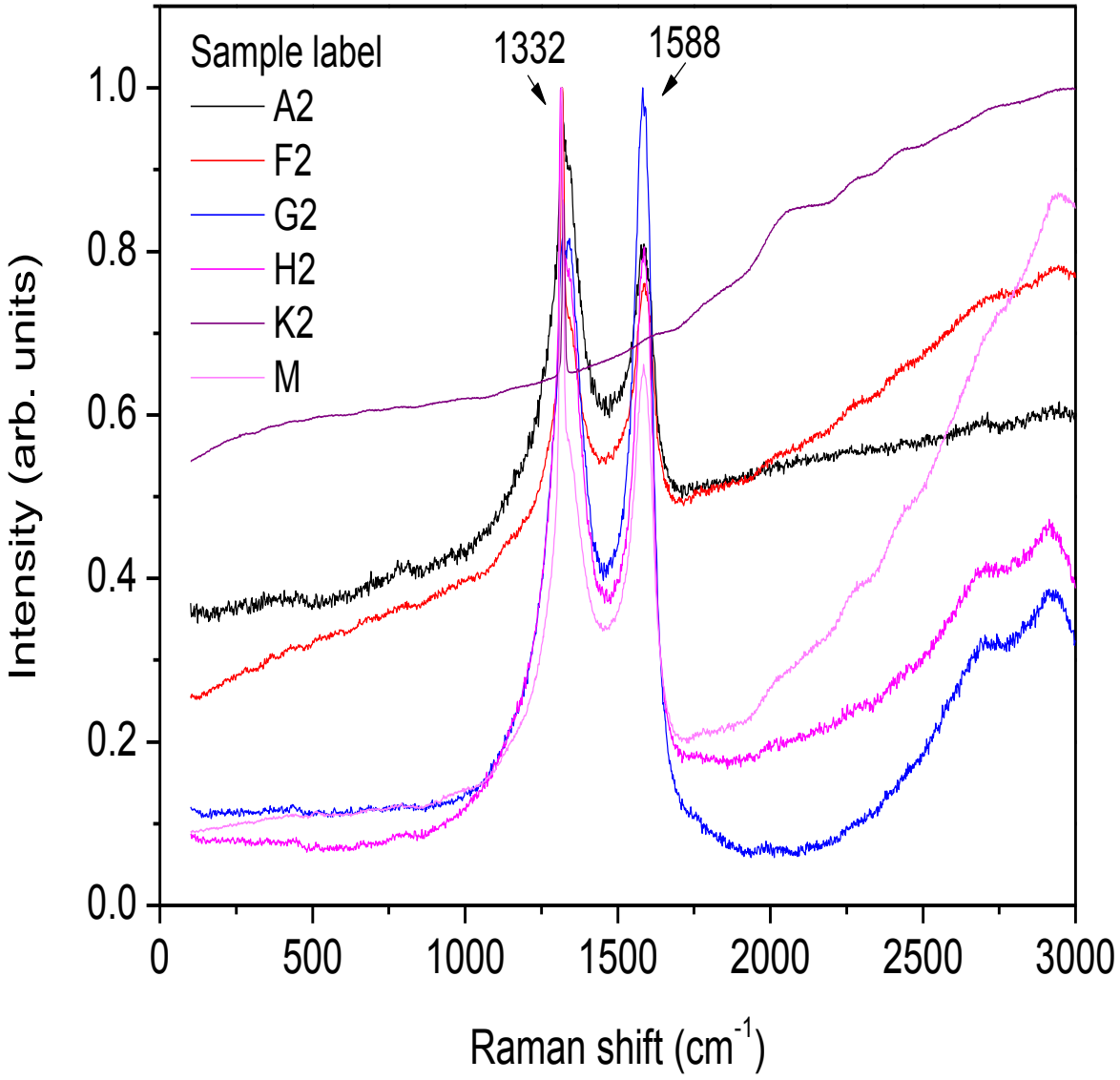

Figure 6. 11: *Raman shift of diamond film annealed at 650°C, 750°C and 850°C under the Oxygen and nitrogen environment. The pressure was recorded to be $3x10^{-3}$ Torr and the oxygen and nitrogen flow rate was kept at 4 sccm for 20 min. The spectra show two peaks one at 1332 cm^{-1} which is for diamond and the other peak at 1588 cm^{-1} which is for graphite.*

6.4 Gas sensing with diamond films

We tested the response of the undoped diamond films to several gasses. In order to realistically test whether diamond can be used as a sensor we first exposed it to humidity (considering that a sensor may be needed to perform in a humid environment, like our region Empangeni and Richards Bay). For this purpose we first deposited a diamond films onto substrates of aluminium oxide that have wires placed underneath so that the sensor may be heated, if so desired. These sensor substrates are similar to those described in Chapter 5 that were used for testing DLC sensors. The sensing tests were performed in a Kinosistec system capable of measuring resistance of the diamond film while automatically changing the temperature of the sensor, the concentrations of the gas as well as the gas type.

Figure 6.12 are results obtained after exposing sensor 1 (diamond sensor) to an environment containing the gas NH_3. The concentration of NH_3 was varied from a low value to a high value, with the time ~ 2000 s corresponding to a concentration of 20 ppm, and increasing concentration by 20 ppm for each successive peak –up to 120 ppm for the highest peak. It is seen therefore that the diamond sensors are sensitive down to about 20 ppm. The recovery time after exposure to NH_3 is about 250 s. A similar trend was found for NO_2

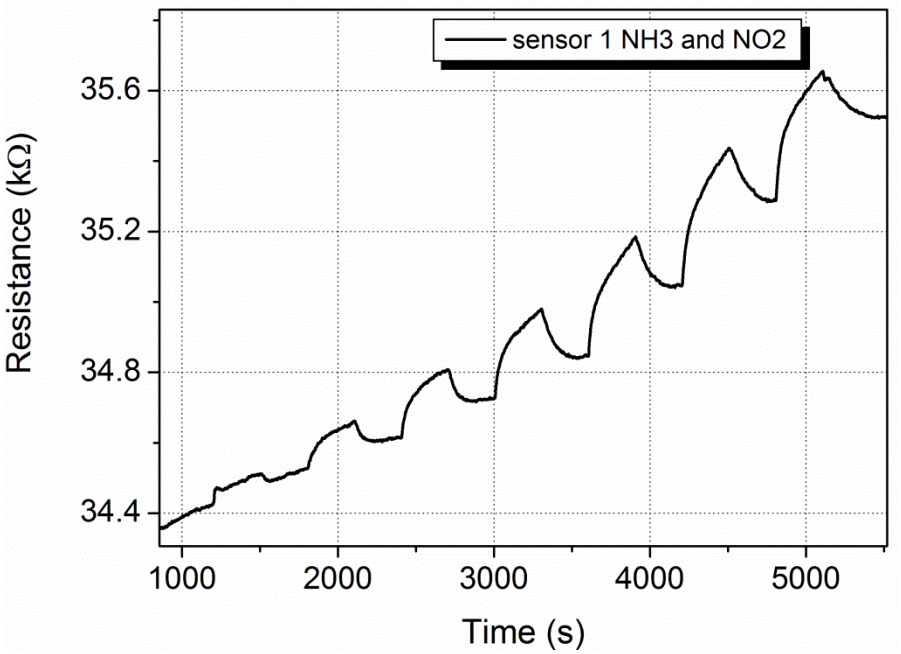

Figure 6. 12: *Response of undoped diamond films to NH_3. The sensors are sensitive down to 20 ppm and the recovery time is about 250 s. Behaviour is similar to that shown by the sensor to NO_2 (curve not given here).*

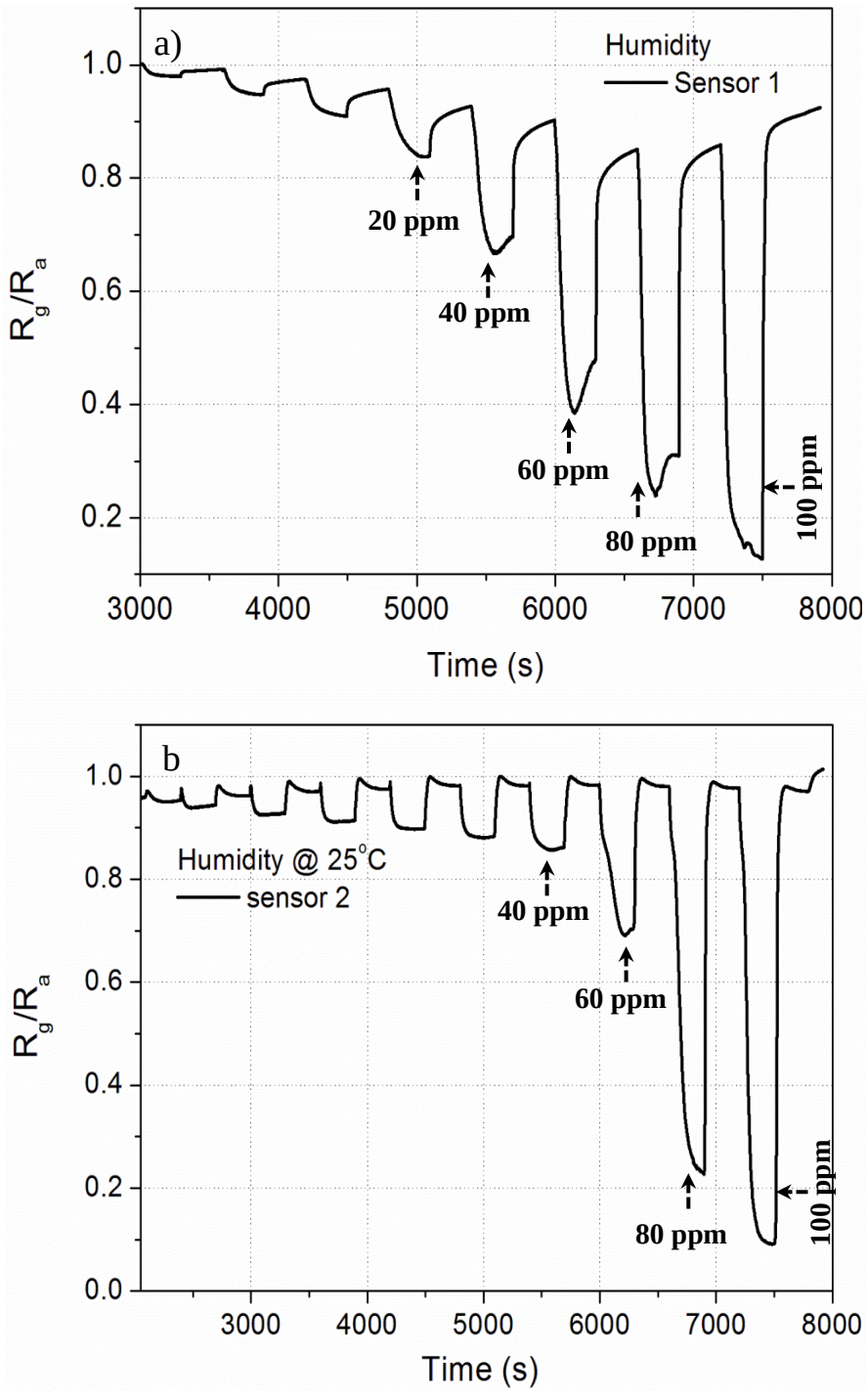

Figure 6. 13: *Response of two diamond thin film gas sensors to humidity. It is seem that the sensors are quite unresponsive to humidity up to concentrations of about 60 ppm. The sensors must therefore be used with caution in humid environments like the coastal regions of KwaZulu-Natal.*

It is important to know whether the sensors can perform as expected in a natural environment, say a region that is humidity like the coastal areas of KwaZulu-Natal. The sensors were therefore subjected to varying degrees of humidity at room temperature. If one compares the amplitudes of the fluctuations between the OFF and ON positions for testing NH_3 compared to testing humidity it is seen that the resonse to humidity have lower amplitudes. This is desirable for a sensor. It means that the sensor is not highly sensitive to humidity (cannot mistake humidity with the gas it measures). Caution must however be exercised when using these sensors where there are high levels of humidity.

6.5 Conclusion

Diamond films were deposited onto silicon wafers using the method of spin coating. Diamond powder was mixed with methanol to form a consistent paste and then droplets of the paste were dropped onto a rotating silicon wafer (spin coater speed, 300 rpm). The films were then characterised by Electron Microscopy, from which we concluded that uniform films had been formed. The films consisted of diamond grains of about 1 μm in diameter. In order to make these films to be able to conduct electricity (for gas sensing purposes), we used Chemical Vapour Deposition (CVD) to grow the diamond grains. This was done within a heated chamber under vacuum. The pressure was maintained at $3x10^{-3}$ Torr while bleeding C_2H_2 into the chamber. During deposition, samples were kept at temperatures, 650 ^oC,750 ^oC and 850 ^oC. Some of the films were doped with either nitrogen or oxygen. The doping levels were measured using EDX on the SEM and were found to be between 1.3 and 2 for both nitrogen and oxygen.

The continuity of the films was investigated using Rutherford Backscattering Spectrometry at energy of 1-3 MeV. It was found that for those samples for which CVD had not been done, the Si signal in the RBS spectrum is at its surface position. The films therefore are not continuous before CVD or there are some holes in the films i.e. the some energetic alpha particles can hit the wafer without having gone through the diamond film. After CVD, especially at higher temperatures, the signal from Si in the RBS spectrum receded to lower energies. This means that the film now covers the Si wafer fully. RBS however cannot tell whether the material that covers the Si wafer is diamond or some other carbonaceous material

–just that it is carbon. Raman analysis showed that the samples do not graphitise if subjected to temperatures of 850 ^{o}C or below. It showed that those films on which CVD had been performed contain some graphite. The graphite however is desirable in order to connect the films and make them electrically conducting.

Undoped diamond films may be used to test for a gas such as NH3 or NO2. These are poisonous gasses and finding materials that can be used to test for them is important.

6.5 References

[1] Angus J.C and Hayman C.C., *"Low-pressure, metastable growth of diamond and diamond-like phase,*" Science, 241 (1988) 910-913.

[2] Mednikarov. B, Spasov. G, Babeva. T.Z, Sahatchieva. M, Popov .C, Kulisch, *Optical properties of diamond like carbon and nanocrystalline diamond films*, 7 (2005)1409

[3] Kuphaldt T. R. *Lesson in electric circuits' volume iii- semiconductor,* 2000-2010, revised April 05, 2009

[4] Allenspach. R, *Spin –polarized scanning electron microscopy*, 44 (4) (2000) 553-570

[5] Thomson M, Rump: *Rutherford backscattering spectroscopy analysis package*, March 2010.http://www.genplot.com.

[6] Mayer M, *Rutherford Backscattering Spectrometry (RBS) Lectures given at Workshop on Nuclear Data for Science and Technology, Material Analysis, Trieste,* 19 (2003) 55-67.

[7] http://www.matter.org.uk/diffraction/x-ray/x-ray diffraction.htm#

[8] Tai, F.C, Lee, S.C, Wei, C.H and Tyan S.L, *Correlation between I_D/I_G ratio from visible Raman spectra and sp^2/sp^3 ratio from XPS spectra of Annealed hydrogenated DLC film*, Material Transaction,47 (7) (2006)1847-1852

CHAPTER 7: SUMMARY AND CONCLUSION

In this work , Diamond-Like Carbon (DLC) and Diamond films were successfully deposited on various substrates of silicon < 100>/<111> and aluminium strips. DLC films were deposited using sputtering from a graphite target. Diamond films were spin coated from a paste made from diamond powder and methanol. These films were then characterized by means of field emission scanning electron microscopy (FE-SEM); EDS, AFM, RBS, Raman and XRD. Gas sensing using DLC films was also successfully done.

The DLC films on silicon (<100>/<111>) substrates, prepared under various conditions, were found to have smooth uniform surfaces. The root mean square roughness (R_{rms}) of the DLC films and the morphology were investigated using an AFM which showed that the films are flat and smooth. Even after annealing, the films maintained their smooth and uniform surfaces. Raman investigations showed that the sp^3/sp^2 ratio for the films can be improved. Films with higher ratios are those that had a voltage bias and were obtained using a Faraday cage. We think that the voltage bias helps to increase the kinetic energy of the sputtered carbon atoms and these impinging with high energy on the substrate the substrate help improve the sp^3/sp^2 ratio of the DLC film. The Faraday cage is used so that there are no stray fields on the substrate surface. It is generally known that an electric field tend to promote the carbon nanotubes, which have a sp^2 configuration. It is reasoned therefore that having no field might promote sp^3 configuration on the film, leading to a better DLC film. We managed to increase the sp^3 component of the film in this work.

Diamond films were prepared using spin coating from a paste made of diamond powder and methanol. The as prepared diamond films were shown by SEM to consist of grains. The grains were shown to be uniformly distributed over the silicon substrate. Using RBS we could show that the as deposited diamond film is not continuous. Since the final aim is to have diamond films that are conducting, for gas sensing applications, we deposited carbon on the diamond films (using CVD). Temperatures used were 650 °C, 750 ^{o}C and 850 °C. We thereafter used RBS to confirm that the films were fully covered by carbon. We then used Raman spectroscopy and found that the films now had sp^2 bonded carbon over and above the sp^3 carbon from the diamond grains. Some of the diamond films were doped either with nitrogen or oxygen. We used an SEM to show that results from diamond film looks good and

EDX results show that there is content of nitrogen and oxygen present in the doped diamond films. The sensing test on DLC films were performed in a Kinosistec system capable of measuring the resistance of diamond like carbon film while automatically changing the temperature of the sensor, the concentration of each gas as well as the gas type. It is demonstrated that DLC respond more favourable to NO_2 and NH_3 but rather poorly to CO, H_2 and H_2S which is an indicator of good selectivity. The DLC films show highest response in all these gases at room temperature. Reports on DLC as being an active chemical sensor for gases such as NO_2, CO, H_2S, H_2 and NH_3 and as a wide variety of gases are not available in literature.

The future for diamond like carbon films as gas is bright since they have all the desirable characteristic of a good sensor. They are inert to most corrosive gases, they can sense at room temperature, they can sense low concentrations of preferred gasses, they are selective i.e. they do not sense equally all gasses. Diamond films may also be used to sense gasses such as NH_3 and NO_2.

FUTURE WORK

Future work consists of investigating doped DLC films and finding out whether their sensitivities can be improved. This will be done by doping with various metals. Further, the gas sensitivity of diamond films and doped diamond films will also be investigated.

Appendix A

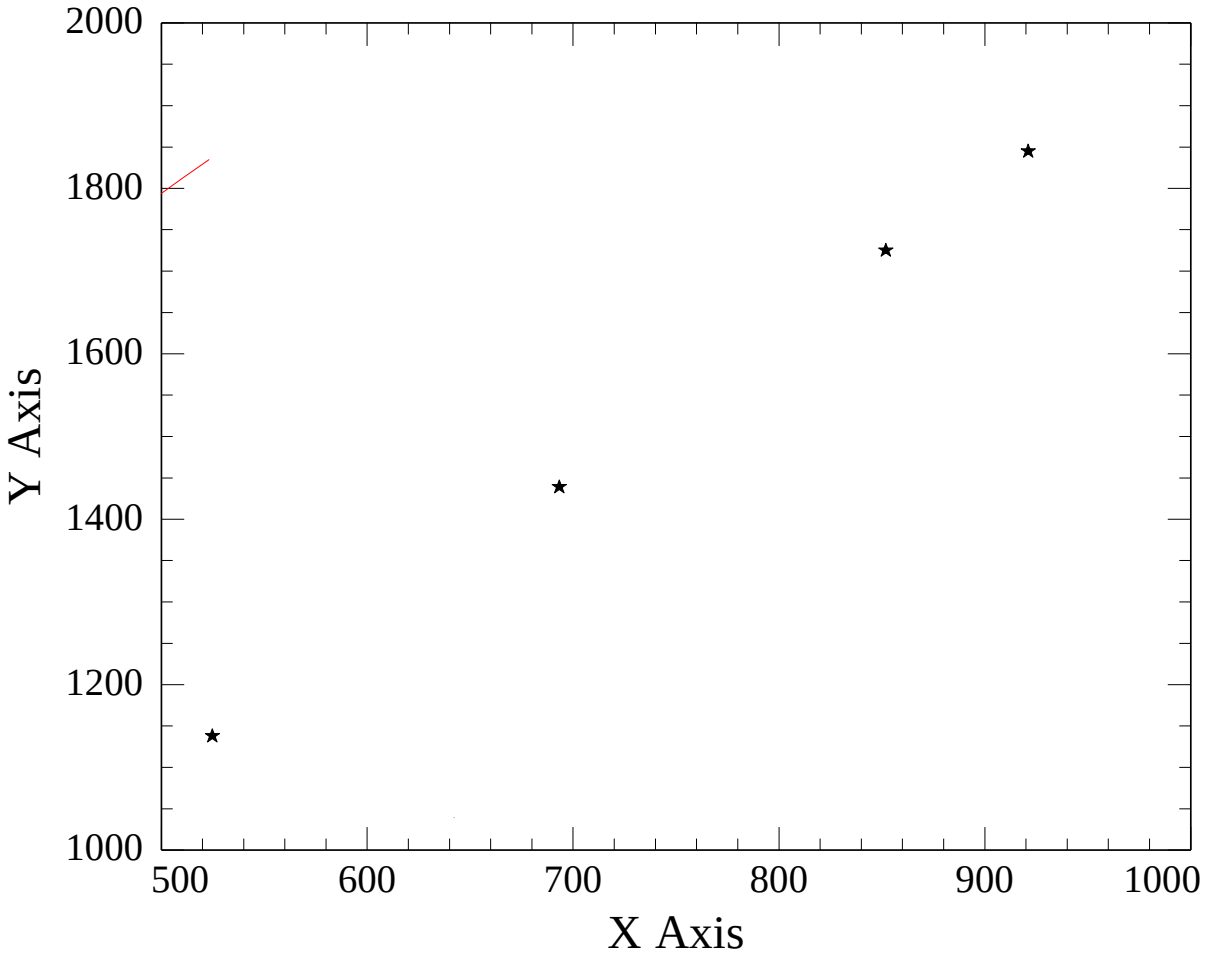

Slope: 1.787614

Intercept: 200.0169

Example:

Beam: 2.000 MeV 4He+ 20.00 uCoul @ 0.00 nA

Geometry: IBM Theta: -10.00 Phi: 15.00 Psi: 0.00

MCA: Econv: **1.787614** **200.0169** First chan: 0.0 NPT: 1024

Detector: FWHM: 20.0 keV Tau: 5.0 Omega: 1.180

Correction: 1.0000